



VNIVERSITATĪ DE VALÈNCIA

Fenomenología de neutrinos
e implicaciones cosmológicas

Julia Garayoa Roca

IFIC, Departamento de Física Teórica

Tesis doctoral

Mayo 2009

NURIA RIUS DIONIS, Profesora Titular del Departamento de Física Teórica de la Universitat de València,

CERTIFICA:

Que la presente memoria “FENOMENOLOGÍA DE NEUTRINOS E IMPLICACIONES COSMOLÓGICAS” ha sido realizada bajo su dirección en el Departamento de Física Teórica de la Universitat de València, por JULIA GARAYOA ROCA i constituye su Tesis para optar al grado de Doctor en Física.

Y para que así conste, en cumplimiento de la legislación vigente, presenta en el Departamento de Física Teórica de la Universitat de València la referida Tesis Doctoral, y firma el presente certificado.

Valencia, a 4 de Mayo de 2009.

Nuria Rius Dionis

Contents

Introducción	7
Introduction	11
1 Neutrino masses	15
1.1 General properties of neutrino masses	15
1.1.1 Neutrino oscillation parameters	16
1.2 The type I seesaw mechanism	17
1.2.1 Seesaw parametrization	19
1.2.2 Supersymmetric seesaw	20
1.3 Alternative models for neutrino masses	21
1.3.1 Inverse seesaw	21
1.3.2 The Higgs Triplet Model: type II seesaw	22
1.3.3 The Fermion Triplet Model: type III seesaw	23
1.3.4 Radiative models	24
1.3.5 Supersymmetric models	25
2 Leptogenesis	27
2.1 Baryon asymmetry of the Universe	27
2.2 Flavored Leptogenesis in the type I seesaw	28
2.2.1 Boltzmann Equations	31
2.2.2 Lower bound on M_1	33
2.2.3 Supersymmetric Leptogenesis	33
2.3 Soft Leptogenesis	35
3 Insensitivity of Leptogenesis with Flavor effects to Low Energy Lep- tonic CP Violation	37
3.1 Introduction	37
3.2 Notation and review	38
3.3 Baryon Asymmetry	40
3.4 CP violation	41
3.5 Discussion	44

4	CP Violation in the SUSY Seesaw: Leptogenesis and Low Energy	45
4.1	Introduction	45
4.2	Framework: Minimal Supergravity	46
4.2.1	Low-energy footprints: LFV and EDMs in MSUGRA	47
4.3	Flavored thermal leptogenesis	51
4.4	Reconstructing leptogenesis from low energy observables	52
4.5	Analytic Estimates	54
4.6	MCMC	56
4.6.1	Bayesian inference	56
4.6.2	The Metropolis-Hastings algorithm	57
4.6.3	Convergence	58
4.6.4	The seesaw sample	59
4.6.5	Run details	61
4.7	Discussion	61
4.7.1	Assumptions	61
4.7.2	Method	62
4.7.3	Results	63
4.8	Summary	65
5	Soft Leptogenesis in the Inverse Seesaw Model	69
5.1	Introduction	69
5.2	Inverse Seesaw Mechanism	70
5.3	The CP Asymmetry	73
5.4	CP Asymmetry in Quantum Mechanics	78
5.5	Boltzmann Equations	82
5.6	Results	90
6	Neutrino mass hierarchy and Majorana CP phases within the Higgs Triplet Model at LHC	95
6.1	Introduction	95
6.2	Doubly charged scalars at the LHC	96
6.3	Numerical analysis and results	99
6.3.1	Description of the analysis	99
6.3.2	Branching ratios	101
6.3.3	Determination of the neutrino mass spectrum	104
6.3.4	Determination of Majorana phases	106
6.4	Summary and concluding remarks	109
7	Conclusions	113
	Conclusiones	117
	Bibliography	121
	Agradecimientos	131

Introducción

El llamado Modelo Estándar de las interacciones fuertes y electrodébiles describe correctamente la mayoría de las observaciones experimentales. En el Modelo Estándar los constituyentes básicos de la materia son los quarks y los leptones, que aparecen replicados en tres familias prácticamente idénticas excepto por su masa. Los quarks interactúan fuertemente y su interacción viene descrita por la Cromodinámica Cuántica (QCD), y tanto los quarks como los leptones interactúan electromagnética y débilmente. Esta interacción electrodébil se describe mediante una teoría “gauge” basada en el grupo $SU(2) \times U(1)$, mientras que la QCD está basada en el grupo $SU(3)$. Los leptones pueden ser cargados, como el electrón y sus réplicas más pesadas, el muón y el tau, o neutros, los neutrinos, que sólo interactúan muy débilmente. En el Modelo Estándar, los neutrinos no tienen masa pues, dados los elementos existentes en el modelo, el término de masa es incompatible con la simetría dinámica de la teoría.

A pesar de su indudable éxito fenomenológico, el Modelo Estándar no puede considerarse como la descripción última y completa de las interacciones fundamentales. En primer lugar, los datos experimentales sobre oscilaciones de neutrinos proporcionan la indicación más importante de física más allá del Modelo Estándar, ya que implican que estas partículas tienen masa. Pero hay también otras preguntas importantes para las que el Modelo Estándar no tiene respuesta. Desde el punto de vista de la física de partículas, el Modelo Estándar no es capaz de explicar el origen de la estructura observada de masas y mezclas fermiónicas, o la unificación de las distintas interacciones en una única teoría dinámica. Desde el punto de vista cosmológico, el Modelo Estándar y el modelo cosmológico actual no son capaces de explicar la asimetría materia-antimateria presente en el Universo. Además existe evidencia experimental de que la materia ordinaria que vemos representa sólo el 4% de toda la materia-energía presente en el Universo. Alrededor del 23% de la materia presente en el Universo no es visible, “materia oscura”, y su naturaleza es desconocida. Y aún peor, la componente más abundante del Universo (representa alrededor del 73%) es la “energía oscura”, que creemos que es la responsable de la expansión acelerada del Universo, pero cuyo origen es completamente desconocido. Para intentar responder a algunas de estas preguntas se han propuesto numerosos modelos llamados “extensiones” del Modelo Estándar.

El descubrimiento de las oscilaciones de neutrinos ha sido uno de los resultados experimentales más importantes de los últimos años en el ámbito de la Física de Partículas, y pueden explicarse cuando se introduce una masa para los neutrinos. Si

los neutrinos tienen masa, los autoestados de masa son, en general, combinaciones lineales de los autoestados de la interacción débil, también llamados autoestados de sabor. Como consecuencia de esta mezcla, los neutrinos pueden ser detectados con un sabor diferente de aquel con que fueron producidos, fenómeno que se conoce como oscilación de neutrinos. Actualmente se observan oscilaciones de neutrinos al medir los flujos de neutrinos atmosféricos y solares, y estas oscilaciones se han confirmado en experimentos totalmente terrestres, Kamland y K2K, en los que el haz inicial de neutrinos se conoce con gran precisión.

Uno de los mecanismos más sencillos para dar masa a los neutrinos, el llamado “seesaw” tipo I, consiste en añadir al Modelo Estándar tres leptones neutros pesados (uno por cada familia), que se mezclan con los neutrinos ligeros. Tras la ruptura espontánea de simetría electrodébil, aparece un término de masa para los neutrinos ligeros. Dada la escala de masas que se deduce de los experimentos de neutrinos que hemos mencionado, los leptones neutros adicionales pueden tener una masa del orden de la llamada escala de Gran Unificación, 10^{15} GeV. Este resultado es extraordinariamente interesante, porque parece indicar que existe una relación entre la masa de los neutrinos y otros dos problemas no resueltos del Modelo Estándar: la unificación de las distintas interacciones y la generación de la Asimetría Bariónica del Universo.

Desde el punto de vista teórico, es posible extender el grupo de simetría “gauge” del Modelo Estándar, $SU(3) \times SU(2) \times U(1)$, a un único grupo gauge que lo contiene, por ejemplo $SU(5)$ o $SO(10)$. Esta extensión posee un profundo significado: cada subgrupo del Modelo Estándar representa una de las interacciones fundamentales, de forma que sería posible unificar todas las interacciones en una única fuerza. La escala de energías a la que se produce esta unificación se denomina escala de Gran Unificación, y es del orden de 10^{15} GeV. Es más, algunos de los grupos de Gran Unificación, por ejemplo $SO(10)$, contienen de forma natural los leptones neutros pesados que generan masas para los neutrinos en el marco del mecanismo seesaw. Esto ha motivado muchos trabajos que intentan describir de forma unificada las masas y mezclas de quarks y leptones, incluyendo, por supuesto, los neutrinos.

La existencia de dos escalas de energía tan diferentes, es decir la escala electrodébil del orden de 100 GeV y la escala de Gran Unificación, da lugar al llamado problema de las jerarquías, ya que el Modelo Estándar se vuelve inestable bajo correcciones radiativas. Existen varias soluciones a este problema, pero una de las mejor motivadas consiste en extender las simetrías del espacio-tiempo introduciendo la llamada Supersimetría, que relaciona partículas con espín diferente (fermiones y bosones). Es remarcable que, con el contenido de partículas del Modelo Estándar Supersimétrico Mínimo, los tres acoplamientos gauge de las interacciones fundamentales convergen a un único valor a la escala de Gran Unificación. Esto se considera un éxito de la Supersimetría, ya que en el Modelo Estándar no se produce esta unificación. Como consecuencia, muchos de los modelos de masas de neutrinos y de Gran Unificación son también supersimétricos.

Los resultados de la nucleosíntesis primordial y las recientes medidas del fondo cósmico de microondas implican que el cociente entre la densidad de bariones y

la de fotones en el Universo debe ser $(6.1 \pm 0.3) \times 10^{-10}$. La producción de esta asimetría bariónica a partir de las interacciones entre las partículas elementales se conoce con el nombre de Bariogénesis. Aunque el Modelo Estándar posee todos los ingredientes necesarios para producir la asimetría bariónica durante la transición de fase electrodébil, predice un valor varios órdenes de magnitud más pequeño que el medido experimentalmente. Por tanto si queremos explicar la Asimetría Bariónica del Universo hay que considerar extensiones del Modelo Estándar. En particular, se ha demostrado que es posible generar esta asimetría bariónica como consecuencia de la desintegración fuera del equilibrio térmico de leptones neutros pesados, mecanismo conocido como Leptogénesis. Este tema es de gran interés actualmente, ya que como hemos dicho, suponiendo la existencia de dichos leptones se puede explicar la masa de los neutrinos. Así, se están realizando numerosos estudios para determinar en cuáles de los modelos de masas de neutrinos propuestos es también posible generar la asimetría bariónica.

Además del mecanismo seesaw tipo I existen otras alternativas para generar la masa de los neutrinos. Son de particular interés aquellos modelos en los que la escala de “nueva física” es más baja que en el seesaw estándar, del orden del TeV, pues en tal caso podría haber nuevos fenómenos observables en los laboratorios. Esto supone una grandísima ventaja ya que estos modelos pueden ser probados por los experimentos presentes o futuros. Así, con el acelerador de protones LHC casi en marcha, es el momento preciso para estudiar este tipo de modelos alternativos al mecanismo seesaw tipo I.

La tesis que aquí se presenta lleva por título “Fenomenología de neutrinos e implicaciones cosmológicas” y pretende ser un análisis de varios aspectos fenomenológicos de la física de neutrinos y sus posibles consecuencias desde el punto de vista cosmológico. En particular hemos estudiado los modelos seesaw tipo I y II, y el modelo seesaw inverso.

Es bien conocido que uno de los ingredientes necesarios para que pueda generarse la asimetría bariónica es que exista violación de CP. Por tanto, si asumimos que la asimetría bariónica fue generada vía el mecanismo de la Leptogénesis, es necesario que exista violación de CP en el sector leptónico. En [1] demostramos que en el contexto del modelo seesaw tipo I, en general, no existe una relación directa entre la violación de CP accesible a bajas energías, y por tanto medible en los laboratorios, y la violación de CP responsable de la Leptogénesis con efectos de sabor.

Posteriormente extendimos este estudio a un escenario supersimétrico. El Modelo Estándar Supersimétrico Mínimo con neutrinos pesados predice la existencia de procesos que violan sabor leptónico y que pueden ser medidos experimentalmente. A saber, la desintegración radiativa de muones y taus. En nuestro trabajo [2] asumimos que los futuros experimentos medirán este tipo de procesos (esto restringe el espacio de parámetros de alta energía de los que no sabemos nada), y demostramos que incluso en este escenario optimista no hay correlación entre la violación de CP a baja energía y Leptogénesis.

También hemos estudiado el modelo seesaw inverso. El interés de este modelo es que los neutrinos pesados son más ligeros que en el caso del seesaw tipo I y los

procesos que violan sabor leptónico no están suprimidos por las masas de los neutrinos, en consecuencia podría haber efectos observables en los aceleradores. Nosotras [3] estudiamos la Leptogénesis Soft en el contexto del modelo seesaw inverso. La Leptogénesis Soft es un nuevo mecanismo para generar la asimetría bariónica que fue propuesto para el caso del seesaw tipo I supersimétrico, y en el que se estudian los efectos térmicos de los términos que rompen supersimetría, y que permiten generar una asimetría leptónica a través de la desintegración fuera de equilibrio de los sneutrinos, compañeros supersimétricos de los neutrinos.

Por último en esta tesis se ha estudiado el modelo del triplete escalar de Gelmini y Roncadelli, también llamado seesaw tipo II, como origen de la masa de los neutrinos. Las componentes de este triplete pueden ser lo suficientemente ligeras como para ser producidas en LHC, y entonces su componente doblemente cargada podría desintegrarse a un par de leptones con la misma carga. El término del lagrangiano que permite esta desintegración es el mismo que es responsable de las masas de los neutrinos. Por esta razón, ver este tipo de eventos en LHC, supondría hacer una medida directa de la matriz de masa de los neutrinos. En nuestro trabajo [4] hemos estudiado qué información puede extraerse a cerca de las propiedades de los neutrinos si en LHC se producen estos procesos.

Introduction

The current Standard Model of Particle Physics describes most of the experimental observations. The matter content of the Standard Model are quarks and leptons, which appear replicated in three families basically identical except for their masses. Only quarks can have strong interactions, described by Quantum Chromodynamics (QCD); while both, quarks and leptons, present weak and electromagnetic interactions. Electroweak interactions are described by the gauge theory based on $SU(2) \times U(1)$ group, whereas QCD is based on $SU(3)$. Leptons can be charged, as the electrons, muons and taus, or neutral, as the neutrinos which only interact weakly. Neutrinos are massless within the Standard Model because a mass term for them is incompatible with the symmetries of the theory.

Despite its undoubted phenomenological success, the Standard Model can not be regarded as the ultimate and complete description of the fundamental interactions. First, the experimental data on neutrino oscillations provide the most important indication of physics beyond the Standard Model, since they imply that these particles have mass. But there are also other important questions for which the Standard Model has no answer. First, from the point of view of particle physics, the Standard Model can not explain the origin of the observed structure of fermion masses and their mixing, or the unification of the different interactions in a single dynamical theory. From the cosmological point of view, the Standard Model and the Cosmological Standard Model do not provide an explanation for the matter-antimatter asymmetry present in the Universe. Moreover we have experimental evidence that the ordinary matter that we see represents only 4% of all the matter-energy present in the Universe. About 23% of the matter is not visible, “dark matter”, and its nature is unknown. And even worse, the most abundant component of the Universe (it represents about 73%) is “dark energy”, which is supposed to drive the accelerated expansion, but its origin is completely unknown. In order to answer some of these questions many models called “extensions” of the Standard Model have been proposed.

The discovery of neutrino oscillations is one of the most important experimental results from recent past years in the field of Particle Physics, and can be explained if we introduce a mass for neutrinos. If neutrinos are massive, the mass eigenstates are, in general, linear combinations of the weak interaction eigenstates, usually called flavor eigenstates. As a result of this mixture, neutrinos can be detected with a different flavor from that with which they were produced, a phenomenon known as neutrino oscillation. Currently neutrino oscillations are observed by measuring the

atmospheric and solar neutrino fluxes, and also in terrestrial experiments, Kamland and K2K, where the initial neutrino beam is known with high accuracy.

One of the simplest ways to generate neutrino masses is the type I seesaw mechanism, where three heavy neutral leptons (one per family) which mix with light neutrinos are added to the Standard Model matter content. After spontaneous electroweak symmetry breaking, a mass term for light neutrinos appears. Given the scale of masses inferred from the neutrino experiments that we have mentioned, the additional neutral leptons can have a mass of the order of the Grand Unification scale, 10^{15} GeV. This result is extremely interesting because it suggests that there is a connexion between neutrino masses and two other open problems in the Standard Model: the unification of the different interactions and the generation of the Baryon Asymmetry of the Universe.

From a theoretical point of view, it is possible to extend the gauge symmetry group of the Standard Model, $SU(3) \times SU(2) \times U(1)$, to a single gauge group that contains it, for instance $SU(5)$ or $SO(10)$. This extension has a deep meaning: each subgroup of the Standard Model represents one of the fundamental interactions, so it would be possible to unify all of them in one single strength. The scale of energies at which this Unification takes place is called Grand Unification scale, and it is of the order of 10^{15} GeV. Moreover, some of the Grand Unification groups, for instance $SO(10)$, naturally contain the heavy neutral leptons which generate neutrino masses within the framework of the seesaw mechanism. This has motivated many papers trying to describe in a unified way the masses and mixings of quarks and leptons, including, of course, neutrinos.

The existence of two such different energy scales, namely the electroweak scale of the order of 100 GeV and the Grand Unification scale, originates the so called hierarchy problem, as the Standard Model becomes unstable under radiative corrections. There are several solutions to this problem, but one of the best motivated is Supersymmetry, which relates particles with different spin (fermions and bosons). It is remarkable that, given the particle content of the Minimal Supersymmetric Standard Model, the gauge couplings of the three fundamental interactions converge into a single value at the Grand Unification scale. This is considered a success of Supersymmetry, since this unification does not occur in the Standard Model. Consequently, most models of neutrino masses and Grand Unified Theories are also supersymmetric.

Primordial nucleosynthesis and the recent measurement of the cosmic microwave background imply that the baryon to photon density ratio in the Universe is $(6.1 \pm 0.3) \times 10^{-10}$. The dynamical production mechanism of this baryon asymmetry is known as Baryogenesis. Although the Standard Model contains all the necessary ingredients to produce the baryon asymmetry during the electroweak phase transition, it predicts a value which is several orders of magnitude smaller than the measured one. So if we want to explain the Baryon Asymmetry of the Universe, some extension of the Standard Model must be considered. In particular, it has been shown that it is possible to generate this baryon asymmetry as a result of the out-of-equilibrium decay of heavy neutral leptons, a mechanism known as Leptogenesis. This issue is

of great interest today, because as we said, assuming the existence of such leptons one can explain neutrino masses. Thus, many studies are being conducted to determine in which models for neutrino masses it is also possible to generate the baryon asymmetry.

In addition to the type I seesaw mechanism there are other alternative models to generate neutrino masses. Of particular interest are those where the scale of new physics is lower than in the standard seesaw, at the TeV scale, because in such a case there could be new phenomena observable at experiments. This is a great advantage because these models could be tested at experiments. With the proton accelerator LHC almost taking data, this may be the right time to study this kind of models.

The thesis presented here is titled “Neutrino phenomenology and cosmological implications” and it is meant to be an analysis of several phenomenological aspects of neutrino physics and their possible consequences from a cosmological point of view. In particular we have studied the seesaw type I and II, and the inverse seesaw.

It is well known that one of the necessary ingredients to generate the baryon asymmetry is CP violation. Therefore, if we assume that the baryon asymmetry was generated via Leptogenesis, there must be CP violation in the lepton sector. In [1] we show that in the framework of the type I seesaw model, in general, there is no direct link between the CP violation accessible at low energies, and thus measurable in neutrino experiments, and the CP violation involved in flavored Leptogenesis.

Subsequently we extended this study to a supersymmetric scenario. The Minimal Supersymmetric Standard Model with heavy neutral leptons predicts the existence of processes that violate flavor and that could be measured experimentally. Namely, the radiative decay of muons and taus. In our work [2] we assume that upcoming experiments will measure this type of processes (this restricts the high-energy parameter space from which we do not know anything), and showed that even in this optimistic scenario there is no correlation between the low energy CP violation and Leptogenesis.

We have also considered the inverse seesaw model. The interest of this model is that the heavy neutrinos can be much lighter than in the type I seesaw and lepton flavor violating processes are not suppressed by neutrino masses, therefore there could be observable effects at accelerators. We studied [3] the mechanism of Soft Leptogenesis in the context of the inverse seesaw model. Soft Leptogenesis is a new mechanism to generate the baryon asymmetry. It was introduced within the supersymmetric type I seesaw model and it considers the thermal effects of the terms that break supersymmetry, since they allow to generate an asymmetry in leptons through the out-of-equilibrium decay of sneutrinos, supersymmetric partners of neutrinos.

Finally in this thesis we have considered the Higgs triplet model, also called type II seesaw, proposed by Gelmini and Roncadelli, as the source of neutrino masses. The scalar components of this triplet can be sufficiently light to be produced at LHC, and then the doubly charged component could decay into a pair of same-sign leptons. The term in the Lagrangian that generates this decay is the same than the one which is responsible for neutrino masses. For this reason, seeing these kind of

events at LHC would be a direct test of the neutrino mass matrix. In our work [4] we studied what can be learnt about neutrinos if LHC discovers such a triplet.

Chapter 1

Neutrino masses

1.1 General properties of neutrino masses

In 1930 Pauli proposed the existence of neutrinos to explain the apparent energy and spin non-conservation in nuclear β decay. 25 years later Reines and Cowan discovered them, they measured the escaping neutrinos from a nuclear reactor in Savannah River.

The experimental challenge of measuring neutrinos continued during the next years. The Sun is a natural fusion nuclear reactor where a huge amount of neutrinos are produced. In the late 60s the Homestake experiment, run by Davis, was the first one built in the attempt of measuring the electron neutrinos coming from the Sun. A systematic discrepancy between the expected neutrino flux and the observed one was established. The hypothesis of massive neutrinos which can mix and oscillate appeared, among others, as a possible explanation to the solar neutrino problem.

A similar problem in the atmospheric neutrino flux was observed. In 1998 SuperKamiokande reported evidence of neutrino oscillations in the atmospheric neutrino flux. The experiments SNO and KamLAND also confirmed neutrino oscillations in the solar neutrino flux.

Today we have a strong experimental evidence that neutrinos are massive, as the rest of fermions of the SM. And we also know that their mass basis is different from the flavor one, as in the case of quarks. The scheme of massive neutrinos which mix and oscillate is the only solution capable of explaining the huge amount of solar [5, 6, 7, 8, 9, 10], atmospheric [11], reactor [12] and accelerator [13, 14] neutrino data collected during the last ten years.

However, when the Standard Model (SM) was being built, during 60s, there was no evidence for neutrino masses. So they were assumed to be massless. Neutrino masses is the first signal of physics beyond the SM. Therefore, from the theoretical point of view, an extension of the SM is needed to explain the neutrino mass generation.

Moreover, we know that massive neutrinos play important roles in some astrophysical and cosmological fields. For instance, neutrinos need to be taken into account in Nucleosynthesis calculations, they can also affect structure formation, and

they are crucial in type II supernova explosions since they carry 99% of the released energy. They could also be the clue for the generation of the Baryon Asymmetry of the Universe, as we discuss in the next chapter.

Neutrinos are neutral fermions with spin 1/2. The fact that neutrinos have no electric charge allows us to write down two types of mass terms for them: Dirac and Majorana mass terms. A Dirac mass has the form $m\bar{\psi}\psi$ and it connects fields with opposite chirality. On the other hand the Majorana mass term, having the form $m\psi^T C^{-1}\psi$, connects fields of the same chirality. The consequence of having Majorana neutrinos is that neutrinos would be their own antiparticle. Therefore lepton number can not be a symmetry of leptons if neutrinos are of the Majorana type.

From the kinematical point of view Majorana neutrinos can not be distinguished from Dirac neutrinos, because both mass terms lead to the same energy-momentum relations. But dynamically, new physical phenomena for Majorana neutrinos are expected. For instance neutrino-less double beta decay.

In the next section we will review the current neutrino oscillation parameters and in the rest of this chapter we will present some of the mechanisms available in literature to generate neutrino masses.

1.1.1 Neutrino oscillation parameters

The flavor neutrino states ν_α , $\alpha = e, \mu, \tau$ involved in electroweak interactions are linear combinations of three mass eigenstates ν_i , $i = 1, 2, 3$. The simplest unitary transformation between the flavor and mass eigenstates is given by the PMNS mixing matrix U:

$$|\nu_\alpha\rangle = \sum_{i=1}^3 U_{\alpha i}^* |\nu_i\rangle, \quad (1.1)$$

where U is a unitary complex matrix containing 3 real mixing angles and 3 phases. The standard parametrization for this matrix is:

$$U = V \text{diag}(e^{i\frac{\alpha_1}{2}}, e^{i\frac{\alpha_2}{2}}, e^{i\frac{\alpha_3}{2}}) \quad \text{with} \quad (1.2)$$

$$V = \begin{pmatrix} c_{12}c_{13} & s_{12}c_{13} & s_{13}e^{-i\delta} \\ -c_{23}s_{12} - s_{13}s_{23}c_{12}e^{i\delta} & c_{23}c_{12} - s_{13}s_{23}s_{12}e^{i\delta} & s_{23}c_{13} \\ s_{23}s_{12} - s_{13}c_{23}c_{12}e^{i\delta} & -s_{23}c_{12} - s_{13}c_{23}s_{12}e^{i\delta} & c_{23}c_{13} \end{pmatrix}$$

where $s_{ij} \equiv \sin \theta_{ij}$, $c_{ij} \equiv \cos \theta_{ij}$, δ is the so-called Dirac CP violating phase, and α_i are the Majorana phases. Note that only relative phases $\alpha_{ij} \equiv \alpha_i - \alpha_j$ are physical, and therefore there are only two independent Majorana phases.

The neutrino mass matrix in the flavor basis can be written in terms of the mass eigenstates and the PMNS mixing matrix:

$$m_\nu = U \text{diag}(m_1, m_2, m_3) U^T \equiv U D_m U^T. \quad (1.3)$$

Oscillation neutrino experiments are only sensitive to neutrino mass squared differences and mixing angles. Recent global fits determine the following solar and

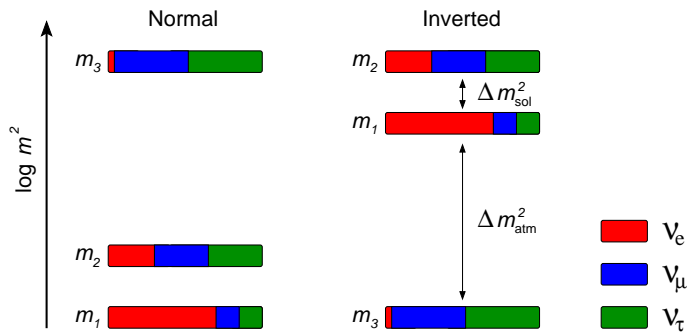


Figure 1.1: Possible neutrino mass hierarchy patterns. $\Delta m_{sol}^2 = \Delta m_{21}^2$ is known to be positive, while the sign of $\Delta m_{atm}^2 = |\Delta m_{31}^2|$ is still unknown and will determine the neutrino mass hierarchy. Positive Δm_{atm}^2 is called normal hierarchy (left pattern), while negative Δm_{atm}^2 is known as inverted hierarchy (right pattern). The colors show the amount of a given flavor states in each mass state, according to current fits for the mixing angles.

atmospheric parameters [15]:

$$\begin{aligned} \sin^2 \theta_{12} &= 0.30 \pm 0.02, & \Delta m_{21}^2 &= (7.65 \pm 0.23) \times 10^{-5} \text{ eV}^2, \\ \sin^2 \theta_{23} &= 0.50 \pm 0.07, & |\Delta m_{31}^2| &= (2.40 \pm 0.12) \times 10^{-3} \text{ eV}^2, \end{aligned} \quad (1.4)$$

where we give 1σ errors and $\Delta m_{ij}^2 \equiv m_i^2 - m_j^2$. For the mixing angle θ_{13} there is only an upper bound,

$$\sin^2 \theta_{13} < 0.05 \quad \text{at } 3\sigma, \quad (1.5)$$

whereas at present nothing is known about the phases δ, α_{ij} . However future neutrino oscillation experiments could determine the Dirac phase. Furthermore, seeing neutrino-less double beta decay would prove the Majorana nature of neutrinos and could put some constraints on the Majorana phases.

The ordering of the 3 mass eigenstates in Eq. (1.3) is not known, and it will be determined by the sign of Δm_{31}^2 . If $\Delta m_{31}^2 > 0$, the lightest neutrino mass is m_1 and we say that the neutrino mass order is normal, normal hierarchy (NH). For $\Delta m_{31}^2 < 0$, the lightest neutrino mass is m_3 and the hierarchy is inverted (IH), as shown in Fig. (1.1). The most stringent bound on the absolute scale of the neutrino mass comes from cosmology, which is sensitive to the sum of the three masses: $\sum_i m_i < 0.5 \text{ eV}$ at 95% CL [16].

1.2 The type I seesaw mechanism

The type I seesaw mechanism [17] provides a simple way to generate small neutrino masses, and has become the standard way to give mass to neutrinos. The idea is to add three singlet right-handed neutrinos (N_i) to the matter content of the SM. The new singlets can couple to the left-handed fermion doublets via the usual yukawa

couplings (λ). Since they are completely neutral, they can also have a Majorana mass. At high energy scales, we can choose a basis where the right-handed Majorana mass matrix (D_{M_i}) and the charged lepton yukawa matrix (Y_{e_α}) are diagonal and real:

$$\mathcal{L} = -Y_{e_\alpha} \bar{\ell}_{L_\alpha} H e_{R_\alpha} - \lambda_{\alpha i} \bar{\ell}_{L_\alpha} \tilde{H} N_i - \frac{D_{M_i}}{2} \bar{N}_i N_i^c + \dots + h.c. \quad (1.6)$$

where the index α labels flavors, l_L are the lepton doublets, e_R are the charged lepton singlets, H is the SM Higgs doublet, and $\tilde{H} = i\tau_2 H^*$, with τ_2 the Pauli matrix. In this basis, the neutrino yukawa matrix is a general complex matrix. Three of the six phases can be removed by redefinition of the lepton doublets, therefore λ contains nine real parameters and three phases. The total number of parameters in the lepton sector is 21 [18].

The yukawa coupling generates a Dirac mass term after electroweak spontaneous symmetry breaking, in the same way as happens for quarks and charged leptons. The complete neutrino mass matrix in the basis (ν_{L_α}, N_i) can be written in blocks as:

$$m_\nu = \begin{pmatrix} 0 & \lambda v_u \\ \lambda^T v_u & M \end{pmatrix}, \quad (1.7)$$

where $v_u = 175$ GeV is the SM Higgs vacuum expectation value. The diagonalization of this mass matrix leads to the neutrino mass eigenvalues and eigenstates. In the limit $M \gg v_u$ one finds three light neutrinos mass eigenstates with masses of order $\frac{(\lambda v_u)^2}{M}$ and three heavy neutrino mass eigenstates with masses of order M . The smallness of the light neutrino mass eigenstates finds an explanation in the hierarchy $M \gg v_u$.

We can do a simple estimation of the energetic scale of the right-handed neutrinos. If we take the neutrino yukawa couplings of the order of the top quark yukawa coupling, $Y \sim 1$, and we use the cosmological bound on light neutrino masses [16] ($\sim \frac{(\lambda v_u)^2}{M}$), we obtain an upper bound for the right-handed neutrino mass $M \sim 10^{15}$ GeV. This estimation gives an idea of the energetic scale for new physics, and shows the difficulty of proving the seesaw as the source of neutrino masses.

On the other hand, one virtue of the seesaw mechanism is that it provides a very elegant solution for the baryon asymmetry problem of the Universe, through the mechanism of Leptogenesis which we describe in the next chapter.

Finally, we stress that the main theoretical drawback of the model is that singlet right-handed neutrinos give corrections $\sim |M|^2$ to the Higgs mass through loop effects. This is known as the hierarchy problem. Supersymmetry can solve this problem because these dangerous contributions to the Higgs mass are exactly canceled by the sneutrino ones. We describe the type I seesaw mechanism in the context of the Minimal Supersymmetric Standard Model later in this chapter.

1.2.1 Seesaw parametrization

Top-down parametrization

The parameters of the seesaw as described above, in terms of the diagonal matrix D_M and the neutrino yukawa matrix, is usually referred to as the “top-down parametrization”. In this parametrization one uses as input parameters those acting on the right-handed sector.

The neutrino yukawa matrix can be written in terms of a diagonal matrix with real eigenvalues by doing the transformation:

$$\lambda = V_L^\dagger D_\lambda V_R, \quad (1.8)$$

where V_L and V_R are complex unitary matrices. In a “top-down parametrization” the set of input parameters are D_M , D_λ , V_L and V_R .

Let us now show how to write the light neutrino masses in terms of the input parameters. At low energies ($\ll M$), we can integrate out the heavy right-handed neutrinos in the Lagrangian Eq. (1.6). Thus we obtain an effective lagrangian [19]:

$$\mathcal{L}_{lep}^{eff} = -Y_{e\alpha} \bar{\ell}_{L\alpha} H e_{R\alpha} - \frac{1}{2} (\lambda_{\alpha i} \bar{\ell}_{L\alpha} \tilde{H}) D_{M_i}^{-1} (\lambda_{\beta i}^T \ell_{L\beta}^C \tilde{H}^\dagger) + h.c. \quad (1.9)$$

After electroweak symmetry breaking, the left-handed neutrinos acquire a Majorana mass $\sim -\frac{1}{2} \nu_L^T C^{-1} m_\nu \nu_L$ given by:

$$m_\nu = \lambda D_M^{-1} \lambda^T v_u^2 \quad (1.10)$$

This light neutrino mass matrix can be diagonalized by the unitary matrix U , the PMNS mixing matrix whose parametrization we have already introduced in Eq. (1.2):

$$m_\nu = U D_m U^T. \quad (1.11)$$

Therefore within the top-down parametrization the light neutrino mass matrix can be obtained through Eq. (1.10).

Bottom-up parametrization

From a phenomenological point of view it is more interesting to use a parametrization where the input parameters are at the electroweak scale, accessible to experiments. This is the aim of a “bottom-up parametrization” [20, 21], where input parameters are those acting on the left-handed sector, which are potentially more accessible. Thus, input parameters are D_m , U , D_λ and V_L .

It is straight-forward to show that the rest of parameters can be extracted from these inputs. The singlet neutrino Majorana mass matrix is:

$$M^{-1} = V_R D_M^{-1} V_R^T = D_\lambda^{-1} V_L U D_m U^T V_L^T D_\lambda^{-1} v_u^{-2}, \quad (1.12)$$

with matrix V_R diagonalizing the inverse right-handed neutrino mass matrix.

Casas-Ibarra parametrization

Finally we introduce the ‘‘Casas-Ibarra parametrization’’ [22]. The aim of this parametrization is to use as input parameters those accessible at neutrino experiments, and encode all the unknown information in a complex matrix R . It uses as input parameters D_m , U , D_M and a general complex orthogonal matrix R . It can be shown that the most general neutrino yukawa matrix can be written as:

$$\lambda v_u = U D_m^{1/2} R D_M^{1/2} \quad (1.13)$$

With the Casas-Ibarra parametrization one loses the information on the high-energy theory. On the other hand, it turns out to be very useful to perform calculations.

1.2.2 Supersymmetric seesaw

Supersymmetry is desirable in a seesaw scenario because it solves the hierarchy problem present in the SM. The superpotential of the leptonic sector in a supersymmetric seesaw model with three right-handed neutrinos is:

$$W_{lep} = (L_L H_d) Y_e E^c + (L_L H_u) \lambda N^c + N^c \frac{M}{2} N^c. \quad (1.14)$$

In this expression, λ , Y_e and M are 3×3 matrices, and flavor indices are suppressed. The H_u, H_d are the supermultiplets containing the two scalar Higgs doublets, L_L are those containing the left-handed lepton fields, while E contain the right-handed charged leptons and N the right-handed singlets. Without loss of generality one can work in the basis where Y_e and M are diagonal, so that the superpotential gives the same Lagrangian for leptons as the one written in Eq. (1.6).

Since supersymmetry is broken, to this Lagrangian we must add the soft SUSY breaking terms :

$$-\mathcal{L}_{SSB} = \tilde{m}_0^2 \sum_f \tilde{f}^\dagger \tilde{f} + \left\{ \frac{B D_{M_i}}{2} \tilde{N}_i^c \tilde{N}_i^c + a_0 (y_{e\alpha} \tilde{\ell}_{L\alpha} H_d \tilde{e}_{R\alpha}^c + \lambda_{\alpha i} \tilde{\ell}_{L\alpha} H_u \tilde{N}_i^c) + h.c. \right\} \quad (1.15)$$

where \tilde{f} collectively represents sfermions. This soft part is written at some high scale M_X where, in MSUGRA, the soft masses are universal and the trilinear couplings are proportional to the corresponding Yukawas. MSUGRA is then characterized by four parameters: the scalar (m_0) and gaugino ($m_{1/2}$) masses, shared by all of them at the GUT scale; the trilinear coupling involving scalars, a_0 , at the GUT scale; and finally the Higgs vev ratio, $\tan \beta = v_u/v_d$.

The generation of light neutrino masses via the type I seesaw mechanism in the Minimal Supersymmetric version of the SM (MSSM), works exactly in the same way as in the SM. So neutrino masses can be written as in Eq. (1.10), with $v_u = \langle H_u \rangle$.

Let us note that, in the supersymmetric type I seesaw, neutrino yukawa couplings induce, through Renormalization Group Equations (RGE) running from high to low

energies, lepton flavor and CP violating contributions to the slepton masses. At leading order this correction is [23, 24, 25, 26]:

$$\Delta\tilde{m}_{L_{\alpha\beta}} = -\frac{3m_0^2 + a_0^2}{16\pi^2}\lambda_{\alpha i}\log\frac{M_i^2}{M_X^2}\lambda_{i\alpha}^\dagger. \quad (1.16)$$

At one loop, the off-diagonal slepton mass terms can lead to lepton flavor violating (LFV) processes at observable rates. This is very interesting because the slepton mass matrix becomes a low energy footprint of the seesaw mechanism. Of course, it is possible that there are additional contributions to the slepton matrix different from the neutrino ones. This could happen if, for instance, the soft terms were not universal as we are assuming. Therefore, measuring a non-diagonal slepton matrix would not be a proof of the seesaw, but it would put some bounds on neutrino yukawas [20].

In chapter 4 we use this nice feature to study if any correlation between the CP violating phases relevant in Leptogenesis and low energy Supersymmetry can be established.

1.3 Alternative models for neutrino masses

The seesaw mechanism is the standard mechanism to generate neutrino masses. However, generically, the large mass of the right-handed neutrinos makes extremely difficult to test it. Even if we use the bottom-up parametrization described above, and we assume the most promising supersymmetric scenario where the full slepton mass matrix can be measured [20], it would be impossible to reconstruct the full neutrino yukawa matrix and the right-handed neutrino masses. Imposing approximate symmetries, for instance lepton number, would allow to lower the energetic scale with observable effects of the type I seesaw [27].

Given this unpromising scenario seems reasonable to consider alternative neutrino mass models where the energetic scale of new physics is lower, so that they are potentially testable. In this section we present some of these alternative mechanisms for neutrino masses.

First we will present a modification of the standard seesaw, the inverse seesaw model, which allows for much lighter right-handed neutrinos. We will also describe the called type II and type III seesaw mechanisms. We will refer to models with explicit lepton flavor violation where neutrino masses are generated via radiative corrections. Finally we will comment on the possibility that the origin of neutrino mass is low scale supersymmetry.

1.3.1 Inverse seesaw

This model [28] is a modification of the seesaw where the lepton content is not minimal. The model incorporates two singlet fermions N_i and S_i per generation

which couple to the lepton sector:

$$\mathcal{L} = -\lambda_{\alpha i} \bar{\ell}_{L\alpha} \tilde{H} N_i - M_{ij} \bar{S}_i N_j - \mu_{ij} \bar{S}_i S_j^c . \quad (1.17)$$

We assign lepton number $L = 1$ to the singlets S_i and N_i . Therefore the mass term $\sim \mu$ violates lepton number. In the original formulation of the model, the singlets S_i were superstring inspired E(6) singlets, in contrast to the right-handed neutrinos N_i , which are in the spinorial representation. More recently this mechanism has also arisen in the context of left-right symmetry [29] and SO(10) unified models [30].

After electroweak symmetry breaking the 9×9 mass matrix of the neutral lepton sector in (ν_L, N, S) basis is given by:

$$\mathcal{M} = \begin{pmatrix} 0 & m_D & 0 \\ m_D^T & 0 & M^T \\ 0 & M & \mu \end{pmatrix} , \quad (1.18)$$

where $m_D = \lambda v_u$, M are arbitrary 3×3 complex matrices in flavor space and μ is complex symmetric. In models where lepton number is spontaneously broken by a vacuum expectation value $\langle \sigma \rangle$, $\mu = \lambda \langle \sigma \rangle$ [31]. The matrix \mathcal{M} can be diagonalized by a unitary transformation, leading to nine mass eigenstates n_a : three of them correspond to the observed light neutrinos, while the other three pairs of two component leptons combine to form three quasi-Dirac leptons.

In this ‘‘inverse seesaw’’ scheme, assuming $m_D, \mu \ll M$ the effective Majorana mass matrix for the light neutrinos is approximately given by:

$$m_\nu = m_D^T M^{T-1} \mu M^{-1} m_D , \quad (1.19)$$

while the three pairs of heavy neutrinos have masses of order M , and the admixture among singlet and doublet $SU(2)$ states is suppressed by m_D/M . Although M is a large mass scale suppressing the light neutrino masses, in contrast to the Majorana mass ($\Delta L = 2$) of the right-handed neutrinos in the standard seesaw mechanism, it is a Dirac mass ($\Delta L = 0$), and it can be much smaller, since the suppression in Eq. (1.19) is quadratic and moreover light neutrino masses are further suppressed by the small parameter μ which characterizes the lepton number violation scale.

Notice that in the $\mu \rightarrow 0$ limit lepton number conservation is restored. Then, the three light neutrinos are massless Weyl particles and the six heavy neutral leptons combine exactly into three Dirac fermions.

In chapter 5 we consider the supersymmetric version of this model and we study the mechanism of Soft Leptogenesis.

1.3.2 The Higgs Triplet Model: type II seesaw

This model was first proposed by Gelmini and Roncadelli [32]. A $SU(2)_L$ Higgs triplet with hypercharge $Y = 2$ is added to the SM, then the following normalizable term can appear in the Yukawa sector of the Lagrangian:

$$\mathcal{L}_\Delta = -\lambda_{\alpha\beta} l_{L\alpha}^T C^{-1} i\tau_2 \Delta l_{L\beta} + h.c. , \quad (1.20)$$

where the indices $\alpha, \beta = e, \mu, \tau$ label flavors, $l_{L\alpha}$ are the lepton doublets, C is the charge conjugation matrix, τ_2 is the Pauli matrix, Δ denotes the scalar triplet, and $\lambda_{\alpha\beta}$ is a symmetric complex Yukawa matrix. The components of the triplet are given by:

$$\Delta = \begin{pmatrix} \Delta^+/\sqrt{2} & \Delta^{++} \\ \Delta^0 & -\Delta^+/\sqrt{2} \end{pmatrix}. \quad (1.21)$$

We assign lepton number $L = -2$ to the triplet, so that the coupling in Lagrangian Eq. (1.20) conserves lepton number. To this lagrangian one also adds a scalar potential which contains all the allowed terms involving the Higgs triplet and the SM Higgs doublet. In the original version of the model, lepton number was spontaneously broken, leading to a Majoron and a light neutral scalar such that the Z gauge boson would decay into these two scalars. Since there is no room for such a decay according to LEP measurements, we explicitly break lepton number by a cubic term in the Higgs potential $\sim \mu H \Delta H$.

If the neutral component of the triplet acquires a vacuum expectation value (VEV) v_T , $\langle \Delta^0 \rangle \equiv v_T/\sqrt{2}$ a Majorana mass term for neutrinos is generated at tree level, proportional to v_T :

$$-\frac{1}{2} \nu_{L\alpha}^T C^{-1} m_{\nu_{\alpha\beta}} \nu_{L\beta} + h.c. \quad \text{with} \quad m_{\nu_{\alpha\beta}} = \sqrt{2} v_T f_{\alpha\beta}. \quad (1.22)$$

Such a triplet arises naturally in many extensions of the Standard Model, for example in left-right symmetric models [33], or in Little Higgs theories [34, 35]. Assuming that all other mass parameters in the scalar potential are of the electroweak scale v_u , the minimization of the potential leads to the relation for the triplet VEV $v_T \sim \mu$, see e.g. [36]. In order to obtain small neutrino masses this VEV and/or the corresponding Yukawa couplings have to be very small.

If a very high energy scale $M \gg v_u$ is associated to the triplet, one obtains the well-known seesaw (type-II) relation $v_T \sim v_u^2/M$ as explanation for the smallness of neutrino masses [37, 38, 39].

We can also consider a different scenario where the triplet states have masses not too far from the electroweak scale, such that the components of the triplet can be produced at colliders [40, 41] or lead to sizable rates of LFV processes [42]. The hierarchy $\mu \ll v_u$ may find an explanation for example through extra dimensions [43].

In chapter 6 we consider this model for neutrino masses and we study what can be learnt from neutrinos if LHC discovers such a triplet.

1.3.3 The Fermion Triplet Model: type III seesaw

The type III seesaw model considers the addition of $SU(2)$ fermionic triplets to the SM:

$$\Sigma = \begin{pmatrix} \Sigma^0/\sqrt{2} & \Sigma^+ \\ \Sigma^- & -\Delta^0/\sqrt{2} \end{pmatrix}. \quad (1.23)$$

The fermion triplets have a gauge invariant mass term and couple to the lepton sector via a Yukawa interaction:

$$\mathcal{L} = -\frac{1}{2}\text{Tr}[\bar{\Sigma}M_{\Sigma}\Sigma^c] - \bar{l}_L Y_{\Sigma}^* \Sigma \tilde{H} + h.c. \quad (1.24)$$

Without loss of generality, one can work in the basis where M_{Σ} is diagonal and real. After spontaneous electroweak symmetry breaking, the yukawa coupling generates a Dirac mass term for neutral leptons, so that:

$$\mathcal{L} = -\frac{M_{\Sigma}}{2}\bar{\Sigma}^0\Sigma^{0c} - \frac{v_u Y_{\Sigma}}{2}\bar{\Sigma}^0\nu_L \quad (1.25)$$

As in the type I seesaw, at least two fermion triplets are needed in order to have two non-vanishing light neutrino masses. The effective Majorana light neutrino masses can be obtained in a analogous way as in the type I seesaw model:

$$m_{\nu} = Y_{\Sigma}M_{\Sigma}^{-1}Y_{\Sigma}^T v_u^2 \quad (1.26)$$

Within this model lepton flavor violating processes can occur at higher rates than in the usual type I seesaw [44]. Combinations of both type II and type III seesaws at energetic scales accesible to LHC have also been studied [45].

1.3.4 Radiative models

We refer here to the class of models where neutrino masses are generated at the loop level. In this case, the smallness of neutrino masses is achieved by loop and yukawa suppression.

One possibility is the Zee-Babu model [46]. In addition to the SM fields, the model contains a singly (h^+) and a doubly (k^{++}) charged complex singlets with hypercharges ± 1 and ± 2 respectively. They couple to the lepton sector via the yukawa couplings:

$$\mathcal{L} = -f_{\alpha\beta}l_{L\alpha}^T C^{-1}i\tau_2 l_{L\beta} h^+ - g_{\alpha\beta}e_{R\alpha}^{\overline{C}} e_{R\beta} k^{++} + h.c. , \quad (1.27)$$

where α and β are flavor indices, $l_{L\alpha}$ are the lepton doublets, $e_{R\alpha}$ are the charged lepton singlets, C is the charge conjugation matrix, and τ_2 is the Pauli matrix. $f_{\alpha\beta}$ is a complex antisymmetric yukawa matrix, and $g_{\alpha\beta}$ a complex symmetric yukawa matrix. The scalar potential of the model contains all the gauge invariant couplings involving the new scalars and the SM Higgs doublet, including the trilinear coupling $\sim \mu h^2 k$. Lepton number $L = -2$ is associated to both scalars, thus this trilinear coupling breaks lepton number explicitly.

Neutrino masses are generated at two loops, via the couplings in the lagrangian Eq. (1.27) and the trilinear coupling $\sim \mu$. The neutrino mass matrix is approximately given by [47]:

$$m_{\nu_{\alpha\beta}} = \frac{v_u^2 \mu}{48\pi^2 M^2} \tilde{I} [f Y g^{\dagger} Y^T f^T]_{\alpha\beta}, \quad (1.28)$$

where M is the mass scale of the scalars, \tilde{I} is a loop factor which depends on the mass of the scalars, and Y is the charged lepton yukawa matrix. It is important to note that, in the limit $\mu \rightarrow 0$, neutrino masses vanish and lepton number conservation is recovered.

Since neutrino masses are suppressed by 5 yukawa couplings, these new scalars can be relatively light. In fact they could be light enough to be produced at present colliders. Moreover, these scalars can mediate LFV processes such as $\mu \rightarrow e\gamma$ or $\mu \rightarrow eee$, leading to sizable rates measurable at future experiments. This recent analysis [47] shows the viability of the model and the possibility of confirming or rejecting it at the running experiments LHC and MEG.

Another possibility is the Zee model [48], in which a complex scalar singlet and a scalar doublet are added to the SM and neutrino masses are generated at one loop.

1.3.5 Supersymmetric models

Supersymmetric models with R-parity violation can lead to lepton number violation and generate neutrino masses. R-parity is a multiplicative symmetry defined as:

$$R_p = (-1)^R = (-1)^{3B+L+2S}, \quad (1.29)$$

where B denotes baryon number, L lepton number and S the spin of the particle. R-parity is conserved in the MSSM. However if one allows R-parity violating terms in the superpotential, one obtains a source of lepton number violation. For instance one could have a bilinear term that mixes neutrinos and neutralinos and violates lepton number in one unit. Thus, a non-vanishing Majorana mass for neutrinos can be obtained at tree level [49]. In general, radiative corrections may lead to new mass terms. Usually one expects the tree level mass to be of the order of the atmospheric mass splitting and loop corrections to generate the solar one. Therefore, one naturally obtains a hierarchical neutrino mass spectrum.

Chapter 2

Leptogenesis

2.1 Baryon asymmetry of the Universe

Our Universe is made of matter: protons, neutrons and electrons; the only evidence of antimatter are the antiprotons observed in cosmic rays, but the measured rate is consistent with secondary production of antiprotons in high energy collisions. There is a matter-antimatter asymmetry, baryon asymmetry of the Universe (BAU), and it is maximal. One can define the BAU as the difference between the number of baryons and antibaryons in the Universe per unit volume: $n_B - n_{\bar{B}}$. Since the Universe is expanding, this quantity is not constant during the history of the Universe. So, it turns out convenient to normalize this quantity to the photon number density or the entropy density of the Universe. The current experimental values of these two quantities are [50]:

$$\begin{aligned}\eta &\equiv \frac{n_B - n_{\bar{B}}}{n_\gamma} = (6.1 \pm 0.3) \times 10^{-10}, \\ Y_B &\equiv \frac{n_B - n_{\bar{B}}}{s} = (8.7 \pm 0.4) \times 10^{-11}\end{aligned}\tag{2.1}$$

The numerical value of the BAU can be inferred from two different observations: Big Bang Nucleosynthesis [51] data and Cosmic Microwave Background temperature anisotropies, measured recently by WMAP [52]. The fact that these two completely different measurements give compatible results is a success of modern cosmology. In this thesis we will use the WMAP measurement given above as reference value.

We do not think that the BAU was an initial condition of the Universe. Even if it were, we expect that during inflation any preexisting asymmetry was diluted, because of the accelerated expansion. This means that the BAU was dynamically generated at some point during the early Universe. This generation of the BAU is the mechanism known as Baryogenesis.

In 1964 [53], Sakharov showed that there are three necessary ingredients for Baryogenesis:

- First, if we assume that there is no preexisting asymmetry, it is clear that we need an interaction that violates baryon number.

- Second, we need C and CP violation. Otherwise, processes involving antibaryons would generate a baryon asymmetry exactly equal but opposite in sign, to the one generated by those involving baryons.
- Finally, we need out of equilibrium conditions. The equilibrium distribution of a particle depends only on its mass, and since the mass of a particle and its antiparticle is the same, we need the above interactions to occur out of equilibrium.

In the SM baryon (B) and lepton (L) number are violated at the quantum level, due to the triangle anomaly, with the combination B-L being conserved [54]. This leads to a kind of processes that violate baryon (and lepton) number, the so called sphaleron processes [55]. At zero temperature sphaleron interactions are extremely suppressed. But at higher temperatures, above the electroweak phase transition, they are in equilibrium and can occur at an observable rate. It is also well known that C and CP are symmetries violated in Nature. And out-of-equilibrium conditions can take place during the electroweak phase transition. Therefore, the SM contains all the necessary ingredients for Baryogenesis. However it turns out that the amount of CP violation is too small, and the phase transition is not strongly first order in SM to generate the right BAU. Therefore an extension of the SM is needed to explain the matter-antimatter asymmetry of the Universe.

In [56], Fukujita and Yanagida proposed an alternative mechanism to produce the BAU. Since sphaleron processes conserve the combination B-L, it is possible to generate an asymmetry in baryon number from one in lepton number. This scenario can take place in the context of the seesaw mechanism, where right-handed neutrinos, whose interactions violate lepton number, are added to the matter content of SM. The yukawa couplings of the right-handed neutrinos provide the necessary source of CP violation, and the out-of-equilibrium condition can be satisfied if the yukawa interaction rates are small compared to the expansion of the Universe. Then sphaleron processes can partially convert the leptonic asymmetry into baryonic asymmetry.

The above mechanism is known as Leptogenesis and has attracted physicist's attention during the last years because it connects two open questions in particle physics and cosmology: neutrino masses and the generation of the BAU. A recent and very useful review is [57].

2.2 Flavored Leptogenesis in the type I seesaw

In this section we try to outline the mechanism of thermal leptogenesis in the standard seesaw model.

The heavy right-handed neutrinos (N_i) violate lepton number in their decay into a lepton and a Higgs: $N_i \rightarrow l_\alpha H, \bar{l}_\alpha \bar{H}$. This decay rate is governed by the neutrino yukawa matrix, which in general is a complex matrix. Therefore CP violation is

expected. The N_1 decay rate is:

$$\Gamma_D = \sum_{\alpha} \Gamma_{\alpha} = \frac{[\lambda^{\dagger}\lambda]_{11} M_1}{8\pi} \quad (2.2)$$

The leading order of the CP asymmetry in these decays is computed [58] by evaluating the interference between the tree-level and one-loop diagrams contributing to the process. Here we show the asymmetry produced in the decay of N_1 into leptons of a given flavor:

$$\begin{aligned} \epsilon_{\alpha} &= \frac{\Gamma(N_1 \rightarrow \ell_{\alpha} H) - \Gamma(N_1 \rightarrow \bar{\ell}_{\alpha} \bar{H})}{\Gamma(N_1 \rightarrow \ell H) + \Gamma(N_1 \rightarrow \bar{\ell} \bar{H})} \\ &\simeq \frac{3M_1}{16\pi v_u^2 [\lambda^{\dagger}\lambda]_{11}} \text{Im} \{ [\lambda]_{\alpha 1} [m_{\nu}^{\dagger} \lambda]_{\alpha 1} \}, \end{aligned} \quad (2.3)$$

By making use of Eq. (1.10) in the above expression, one can demonstrate that at least two generations of right-handed neutrinos are needed to have a non-vanishing CP asymmetry. The asymmetry comes from phases in the yukawa couplings, thus in general it contains contributions from low energy phases (phases in the PMNS mixing matrix) and unmeasurable high energy phases. A correlation between the values of the low energy phases and successful leptogenesis can not be established in general. This question is the main issue of chapters 3 and 4.

Most of leptogenesis studies assume hierarchical singlet neutrinos and focus on the asymmetry generated by the lightest right-handed neutrino N_1 . The asymmetries generated by the heavier states $N_{2,3}$ tend to be diluted by $\Delta L = 2$ processes mediated by N_1 . Scenarios where the asymmetry generated by N_2 is not destroyed have been studied [59, 60, 61].

The general picture is as follows: at $T \gtrsim M_1$, the N_1 are thermally produced by scattering processes, $q_L t_R \rightarrow H \rightarrow \ell_{\alpha} N_1$ and $l_{\alpha} t_R \rightarrow H \rightarrow q_L N_1$, and inverse decays, $l_{\alpha} H \rightarrow N_1$. A lepton asymmetry is generated in the thermal plasma during N_1 production. At $T \sim M_1$, N_1 , CP violating decays generate an asymmetry which is opposite in sign to the former one. The existence of out-of-equilibrium wash-out processes, namely inverse decays and $\Delta L = 2$ scatterings, $l_{\alpha} H \rightarrow N_1 \rightarrow \bar{l}_{\alpha} \bar{H}$, prevent an exact cancellation between the two contributions. Once the out-of-equilibrium condition is achieved, the existing asymmetries in each flavor may survive.

Since the Universe is expanding, the out-of-equilibrium condition is fulfilled at temperatures at which the neutrino yukawa interactions are slow compared to the expansion rate of the Universe: $\Gamma_T < H|_T$, where:

$$H = 1.66 g_*^{1/2} \frac{T^2}{m_{Pl}}, \quad (2.4)$$

$g_* = 106.75$ for SM, it represents the number of degrees of freedom in the thermal plasma, and $m_{Pl} = 1.22 \times 10^{19}$ GeV is the Planck Mass. For $T < M_1/100$ all the interactions are frozen and the existing asymmetry remains constant until sphalerons partially convert it into a baryon asymmetry.

The realization of the out-of-equilibrium dynamics depends on the region of the parameter space under consideration. It is convenient to define the following quantities, which represent respectively the singlet neutrino decay rate Γ_D and the expansion rate of the Universe H at temperature $T = M_1$, and are of the order of the light neutrino mass scale:

$$\tilde{m} \equiv \sum_{\alpha} \tilde{m}_{\alpha\alpha} = 8\pi \frac{v_u^2}{M_1^2} \Gamma_D = \frac{[\lambda^\dagger \lambda]_{11}}{M_1} v_u^2 \quad (2.5)$$

$$\tilde{m}_{\alpha\alpha} = \frac{|\lambda_{\alpha 1}|^2}{M_1} v_u^2 \quad (2.6)$$

$$m_* \equiv 8\pi \frac{v_u^2}{M_1^2} H|_{T=M_1} \quad (2.7)$$

The parameter $K \equiv \tilde{m}/m_* = \Gamma_D/H(T = M_1)$ can be used to define the type of wash-out regime. We first discuss the strong wash-out regime, where $K > 1$. In this case, at $T \sim M_1$ neutrino interactions are already in equilibrium. This means that at higher temperatures $T > M_1$ the singlet neutrinos N_1 were thermally produced, and at $T \sim M_1$ their distribution has reached the equilibrium abundance. Therefore the existing lepton asymmetry at that time is null. Then the N_1 populating the hot plasma start to decay generating a lepton asymmetry. Inverse decays wash-out the produced asymmetry while they are fast enough. Once inverse decays are out-of-equilibrium, at temperatures for which $\Gamma_{ID}(T) < H(T)$, this cancellation stops and an asymmetry survives.

In the weak wash-out regime: $K < 1$. In this case, at temperatures $T \sim M_1$, the N_1 have not reached their equilibrium density. Hence the asymmetry produced during thermal production of N_1 does not vanish. As the temperature goes down, N_1 start to decay producing an asymmetry opposite in sign to the one produced during thermalization. Thanks to the out-of-equilibrium inverse decays, an exact cancellation is avoided.

It was a common thing in Leptogenesis calculations to work in the one-flavor approximation by summing over all three flavors. However it has been recently shown [62, 63, 64] that flavors can play a role in Leptogenesis. If a flavor is distinguishable in the thermal bath, then the corresponding lepton asymmetry follows an independent evolution, because the asymmetry generated in a given flavor α can only be washed-out by leptons of that flavor l_α . This occurs when the charged lepton yukawa Y_α interaction rate $\Gamma_\alpha \simeq 5 \times 10^{-3} Y_\alpha^2 T$ is in equilibrium, faster than the expansion rate H and the N_1 inverse decay rate.

At temperatures $T > 10^{12}$ GeV all flavors are out-of-equilibrium, and the single flavor approximation is valid. In the temperature range $10^9 < T < 10^{12}$ GeV τ s are in equilibrium. Therefore the out-of-equilibrium N_1 decays generate an asymmetry in flavor τ and in flavor o , where l_o defines the flavor combination orthogonal to τ into which N_1 decays: $\hat{\ell}_o = (\lambda_{\mu 1} \hat{\mu} + \lambda_{e 1} \hat{e}) / (\sqrt{|\lambda_{\mu 1}|^2 + |\lambda_{e 1}|^2})$. The asymmetries stored in these two flavors evolve independently.

The inclusion of flavor in Leptogenesis affects the wash-out processes. For instance, it might be possible that we are in a strong wash-out scenario for all flavors except one, for which the yukawas are small. This situation can lead to an enhancement of the surviving lepton asymmetry.

2.2.1 Boltzmann Equations

In order to track the lepton asymmetry in each flavor along the history of the Universe, one should solve the set of Boltzmann equations that describe the out-of-equilibrium dynamics for the kinetic distributions of all the particles involved [65]. The Boltzmann equation for a given species X is:

$$\frac{\partial f_X}{\partial t} - Hp \frac{\partial f_X}{\partial p} = -\frac{1}{2E} C[f_X], \quad (2.8)$$

where f_X is the momentum distribution of the particle X , t is the time, p and E are the momentum and energy of the particle, H is the Hubble parameter, and the collision integral is given by:

$$\begin{aligned} C[f_X] &= \sum_{j,l,m} \Lambda_{lm\dots}^{j\dots} [f_l f_m \dots (1 \pm f_X)(1 \pm f_j) \dots W(lm \dots \rightarrow Xj \dots) - \\ &\quad - f_X f_j \dots (1 \pm f_l)(1 \pm f_m) \dots W(Xj \dots \rightarrow lm \dots)] \end{aligned}$$

where $(1 \pm f)$ are the Bose enhancement and Pauli blocking factors,

$$\Lambda_{lm\dots}^{j\dots} = \int \frac{d^3 p_j}{(2\pi)^3 2E_j} \dots \int \frac{d^3 p_l}{(2\pi)^3 2E_l} \int \frac{d^3 p_m}{(2\pi)^3 2E_m} \dots,$$

and $W(Xj \dots \rightarrow lm \dots)$ is the squared transition amplitude in which particle X is involved, summed over initial and final spins.

The number density is:

$$n_X = g_X \int \frac{d^3 p}{(2\pi)^3} f_X(\vec{p}), \quad (2.9)$$

where g_X is the number of internal degrees of freedom. If we integrate Eq. (2.8) over the momentum of the X particle, we obtain:

$$\begin{aligned} \frac{dn_X}{dt} + 3Hn_X &= \sum_{j,l,m} \Lambda_{lm\dots}^{Xj\dots} [f_l f_m \dots (1 \pm f_X)(1 \pm f_j) \dots W(lm \dots \rightarrow Xj \dots) - \\ &\quad - f_X f_j \dots (1 \pm f_l)(1 \pm f_m) \dots W(Xj \dots \rightarrow lm \dots)]. \end{aligned} \quad (2.10)$$

In the case of Leptogenesis the key processes that need to be taken into account are the decays, inverse decays and $\Delta L = 2$ scatterings mediated by N_1 . Here we show the so called integrated Boltzmann equations for the the right-handed neutrino $Y_{N_1} = n_{N_1}/s$, and the asymmetries in different flavors $Y_{\mathcal{L}_\alpha} \equiv Y_{l_\alpha} - Y_{\bar{l}_\alpha} = (n_{l_\alpha} - n_{\bar{l}_\alpha})/s$

normalized to the entropy density s , under the following assumptions: thermal equilibrium for the Higgs, and kinetic equilibrium for leptons. We also neglect Bose enhancement and Pauli blocking factors, and only terms which are quadratic in the neutrino yukawa couplings are considered, which is a good approximation as long as all the neutrino yukawa couplings are small:

$$\frac{dY_{N_1}}{dz} = -Kz(Y_{N_1} - Y_{N_1}^{eq})\frac{K_1(z)}{K_2(z)}, \quad (2.11)$$

$$\frac{dY_{\mathcal{L}_\alpha}}{dz} = \epsilon_\alpha Kz(Y_{N_1} - Y_{N_1}^{eq})\frac{K_1(z)}{K_2(z)} - \frac{z^3}{4}K_\alpha K_1(z)Y_{\mathcal{L}_\alpha}, \quad (2.12)$$

where the dimensionless parameter z is defined as $z = M_1/T$, $K_i(z)$ are the modified Bessel functions of the second kind of order i , and the decay parameter $K = \sum_\alpha K_\alpha$, $K_\alpha = \Gamma_\alpha/H(T = M_1)$ is the parameter that describes the type of wash-out regime, as we discussed in the previous section.

It is clear from the Boltzmann equations in Eq. (2.11) that the three Sakharov conditions are satisfied. Lepton number is violated by N_1 interactions. If singlet neutrinos were always in equilibrium, no asymmetry would be generated. And if the CP asymmetry vanishes, so does the lepton asymmetry.

An analytical solution for Eqs. (2.11) can be obtained [66, 64]. Using those approximated solutions, the final baryon asymmetry can be parametrized as:

$$Y_B \simeq C Y_{N_1}^{eq} \sum_\alpha \epsilon_\alpha \eta_\alpha, \quad (2.13)$$

where C is the fraction of lepton asymmetry converted into baryon asymmetry by sphalerons [67]. The SM value is $C = 12/37$. The equilibrium distribution for the singlet neutrinos is given by:

$$Y_{N_1}^{eq} = \frac{n_{N_1}^{eq}}{s} = \frac{135\xi(3)}{4\pi^4 g_*}, \quad (2.14)$$

the CP asymmetry for the type I seesaw was given in Eq. (2.3), and η_α is the efficiency factor which depends on the type of wash-out regime, and whose approximate value can be written in terms of the parameters m_* and $\tilde{m}_{\alpha\alpha}$ [57]:

$$\begin{aligned} \eta_\alpha &\sim \frac{m_*}{\tilde{m}_{\alpha\alpha}} && \text{strong } (\tilde{m} > m_*, \tilde{m}_{\alpha\alpha} > m_*) \\ \eta_\alpha &\sim \frac{\tilde{m}_{\alpha\alpha}}{m_*} && \text{intermediate } (\tilde{m} > m_*, \tilde{m}_{\alpha\alpha} < m_*) \\ \eta_\alpha &\sim \frac{\tilde{m}_{\alpha\alpha}\tilde{m}}{m_*^2} && \text{weak } (\tilde{m} < m_*, \tilde{m}_{\alpha\alpha} < m_*) \end{aligned} \quad (2.15)$$

Most studies of leptogenesis use the integrated Boltzmann equations Eq. (2.11) to follow the evolution of the heavy particle number density and the lepton asymmetry. This approach, as we have mentioned, assumes Maxwell-Boltzmann statistics,

as well as kinetic equilibrium for all particles, including the heavy species. This assumption is normally justified in freeze-out calculations, where elastic scattering is assumed to be much faster than inelastic reactions. However in the present context, kinetic equilibrium in the heavy species would have to be maintained by the decays and inverse decays alone, and it is not obvious that the integrated Boltzmann equation is always a good approximation. In general, $1 \leftrightarrow 2$ processes are inefficient for thermalization compared to $2 \leftrightarrow 2$ processes, and in some parameter ranges there can be large deviations from kinetic equilibrium. In [68], the impact of this difference on the lepton asymmetry produced during Leptogenesis has been studied, and it was found that in the strong washout regime the final asymmetry is changed by 15 – 30% when the full Boltzmann equation is used.

2.2.2 Lower bound on M_1

In [69] it was shown that a model independent upper bound on the CP asymmetry in Eq. (2.3) exists, for a seesaw model with hierarchical right-handed neutrinos.

This analysis shows that the CP asymmetry and the lightest right-handed neutrino mass are not independent parameters. If one adds the requirement of successful leptogenesis to the picture, a lower bound on the lightest right-handed neutrino mass can be obtained. In the case of interest for us, thermal production of the singlet neutrinos, this lower bound is $M_1 \gtrsim 10^9$ GeV. A thermal production of N_1 requires a reheating temperature of the order of M_1 .

If supersymmetry is considered, this bound could be in trouble with the upper bound on the reheating temperature that prevents the overproduction of gravitinos. This is the so called gravitino problem, which we will comment in the next section.

2.2.3 Supersymmetric Leptogenesis

In this section we present the new features of the Leptogenesis mechanism in a supersymmetric model. We concentrate in the MSSM with three hierarchical right-handed neutrinos and sneutrinos.

Once supersymmetry is included into the picture, also the sneutrinos can contribute to produce the lepton asymmetry, which will be later reprocessed by sphalerons into a baryon asymmetry:

$$\begin{aligned} N_1 &\rightarrow l_\alpha H, \bar{l}_\alpha \bar{H}, \tilde{l}_\alpha h, \tilde{l}_\alpha^\dagger h^\dagger \\ \tilde{N}_1 &\rightarrow \tilde{l}_\alpha H, \bar{l}_\alpha \bar{h} \\ \tilde{N}_1^\dagger &\rightarrow \tilde{l}_\alpha^\dagger H^\dagger, l_\alpha h \end{aligned}$$

Neglecting soft supersymmetry breaking terms, the decay rates and the CP asymmetries in these decays are equal for neutrinos and sneutrinos. The numerical value of the CP asymmetry ϵ_α doubles the SM value, Eq. (2.3). Since the number of decay channels doubles, the decay rate also doubles the SM value:

$$\Gamma_D = \sum_\alpha \Gamma_\alpha = \frac{[\lambda^\dagger \lambda]_{11}}{4\pi} M_1, \quad (2.16)$$

where Γ_α verifies: $\Gamma_\alpha = \Gamma_\alpha^f = \Gamma_\alpha^s = \tilde{\Gamma}_\alpha^f/2 = \tilde{\Gamma}_\alpha^s/2$, with $\Gamma_\alpha^{f(s)}$ the decay of N_1 into leptons or sleptons, and $\tilde{\Gamma}_\alpha^{f(s)}$ the decay of \tilde{N}_1 and \tilde{N}_1^\dagger into fermions or scalars.

It is straight-forward to see how the integrated Boltzmann equations are modified in the supersymmetric case. The Boltzmann equations for the neutrino and sneutrino distributions, and the total lepton number asymmetry are:

$$\frac{dY_{N_1}}{dz} = -Kz(Y_{N_1} - Y_{N_1}^{eq})\frac{K_1(z)}{K_2(z)}, \quad (2.17)$$

$$\frac{d(Y_{\tilde{N}_1} + Y_{\tilde{N}_1^\dagger})}{dz} = -Kz(Y_{\tilde{N}_1} - Y_{\tilde{N}_1}^{eq})\frac{K_1(z)}{K_2(z)} - Kz(Y_{\tilde{N}_1^\dagger} - Y_{\tilde{N}_1^\dagger}^{eq})\frac{K_1(z)}{K_2(z)}, \quad (2.18)$$

$$\begin{aligned} \frac{d(Y_{\mathcal{L}_\alpha} + Y_{\tilde{\mathcal{L}}_\alpha})}{dz} &= \epsilon_\alpha Kz(Y_{N_1} - Y_{N_1}^{eq})\frac{K_1(z)}{K_2(z)} - \frac{z^3}{4}K_\alpha K_1(z)(Y_{\mathcal{L}_\alpha} + Y_{\tilde{\mathcal{L}}_\alpha}) + \\ &+ \epsilon_\alpha Kz(Y_{\tilde{N}_1} - Y_{\tilde{N}_1}^{eq})\frac{K_1(z)}{K_2(z)} - \frac{z^3}{4}K_\alpha K_1(z)(Y_{\mathcal{L}_\alpha} + Y_{\tilde{\mathcal{L}}_\alpha}) + \\ &+ \epsilon_\alpha Kz(Y_{\tilde{N}_1^\dagger} - Y_{\tilde{N}_1^\dagger}^{eq})\frac{K_1(z)}{K_2(z)} - \frac{z^3}{4}K_\alpha K_1(z)(Y_{\mathcal{L}_\alpha} + Y_{\tilde{\mathcal{L}}_\alpha}), \end{aligned} \quad (2.19)$$

where $Y_{\mathcal{L}_\alpha} = Y_{L_\alpha} - Y_{\tilde{L}_\alpha}$ and $Y_{\tilde{\mathcal{L}}_\alpha} = Y_{\tilde{L}_\alpha} - Y_{\tilde{L}_\alpha^\dagger}$ are the lepton number asymmetries stored in leptons and sleptons, respectively, and $K = \sum_\alpha K_\alpha$, $K_\alpha = \Gamma_\alpha/H(T = M_1)$ with Γ_α defined in Eq. (2.16).

Since the form of the equation is the same as in the non supersymmetric case, the approximate solution given in Eq. (2.13) stands:

$$Y_B \simeq C (Y_{N_1} + Y_{\tilde{N}_1} + Y_{\tilde{N}_1^\dagger}) \sum_\alpha \epsilon_\alpha \eta_\alpha, \quad (2.20)$$

in the MSSM $C=10/31$, the neutrino equilibrium distribution was given in Eq. (2.14) and the sneutrino one is $4/3 Y_{N_1}$. The efficiency factors have the same functional form as in the SM, Eq. (2.15), with $\tilde{m}_{\alpha\alpha}$ and m_* defined as:

$$\tilde{m} = \sum_\alpha \tilde{m}_{\alpha\alpha} = \sum_\alpha \frac{|\lambda_{\alpha 1}|^2}{M_1} v_u^2, \quad (2.21)$$

$$m_* = \frac{4\pi v_u^2 H(T = M_1)}{M_1^2}, \quad (2.22)$$

where $H = 1.66g_*^{1/2}T^2/m_{Pl}$, and the number of degrees of freedom in MSSM is $g_* = 228.75$. Note that the value of m_* in the MSSM is about a factor $\sqrt{2}$ smaller than the SM value. The final numerical value for the generated baryon asymmetry is approximately a factor $\sqrt{2}$ larger than the SM one, in the limit of strong wash-out for all flavors.

Concerning flavor effects, some comments are in order. Since in the MSSM charged lepton yukawas are larger than in SM: $Y_\alpha = m_\alpha/(\cos\beta \times 174\text{GeV})$, they come into equilibrium earlier. At very high temperatures $T > \tan^2\beta 10^{12} \text{ GeV}$ ¹,

¹We approximate $\tan\beta \simeq 1/\cos\beta$ because $\sin\beta \sim 1$ and $\tan\beta$ is a more familiar parameter.

the charged lepton yukawa interactions are out of equilibrium ($\Gamma_{\ell_\alpha} \ll H$) and there are no flavor effects, so leptogenesis can be studied in one-flavor case. However, as the temperature drops, the τ interactions come into equilibrium. In the range $\tan^2 \beta 10^9 \lesssim T \lesssim \tan^2 \beta 10^{12}$ GeV, we have an intermediate two-flavor regime, so that the lepton asymmetry produced in the τ evolves separately from the lepton asymmetry created in the linear combination: $\hat{\ell}_o = (\lambda_{\mu 1} \hat{\mu} + \lambda_{e 1} \hat{e}) / (\sqrt{|\lambda_{\mu 1}|^2 + |\lambda_{e 1}|^2})$. For $T \lesssim \tan^2 \beta 10^9$ GeV, also the μ Yukawa interactions come into chemical equilibrium and all the three flavors become distinguishable.

Finally, let us say a few words about the gravitino problem [70]. In the early Universe gravitinos can be copiously produced and their late decay can jeopardize successful nucleosynthesis. In order to avoid the overproduction of gravitinos, an upper bound on the reheat temperature T_{RH} exists. Since Leptogenesis takes place at temperatures $T \sim M_1$, this bound can be translated into an upper bound on the singlet neutrino mass, $M_1 \lesssim 5 T_{RH}$. It can exist some tension between this upper bound on M_1 and the upper bound coming from the requirement of successful Leptogenesis, $M_1 > 10^9$ GeV.

There are various ways to obtain $T_{RH} \sim 10^9 - 10^{10}$ GeV. If the gravitino is unstable, the nucleosynthesis bound leads to very stringent upper bounds on the reheating temperature after inflation [71]: $T_{RH} \lesssim 10^4 - 10^5$ GeV for $m_{3/2} \lesssim 10$ TeV, or $T_{RH} \lesssim 10^9 - 10^{10}$ GeV for $m_{3/2} > 10$ TeV. A sufficiently high reheat temperature is obtained for very heavy gravitinos because they decay before BBN. Alternatively, if the gravitino is the stable LSP, a correct dark matter relic density can be obtained for $T_{RH} \sim 10^9 - 10^{10}$ GeV. In this scenario, one must ensure that the decay of the NLSP does not perturb BBN. This can be obtained, for instance by choosing the NLSP with care [72] or by having it decay before BBN via R -parity violating interactions [73].

2.3 Soft Leptogenesis

It is well known that Supersymmetry must be broken if it exists. It has been shown recently [74, 75, 76] that Leptogenesis can be successful if we consider the soft supersymmetry breaking parameters as the source of lepton number and CP violation.

Soft supersymmetry breaking terms involving the singlet sneutrinos remove the mass degeneracy between the two real sneutrino states of a single neutrino generation, and provide new sources of lepton number and CP violation. As a consequence, the mixing between the two sneutrino states generates a CP asymmetry in the decay, which can be sizable for a certain range of parameters. The lower bound on M_1 does not apply in this new mechanism for leptogenesis, and in fact it has been shown that the asymmetry is large enough for a right-handed neutrino mass scale relatively low, in the range $10^5 - 10^8$ GeV. This value for the right-handed neutrino mass is well below the reheat temperature limits, what solves the cosmological gravitino problem.

Moreover, contrary to the traditional leptogenesis scenario, where at least two generations of right-handed neutrinos are required to generate a CP asymmetry in neutrino/sneutrino decays, in this new mechanism for leptogenesis the CP asymmetry in sneutrino decays is present even if a single generation is considered.

In chapter 5 we analyze this mechanism in the context of the inverse seesaw model.

Chapter 3

Insensitivity of Leptogenesis with Flavor effects to Low Energy Leptonic CP Violation

3.1 Introduction

CP violation is required to produce the puzzling excess of matter over anti-matter observed in the Universe [53]. If this Baryon Asymmetry of the Universe (BAU) was made via leptogenesis [56, 77, 66], then CP violation in the lepton sector is needed. The required CP violation is encoded in the CP violating phases of the lepton sector. Three of them are the well known Dirac and Majorana phases of the PMNS mixing matrix, that are in principle measurable. So any observation thereof, for instance in neutrino oscillations, would support leptogenesis by demonstrating that CP is not a symmetry of the leptons. It is interesting to explore whether a stronger statement can be made about this tantalizing link between low-energy observable CP violation and the BAU.

In the paper [1], we address a phenomenological question: “is the baryon asymmetry *sensitive* to the phases of the lepton mixing matrix (PMNS matrix)?”. Electroweak precision data was said to be sensitive to the top mass, meaning that a preferred range for m_t could be extracted from the data. Here, we wish to ask a similar question, assuming the baryon asymmetry is generated, via leptogenesis, from the decay of the lightest right-handed (RH) neutrino: given the measured value of the baryon asymmetry, can an allowed range for the PMNS phases be obtained?

It was shown in [78] that the BAU produced by thermal leptogenesis in the type I seesaw, without flavor effects, is insensitive to PMNS phases. That is, the PMNS phases can be zero while leptogenesis works, and the CP asymmetry of leptogenesis can vanish for arbitrary values of the PMNS phases. In fact, the “unflavored” asymmetry is controlled by phases from the RH sector only, and it would vanish were this sector CP conserving. However, it was recently realized that lepton flavor matters in leptogenesis [62, 63, 64]: in the relevant temperature range $10^9 \rightarrow 10^{12}$ GeV, the final baryon asymmetry depends separately on the lepton asymmetry in

τ s, and on the lepton asymmetry in muons and electrons. So in our work, we revisit the question addressed in [78], but with the inclusion of flavor effects.

The question we address, and the answer we find, differ from recent discussions [79, 80, 81, 82, 83, 84, 85] in that we wish to do a bottom-up analysis of the three generation seesaw. Ideally, we wish to express the baryon asymmetry in terms of observables, such as the light neutrino masses and PMNS matrix, and free parameters. Then, by inspection, one could determine whether fixing the baryon asymmetry constrained the PMNS phases.

3.2 Notation and review

We consider a seesaw model [17], where three heavy ($M \gtrsim 10^9$ GeV) Majorana neutrinos N_i are added to the Standard Model, as described in section 1.2:

$$\mathcal{L} = -Y_{e\alpha} \bar{\ell}_{L\alpha} H e_{R\alpha} - \lambda_{\alpha i} \bar{\ell}_{L\alpha} \tilde{H} N_i - \frac{D_{M_i}}{2} \bar{N}_i N_i^c + \dots + h.c., \quad (3.1)$$

where α is a flavor index, and the order on the Yukawa matrices Y_e, λ is left-right. We work in the basis where the charged lepton yukawa matrix and the Majorana mass matrix for right-handed neutrinos are diagonal and real.

There are 6 phases among the 21 parameters of this Lagrangian. We can work in the mass eigenstate basis of the charged leptons and the N_i , and write the neutrino Yukawa matrix as:

$$\lambda = V_L^\dagger D_\lambda V_R, \quad (3.2)$$

where D_λ is real and diagonal, and V_L, V_R are unitary matrices, each containing three phases. So at the high scale, one can distinguish CP violation in the left-handed doublet sector (phases that appear in V_L) and in the right-handed singlet sector (phases in V_R). Leptogenesis can work when there are phases in either or both sectors.

As we described in section 1.2, at energies accessible to experiment, well below the N_i mass scale, the light left-handed neutrinos acquire an effective Majorana mass matrix Eqs. (1.3, 1.10):

$$m_\nu = \lambda M^{-1} \lambda^T v_u^2 = U D_m U^T, \quad (3.3)$$

where $v_u = 174$ GeV is the Higgs vev, D_m is diagonal with real eigenvalues, and U is the PMNS matrix. There are nine parameters in m_ν , which is “in principle” experimentally accessible. Two mass differences and two angles of U are measured, leaving the mass scale, one angle and three phases of U unknown.

From the above we can write:

$$D_m = U^\dagger V_L^\dagger D_\lambda V_R D_M^{-1} V_R^T D_\lambda V_L^* U^* v_u^2, \quad (3.4)$$

so we see that the PMNS matrix will generically have phases if V_L and/or V_R are complex. Like leptogenesis, it receives contributions from CP violation in the LH

and RH sectors. Thus it seems “probable”, or even “natural”, that there is some relation between the CP violation of leptogenesis and of the PMNS matrix. However, the notion of relation or dependence is nebulous [21], so we address the more clear and simple question of whether the baryon asymmetry is *sensitive* to PMNS phases. By this we mean: if the total baryon asymmetry is fixed, and we assume to know all the neutrino masses and mixing angles, can we predict ranges for the PMNS phases?

We suppose that the baryon asymmetry is made via leptogenesis, in the decay of the lightest singlet neutrino N_1 , with $M_1 \sim 10^{10}$ GeV. Flavor effects are relevant in this temperature range [62, 63, 64]¹. N_1 decays to leptons ℓ_α , an amount ϵ_α more than to anti-leptons $\bar{\ell}_\alpha$, and this lepton asymmetry is transformed to a baryon asymmetry by SM processes (sphalerons). We will further suppose that the partial decay rates of N_1 to each flavor are faster than the expansion rate of the Universe H . This implies that N_1 decays are close to equilibrium, and there is a significant washout of the lepton asymmetry due to N_1 interactions (strong washout regime); we discuss later why this assumption does not affect our conclusions.

Flavor effects are relevant in leptogenesis [62, 63, 64] because the final asymmetry cares which leptons ℓ are distinguishable. N_1 interacts only via its Yukawa coupling, which controls its production and destruction. The washout of the asymmetry, by decays, inverse decays and scatterings of N_1 , is therefore crucial for leptogenesis to work, because otherwise the opposite sign asymmetry generated at early times during N_1 production would cancel the asymmetry produced as they disappear. To obtain the washout rates (for instance, for $\ell + H \rightarrow N_1$), one must know the initial state particles, that is, which leptons are distinguishable.

At $T \sim M_1$, when the asymmetry is generated, SM interactions can be categorized as much faster than H , of order H , or much slower. Interactions that are slower than H can be neglected. H^{-1} is the age of the Universe and the timescale of leptogenesis, so the faster interactions should be resummed— for instance into thermal masses. In the temperature range $10^9 \lesssim T \lesssim 10^{12}$ GeV, interactions of the τ Yukawa are faster than H , so the ℓ_τ doublet is distinguishable (has a different “thermal mass”) from the other two lepton doublets. The decay of N_1 therefore produces asymmetries in $B/3 - L_\tau$, and in $B/3 - L_o$, where ℓ^o (“other”) is the projection in ℓ^e and ℓ^μ space, of the direction into which N_1 decays [87]:

$$\hat{\ell}_o = \frac{\lambda_{\mu 1} \hat{\mu} + \lambda_{e 1} \hat{e}}{\sqrt{|\lambda_{\mu 1}|^2 + |\lambda_{e 1}|^2}}. \quad (3.5)$$

Following [64], we approximate these asymmetries to evolve independently. In this case, the baryon to entropy ratio can be written as the sum over flavor of the flavored CP asymmetries ϵ_α times a flavor-dependent washout parameter $\eta_\alpha < 1$ which is obtained by solving the relevant flavored Boltzmann equations [62, 63, 64]:

$$Y_B \simeq \frac{12}{37} \frac{1}{3g_*} (\epsilon_\tau \eta_\tau + \epsilon_o \eta_o), \quad (3.6)$$

¹provided the decay rate of N_1 is slower than the interactions of the τ Yukawa [86]

where $g_* = 106.75$ counts entropy, and the $12/37$ is the fraction of a $B-L$ asymmetry which, in the presence of sphalerons, is stored in baryons.

In the limit of hierarchical RH neutrinos, the CP asymmetry in the decay $N_1 \rightarrow \ell_\alpha H$ can be written as:

$$\epsilon_\alpha \simeq -\frac{3M_1}{16\pi v^2[\lambda^\dagger\lambda]_{11}}\text{Im}\{[\lambda]_{\alpha 1}[m_\nu^\dagger\lambda]_{\alpha 1}\}, \quad (3.7)$$

where m_ν is defined in Eq. (3.3).

In the case of strong washout for all flavors, which corresponds to $\Gamma(N_1 \rightarrow \ell_\alpha H) > H_{(T=M_1)}$ for $\alpha = \tau, o$, the washout factor is approximately [64, 88]:

$$\eta_\alpha \simeq 1.3 \left(\frac{m_*}{6A_{\alpha\alpha}\tilde{m}_{\alpha\alpha}} \right)^{1.16} \rightarrow \frac{m_*}{5A_{\alpha\alpha}\tilde{m}_{\alpha\alpha}}, \quad (3.8)$$

where there is no sum on α , $m_* \simeq 10^{-3}$ eV, and $A_{\tau\tau} \simeq A_{oo} \sim 2/3$ [87, 64]². The (rescaled) N_1 decay rate is:

$$\tilde{m} = \sum_\alpha \tilde{m}_{\alpha\alpha} = \sum_\alpha \frac{|\lambda_{\alpha 1}|^2}{M_1} v^2. \quad (3.9)$$

3.3 Baryon Asymmetry

Combining Eqs. (3.6,3.7,3.8), we obtain:

$$Y_B \propto \epsilon_\tau/\tilde{m}_{\tau\tau} + \epsilon_o/\tilde{m}_{oo}, \quad (3.10)$$

where α is not summed,

$$\frac{\epsilon_\alpha}{\tilde{m}_{\alpha\alpha}} = -\frac{3M_1}{16\pi v^2\tilde{m}} \sum_\beta \text{Im}\{\hat{\lambda}_\alpha m_{\nu_{\alpha\beta}}^\dagger \hat{\lambda}_\beta\} \frac{|\lambda_\beta|}{|\lambda_\alpha|}, \quad (3.11)$$

and the Yukawa couplings of N_1 have been written as a phase factor times a magnitude : $\hat{\lambda}_\alpha|\lambda_\alpha| = \lambda_{\alpha 1}$. So the baryon asymmetry can be approximated as:

$$Y_B \simeq Y_B^{bd} \left(\frac{\text{Im}\{\hat{\lambda}_\tau \cdot m_\nu^\dagger \cdot \hat{\lambda}_\tau\}}{\sqrt{\Delta m_{\text{atm}}^2}} + \frac{\text{Im}\{\hat{\lambda}_o \cdot m_\nu^\dagger \cdot \hat{\lambda}_o\}}{\sqrt{\Delta m_{\text{atm}}^2}} + \frac{\text{Im}\{\hat{\lambda}_\tau \cdot m_\nu^\dagger \cdot \hat{\lambda}_o\}}{\sqrt{\Delta m_{\text{atm}}^2}} \left[\frac{|\lambda_o|}{|\lambda_\tau|} + \frac{|\lambda_\tau|}{|\lambda_o|} \right] \right) \frac{1}{A_{\tau\tau}}. \quad (3.12)$$

The prefactor of the parentheses:

$$Y_B^{bd} = -\frac{12}{37} \frac{M_1 \sqrt{\Delta m_{\text{atm}}^2}}{16\pi v^2} \frac{m_*}{5g_*\tilde{m}}, \quad (3.13)$$

²The A matrix parametrizes the redistribution of asymmetries in chemical equilibrium.

is the upper bound on the baryon asymmetry, that would be obtained in the strong washout case by neglecting flavor effects. Recall that this equation is only valid in strong washout for all flavors.

This equation reproduces the observation [64], that: (i) for equal asymmetries and equal decay rates of all distinguishable flavors, flavor effects increase the upper bound on the baryon asymmetry by $\sum_a A_{aa}^{-1} \sim 3$. (ii) More interestingly, having stronger washout in one flavor, can increase the baryon asymmetry (via the term in brackets). So models in which the Yukawa coupling $\lambda_{\tau 1}$ is significantly different from $\lambda_{\mu 1}, \lambda_{e 1}$, can have an enhanced baryon asymmetry (with cooperation from the phases).

Finally, this equation is attractive step towards writing the baryon asymmetry as a real function of real parameters (Y_B^{bd} , depending on M_1 and \tilde{m}_1), times a phase factor [89]. In this case, the phase factor is a sum of three terms, depending on the phases of the N_1 Yukawa couplings, light neutrino mass matrix elements normalized by the heaviest mass, and a (real) ratio of Yukawas.

3.4 CP violation

In this section, we would like to use Eq. (3.12) to show that the baryon asymmetry is insensitive to the PMNS phases. The parameters of the lepton sector can be divided into “measurables”, which are the neutrino and charged lepton masses, and the three angles and three phases of the PMNS matrix U . The remaining 9 parameters are unmeasurable. We want to show that for any value of the PMNS phases, there is at least one point in the parameter space of the unmeasurables where a large enough baryon asymmetry is obtained. The approximations leading to Eq. (3.12) are only valid in a subset of the unmeasurable parameter space, but if we can find points in this subspace, we are done. We first show analytically that such points exist, then we do a parameter space scan to confirm that leptogenesis can work for any value of the PMNS phases.

If the phases of the $\lambda_{\alpha 1}$ were independent of the PMNS phases, and a big enough Y_B could be obtained for some value of the PMNS phases, then our claim is true by inspection: for any other values, the phases of the $\lambda_{\alpha 1}$ could be chosen to reproduce the same Y_B . However, there is in general some relation between the phases of m_ν and those of $\lambda_{\alpha 1}$, so we proceed by looking for an area of parameter space where the phases of the $\lambda_{\alpha 1}$ can be freely varied without affecting the “measurables”. Then we check that a large enough baryon asymmetry can be obtained.

Such an area of parameter space can be found using the R matrix parametrization of Casas-Ibarra [22], where the complex orthogonal matrix R is defined such that $\lambda v_u \equiv U D_m^{1/2} R D_M^{1/2}$. Taking a simple R of the form:

$$R = \begin{bmatrix} \cos \phi & 0 & -\sin \phi \\ 0 & 1 & 0 \\ \sin \phi & 0 & \cos \phi \end{bmatrix}, \quad (3.14)$$

and using the standard parametrization of U (see section 1.1.1 and Eq. (1.2), $U = V \text{diag}(e^{i\alpha_1/2}, e^{i\alpha_2/2}, e^{i\alpha_3/2})$), gives:

$$\frac{\lambda_{\tau 1} v}{\sqrt{M_1 m_3}} = U_{\tau 1} \sqrt{\frac{m_1}{m_3}} \cos \phi + U_{\tau 3} \sin \phi \simeq \frac{\sin \phi}{\sqrt{2}}, \quad (3.15)$$

$$\frac{\lambda_{\mu 1} v}{\sqrt{M_1 m_3}} = U_{\mu 1} \sqrt{\frac{m_1}{m_3}} \cos \phi + U_{\mu 3} \sin \phi \simeq \frac{\sin \phi}{\sqrt{2}}, \quad (3.16)$$

$$\frac{\lambda_{e 1} v}{\sqrt{M_1 m_3}} = U_{e 1} \sqrt{\frac{m_1}{m_3}} \cos \phi + U_{e 3} \sin \phi, \quad (3.17)$$

where we took hierarchical neutrino masses. We neglect $\lambda_{e 1}$ because its absolute value is small. With this choice of the unknown R , the phases of the $\lambda_{\alpha 1}$ are effectively independent of the PMNS phases. So for any choice of PMNS phases that would appear on the m_ν of Eq. (3.12), the phases of the Yukawa couplings can be chosen independently, to ensure enough CP violation for leptogenesis.

We now check that a large enough baryon asymmetry can be obtained in this area of parameter space. The parentheses of Eq. (3.12) can be written explicitly as:

$$\text{Im} \left\{ \frac{\sin^2 \phi^*}{|\sin \phi|^2} (m_{\tau\tau} + m_{\mu\mu} + 2m_{\mu\tau}) \right\} \frac{1}{\sqrt{\Delta m_{\text{atm}}^2}}, \quad (3.18)$$

Writing $\phi^* = \rho - i\omega$, the final baryon asymmetry can be estimated from Eq. (3.12) as:

$$\frac{Y_B}{10^{-10}} \simeq - \left(\frac{M_1}{10^{11} \text{GeV}} \right) \frac{\sin \rho \cos \rho \sinh \omega \cosh \omega}{(\sin^2 \rho \cosh^2 \omega + \cos^2 \rho \sinh^2 \omega)^2}, \quad (3.19)$$

which can equal the observed $(8.7 \pm 0.4) \times 10^{-11}$ [52] for $M_1 \sim \text{few} \times 10^{10}$ GeV, and judicious choices of ρ and ω . A similar argument can be made if the light neutrino mass spectrum is inverse hierarchical.

The scatter plots of figure 3.1 show that a large enough baryon asymmetry can be obtained for any value of the PMNS phases.

The plots are obtained by fixing $M_1 = 10^{10}$ GeV, and the measured neutrino parameters to their central values. To mimic the possibility that β ($\equiv \alpha_2/2$) and δ could be determined $\pm 15^\circ$, β - δ space is divided into 50 squares. In each square, the programme randomly generates values for: $\beta, \delta, .001 < \theta_{13} < .2$, the smallest neutrino mass $< \sqrt{\Delta m_{\text{sol}}^2}/10$, and the three complex angles of the R matrix. It estimates the baryon asymmetry from the analytic approximations of [64], and puts a cross if it is big enough. The programme is a proto-Monte-Carlo-Markov-Chain, preferring to explore parameter space where the baryon asymmetry is large enough.

Parametrising with the R matrix imposes a particular measure (prior) on parameter space. This could mean we only explore a class of models. This is ok because the aim is only to show that, for any PMNS phases, a large enough asymmetry *can* be found.

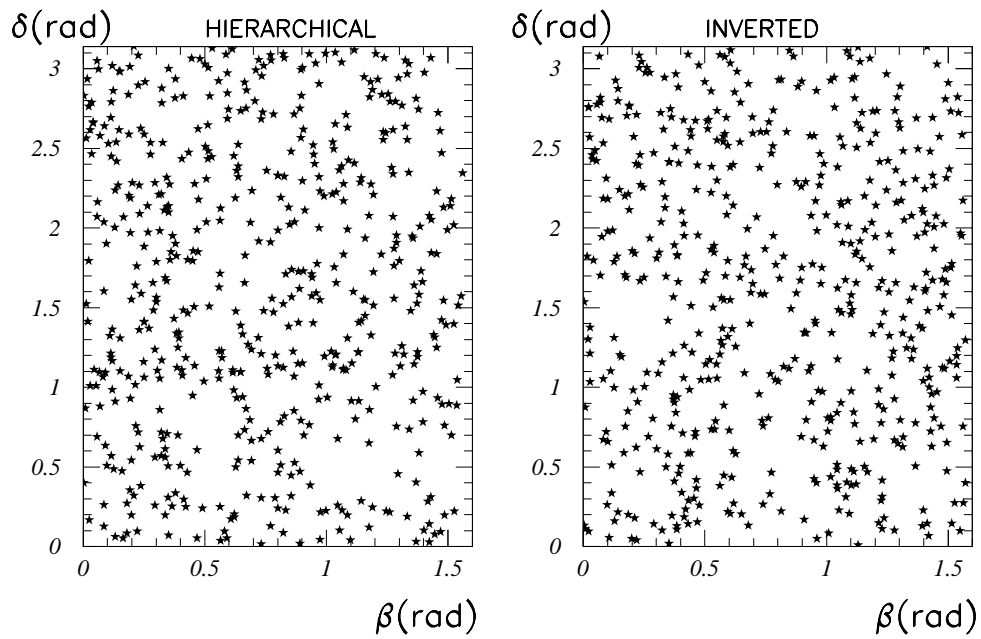


Figure 3.1: A random selection of points where the baryon asymmetry is large enough, for some choice of the unmeasurable parameters of the seesaw. The light neutrino masses are taken non-degenerate, and the Majorana phase of the smallest one can be neglected. The “Dirac” phase δ is defined such that $U_{e3} = \sin \theta_{13} e^{-i\delta}$, and $\beta \equiv \alpha_2/2$ is the majorana phase of $m_2 = |m_2|e^{2i\beta}$. The baryon asymmetry arises in the decay of N_1 of mass $M_1 = 10^{10}$ GeV.

3.5 Discussion

The relevant question, in discussing the “relation” between CP violation in the PMNS matrix and in leptogenesis, is whether the baryon asymmetry is *sensitive* to the PMNS phases. The answer was “no” for unflavored leptogenesis in the Standard seesaw Model [78]. This was not surprising; the seesaw contains more phases than the PMNS matrix, and many unmeasurable real parameters which can be adjusted to obtain a big enough asymmetry. In our paper, we argue that the answer does not change with the inclusion of flavor effects in leptogenesis: for any value of the PMNS phases, it is possible to find a point in the space of unmeasurable seesaw parameters, such that leptogenesis works. This “flavored” asymmetry can be written as a function of PMNS phases, and unmeasurables as entered the unflavored calculation. These can still be adjusted to get a big enough asymmetry. In view of this discouraging conclusion, it is maybe worth to emphasize that CP violation from both the left-handed and right-handed neutrino sectors, contributes both to the PMNS matrix and the baryon asymmetry.

In the demonstration that the baryon asymmetry (produced via thermal leptogenesis) is insensitive to PMNS phases, we found an interesting approximation for the “phase of leptogenesis” (see Eq. (3.12)), when all lepton flavors are in strong washout.

Chapter 4

CP Violation in the SUSY Seesaw: Leptogenesis and Low Energy

4.1 Introduction

In the paper [2], we aim to answer the same phenomenological question addressed in last chapter 3 [1]. Can the BAU be *sensitive* to low-energy phases? In this new study we focus on a supersymmetric seesaw, that has the interesting feature to potentially add new observables in the lepton sector, through the enhancement of flavor and CP violating processes (see *eg* [90] for a review and references on leptonic flavor and CP violation, induced by supersymmetry.).

The intent of this work is to clarify the relation between the CP violation accessible to low-energy experiments, and the CP violation necessary for leptogenesis, in a phenomenological *bottom-up* perspective, with minimal assumptions about the high scale theory. We just assume that the neutrino Yukawa couplings are hierarchical, which is the most natural assumption given the observed values of the charged lepton and quark Yukawas. Neutrino oscillation data then leads to hierarchical singlet masses. We suppose the observed BAU is generated via thermal leptogenesis, and enquire whether this restricts the range of the phases.

Since leptogenesis occurs at a very high-energy scale, a supersymmetric scenario is desirable in order to stabilize the hierarchy between the leptogenesis scale and the electroweak one. However, if supersymmetry exists at all, it must be broken and, in principle, the soft supersymmetry breaking Lagrangian can contain off-diagonal (in flavor space) soft terms, that would enhance lepton flavor violating (LFV) processes. These are strongly constrained by current experiments; this is the so-called supersymmetric flavor problem. In order to avoid it, we focus on the most conservative minimal Supergravity (MSUGRA) scenario with real boundary conditions, where the dynamics responsible for supersymmetry breaking is flavor blind and all the lepton flavor and CP violation is controlled by the neutrino Yukawa couplings. Supersymmetric expectations for LFV [23, 24, 25] and possible relations to leptogenesis [85, 90, 91, 92, 93] and EDMs [94, 95] have been studied by many people.

In this context, we perform a scan over the seesaw parameters, looking for those

points that give a large enough BAU, and where $\mu \rightarrow e\gamma$ and one of $\tau \rightarrow \ell\gamma$ would be seen in upcoming experiments. The aim is to verify if such experimental inputs imply a preferred range of values for the low-energy PMNS phases. We also estimate the contribution to the CP violating electron electric dipole moment. A detailed analysis of the MSUGRA scenario would require a scan also over the supersymmetric parameters, which is beyond the scope of our analysis.

Due to the large number of unknown parameters, instead of doing a usual grid scan in the seesaw parameter space we construct a Markov Chain using a Monte Carlo simulation (MCMC — see *e.g.* [96, 97]). This technique allows to efficiently explore a high-dimension parameter space, and we apply it for the first time to the supersymmetric seesaw model¹. Our work is thus pioneering in the exhaustive scanning of the seesaw parameters, which would be otherwise prohibitive without the MCMC technique.

4.2 Framework: Minimal Supergravity

We consider the superpotential for the leptonic sector in a supersymmetric seesaw model [17] with three hierarchical right-handed neutrinos ($M_1 < M_2 < M_3$), already introduced in section 1.2.2, Eq. (1.14):

$$W_{lep} = (L_L H_d) Y_e E^c + (L_L H_u) \lambda N^c + N^c \frac{M}{2} N^c, \quad (4.1)$$

where flavor indices are suppressed, and L_L , E and N are the supermultiplets containing left-handed lepton fields, right-handed charged leptons and right-handed neutral singlets, respectively. We work in the basis where Y_e and M are diagonal, therefore the neutrino yukawa matrix is in general not diagonal and complex. The previous superpotential leads to a lagrangian for leptons that contains the charged lepton yukawa couplings Y_α , the neutrino yukawa couplings $\lambda_{\alpha i}$ and a Majorana mass term for singlet neutrinos M_i (see section 1.2.2 and Eq. (1.6)).

Since supersymmetry is broken, to this Lagrangian we must add the soft SUSY breaking terms. We consider MSUGRA, so this soft part is written at some high scale M_X where the soft masses are universal and the trilinear couplings are proportional to the corresponding Yukawas, Eq. (1.15):

$$-\mathcal{L}_{SSB} = \tilde{m}_0^2 \sum_f \tilde{f}^\dagger \tilde{f} + \left\{ \frac{BM^i}{2} \tilde{N}_i^c \tilde{N}_i^c + a_0 (y_{e\alpha} \tilde{\ell}_L^\alpha \cdot H_d \tilde{e}_\alpha^c + \lambda_{\alpha i} \tilde{\ell}_L^\alpha \cdot H_u \tilde{N}_i^c) + h.c. \right\}, \quad (4.2)$$

here \tilde{f} collectively represents sfermions. MSUGRA is then characterized by four parameters: the scalar (m_0) and gaugino ($m_{1/2}$) masses, shared by all of them at the GUT scale; the trilinear coupling involving scalars, a_0 , at the GUT scale; and finally the Higgs vev ratio, $\tan\beta$.

¹See [47] for a detailed study of the Zee-Babu model of neutrino masses phenomenology using this technique.

	Present bounds	Future sensitivity
BR($\mu \rightarrow e\gamma$)	$< 1.2 \times 10^{-11}$	10^{-13} (MEG)[99]
BR($\tau \rightarrow \mu\gamma$)	$< 6.8 \times 10^{-8}$	10^{-9} (Belle)[100]
BR($\tau \rightarrow e\gamma$)	$< 1.1 \times 10^{-7}$	
BR($\mu \rightarrow e\bar{\nu}_e\nu_\mu$)	$\sim 100\%$	
BR($\tau \rightarrow \mu\bar{\nu}_\mu\nu_\tau$)	$17.36 \pm 0.05\%$	
BR($\tau \rightarrow e\bar{\nu}_e\nu_\mu$)	$17.84 \pm 0.05\%$	

Table 4.1: Present and predicted bounds on lepton flavor violating processes, and measured branching ratios for $\ell_\alpha \rightarrow \ell_\beta\nu_\alpha\bar{\nu}_\beta$ decays.

Note that in this basis the neutrino Yukawa matrix is the only source of flavor violation in the lepton sector, it contains 6 phases. In general, other sources of CP violation appear in the complex neutrino B-term, in the scalar mass \tilde{m}_0 and in the trilinear coupling a_0 .

Neutrino masses are generated exactly in the same way as in the non supersymmetric case. We refer the reader to sections 1.2 and 1.2.2, and section 3.2 from the previous chapter. We also remind the reader that we use Eq. (3.2) to parametrize the neutrino yukawa matrix, and Eq. (3.3) to write the neutrino mass matrix in terms of the three mass eigenstates. Furthermore, in section 4.4 we will review the input parameters used in our analysis and the parametrizations used for them.

4.2.1 Low-energy footprints: LFV and EDMs in MSUGRA

Present bounds on LFV processes, shown in table 4.1, restrict the size of flavor off-diagonal soft terms. This suggests universal soft terms at some high scale M_X , see Eq. (4.2), like in the MSUGRA scenario. There are also stringent experimental bounds, as we can see in Table (4.2), on the CP violating electric dipole moments, which point towards very small CP phases. To address this ‘‘SUSY CP problem’’², we suppose that all the soft breaking terms (namely a_0 , m_0 and right-handed sneutrino B-term), as well as the μ term, are real. Even under this extremely conservative assumptions, it is well known that because of RGE running from high to low energy scales, the seesaw Yukawa couplings potentially induce lepton flavor and CP violating contributions to the soft terms [23, 24, 25].

We focus on these neutrino Yukawa coupling contributions to LFV and EDMs, assuming MSUGRA with real boundary conditions at M_X . Additional contributions, arising with less restrictive boundary conditions, are unlikely to cancel the ones we discuss, so the upper bounds that will be set if, for instance, no electron EDM is measured by the Yale group, will equally apply. Conversely, if an electron EDM is measured above the range that we predict, it will prove the existence of a source of CP violation other than the neutrino Yukawa phases.

²See *e.g.* [98] for an illuminating discussion.

Present bounds (e cm)	Future sensitivity (e cm)
$d_e < 1.6 \times 10^{-27}$	10^{-29} (Yale group)[101]
$d_\mu < 2.8 \times 10^{-19}$	10^{-24} (Muon EDM Collaboration) [102]
$(-2.2 < d_\tau < 4.5) \times 10^{-17}$	

Table 4.2: Present and anticipated bounds on electric dipole moments. See [90] for a discussion of future experiments.

We are interested in analytic estimates for LFV rates and electric dipole moments. For this, we need the flavor-changing and CP violating contributions to the soft masses, that arise from the neutrino Yukawa. Following [26], we take the one-loop corrections to the flavor off-diagonal doublet slepton masses $\tilde{m}_{L\alpha\beta}^2 \rightarrow \tilde{m}_{L\alpha\beta}^2 + \Delta\tilde{m}_{L\alpha\beta}^2$ and to the trilinear coupling $a_0\lambda \rightarrow a_0\lambda(1 + \Delta a_0)$ to be:

$$\Delta\tilde{m}_{L\alpha\beta}^2 = -\frac{1}{16\pi^2}(3m_0^2 + a_0^2)[C^{(1)}]_{\alpha\beta} - \frac{1}{16\pi^2}(m_0^2 + a_0^2 + 2a_0B)[H]_{\alpha\beta}, \quad (4.3)$$

$$\Delta(a_0)_{\alpha\beta} = -\frac{1}{16\pi^2}[C^{(1)}]_{\alpha\beta} - \frac{1}{16\pi^2}[H]_{\alpha\beta}, \quad (4.4)$$

for $\alpha \neq \beta$ where the matrices H and $C^{(n)}$ are given by:

$$H \equiv \lambda\lambda^\dagger = V_L^\dagger D_\lambda^2 V_L, \quad (4.5)$$

$$C^{(n)} \equiv \lambda \log^n \left(\frac{MM^\dagger}{M_X^2} \right) \lambda^\dagger = V_L^\dagger D_\lambda V_R \log^n \left(\frac{MM^\dagger}{M_X^2} \right) V_R^\dagger D_\lambda V_L, \quad (4.6)$$

we have used the parametrization for the neutrino yukawa matrix from Eq. (3.2). $C^{(1)}$ is the leading log contribution, and terms $\propto H$ arise in the finite part (they could be relevant for EDMs). The one loop corrections to the right handed charged slepton mass matrix, $\tilde{m}_{R\alpha\beta}^2$ only contain the charged lepton Yukawa couplings and therefore can not generate off-diagonal entries. These are generated at two loops, and as we will see later, they can be relevant for the lepton EDMs.

At one loop, sparticles generate the dipole operator (where e without subscript is the electro-magnetic coupling constant):

$$eX_{\alpha\beta}\bar{e}_L^\alpha\sigma^{\mu\nu}e_R^\beta F_{\mu\nu} + h.c. \quad (4.7)$$

which leads to LFV decays ($\ell_\alpha \rightarrow \ell_\beta\gamma$), and induces the flavor diagonal anomalous magnetic and electric dipole moments of charged leptons [90]. For $\alpha = \beta$, the anomalous magnetic moment is $a_\alpha = 4m_{e_\alpha}\text{Re}\{X_{\alpha\alpha}\}$ and the electric dipole moment is $2\text{Im}\{X_{\alpha\alpha}\}$.

In the mass insertion approximation the observable LFV rates are proportional to $|\tilde{m}_{L\alpha\beta}^2|^2 \propto |C_{\alpha\beta}^{(1)}|^2$ and the corresponding branching ratios are of order [24]:

$$\begin{aligned} \frac{BR(\ell_\alpha \rightarrow \ell_\beta \gamma)}{BR(\ell_\alpha \rightarrow \ell_\beta \nu_\alpha \bar{\nu}_\beta)} &\sim \frac{\alpha^3 \tan^2 \beta}{G_F^2 m_{SUSY}^8} |\tilde{m}_{\alpha\beta}^2|^2 \\ &\sim \frac{\alpha^3 \tan^2 \beta}{G_F^2 m_{SUSY}^8} \frac{(3m_0^2 + a_0^2)^2}{(4\pi)^4} |[C]_{\alpha\beta}|^2, \end{aligned} \quad (4.8)$$

a_μ^{EXP}	$(116\ 592\ 080 \pm 63) \times 10^{-11}$ in BNK-E821
$\delta a_\mu = a_\mu^{EXP} - a_\mu^{SM}$	$(276 \pm 81) \times 10^{-11}$ [104]
	$(275 \pm 84) \times 10^{-11}$ [107]
	$(295 \pm 88) \times 10^{-11}$ [105]

Table 4.3: Experimental value and deviation from the SM predictions of the muon anomalous magnetic moment. The errors of δa_μ are the combination in quadrature of the experimental and theoretical ones.

where G_F is the Fermi constant, $\tan \beta = v_u/v_d$, and m_{SUSY} is a generic SUSY mass, which substitutes for the mixing angles and the function of the loop particle masses.

An estimate of m_{SUSY} can be obtained from the data on the anomalous magnetic moment of the muon, as suggested in [103]. A 3.3 or 3.4σ deviation from the Standard Model prediction is observed in the anomalous magnetic moment of the muon (In Table (4.3), is given the experimental value of a_μ and the deviation from the SM prediction [104, 105]). We assume it is due to new physics that can also contribute to flavor violation and EDMs. In the MSUGRA seesaw scenario that we are considering, the main contribution to a_μ comes from 1-loop diagrams with neutralino or chargino exchange and is given by [106]:

$$\delta a_\mu^{SUSY} \simeq \frac{\alpha m_\mu^2}{8\pi \sin^2 \theta_{weak}} \frac{\tan \beta}{m_{SUSY}^2}. \quad (4.9)$$

Assuming [103] that the main contribution to the LFV branching ratio is given by analogous diagrams involving chargino and neutralino exchange, gives, from Eqs. (4.8,4.9) with $m_0 \simeq a_0 \simeq m_{SUSY}$:

$$\frac{BR(\ell_\alpha \rightarrow \ell_\beta \gamma)}{BR(\ell_\alpha \rightarrow \ell_\beta \nu_\alpha \bar{\nu}_\beta)} \sim 10^{-8} |C_{\alpha\beta}|^2 \left(\frac{\delta a_\mu}{10^{-9}} \right)^2. \quad (4.10)$$

Since we aim to explore seesaw parameter space, we set the MSUGRA parameters $m_0 \simeq a_0 \simeq m_{SUSY}$.

In our analysis, we aim for values of $|C_{\alpha\beta}|^2$ that will give $\mu \rightarrow e\gamma$ and either of $\tau \rightarrow \ell\gamma$ in the next round of experiments. We require only one of the τ decays, because the other must be small to suppress $\mu \rightarrow e\gamma$ (recall that we assume the neutrino Yukawas are hierarchical).

The neutrino Yukawa corrections to the soft terms can also enhance the predictions of the CP violating electric dipole moments. In our discussion we can neglect muon and tau EDMs, because the experimental sensitivity on d_μ is currently eight orders of magnitude weaker than on d_e and we expect $d_\mu/d_e \sim m_\mu/m_e$.

There are two potentially important contributions to the charged lepton EDMs induced by the neutrino Yukawa couplings. As discussed in [108, 26], the first non-zero contribution to the complex, flavor diagonal EDMs arises at two-loop order. The matrices Δa_0 and $\Delta \tilde{m}_L^2$ in Eq. (4.3) are the available building blocks to make

an EDM, which turns out to be proportional to the commutator $[H, C]$. This is the dominant contribution at low $\tan\beta$.

We follow [26]³ to estimate:

$$d_e \sim \frac{4\alpha}{(4\pi)^5} \frac{m_e^2}{m_{SUSY}^2} \text{Im}[H C]_{ee} (1.9 \cdot 10^{-11} \text{ e cm}) \sim 10^{-29} \left(\frac{2}{\tan\beta} \right) \text{Im}[H C] \text{ e cm} , \quad (4.11)$$

where we have used $[H, C]/i = 2\text{Im}[H C]$, and the $(2/\tan\beta)$ arises because we extracted m_{SUSY}^2 from the δa_μ .

In the large $\tan\beta$ region, it has been shown [109] that a different contribution to the EDMs can be the dominant one. This new contribution arises at three loops, and it involves the two loop correction to the right handed charged slepton mass matrix $\Delta\tilde{m}_E^2$. It is proportional to the CP violating quantity:

$$D_\alpha = \text{Im} [((\Delta\tilde{m}_E^2)^T m_l \Delta\tilde{m}_L^2)_{\alpha\alpha}] \quad (4.12)$$

where m_l is the (diagonal) charged lepton mass matrix. Despite being a higher loop order, it is typically dominant for $\tan\beta \gtrsim 10$. The two loop expression for $\Delta\tilde{m}_E^2$ can be found in [26]. We approximate this contribution as:

$$d_e \simeq \frac{-e}{2} \frac{8\alpha}{(4\pi)^7} \frac{10m_e \tan\beta}{m_{SUSY}^2} \frac{\text{Im}[\lambda_{ek}^* \lambda_{\alpha k} m_{\tilde{l}_\alpha}^2 \lambda_{\alpha m}^* \lambda_{em}]}{v^2 \cos^2\beta} F(M_k^2), \quad (4.13)$$

where

$$F(M_k^2) = \left(\log \frac{M_X^2}{M_N^2} \log \frac{M_X^2}{M_k^2} \log \frac{M_N^2}{M_k^2} + \log^2 \frac{M_N^2}{M_k^2} \log \frac{M_N^2}{M_m^2} \right), \quad (4.14)$$

and $M_X = 3 \times 10^{16}$ GeV, $M_N = M_2$. It gives an electric dipole moment of order:

$$d_e \sim 10^{-29} \left(\frac{\tan\beta}{50} \right)^2 \frac{\text{Im}[\lambda_{ek}^* \lambda_{\alpha k} m_{\tilde{l}_\alpha}^2 \lambda_{\alpha m}^* \lambda_{em}]}{m_\tau^2} \text{ e cm}.$$

One comment is in order. Throughout this work, we use the approximated formulae (4.10), (4.11) (4.13), where we have set the supersymmetric parameters m_0 and a_0 at a common m_{SUSY} scale. Of course these are very rough approximations, but given that a detailed analysis of the MSUGRA scenario is beyond the scope of this study, which concentrates on the seesaw parameters, it is enough to illustrate our results.

Notice that, since we normalize the LFV branching ratios to the muon g-2 deviation from the SM, there is no enhancement of LFV for large $\tan\beta$. The three loop EDM contribution (4.13) is enhanced, because it has extra powers of $\tan\beta$.

³[26] finds the same structure as [108, 109], but its result is smaller by one power of a large logarithm.

4.3 Flavored thermal leptogenesis

In section 2.2.3 we described the mechanism of Leptogenesis in the context of the supersymmetric seesaw model. We refer the reader to that section, here we only give the relevant expressions for this work.

The baryon to entropy ratio produced by the decay close to equilibrium of neutrinos and sneutrinos into leptons and sleptons, can be written in all flavor regimes, as:

$$Y_B \simeq \frac{10}{31} \frac{n_N + n_{\tilde{N}} + n_{\tilde{N}^\dagger}}{s} \sum_{\alpha} \epsilon_{\alpha} \eta_{\alpha} \simeq \frac{10}{31} \frac{315 \zeta(3)}{4\pi^4 g_*} \sum_{\alpha} \epsilon_{\alpha} \eta_{\alpha}. \quad (4.15)$$

The numerical prefactor indicates the fraction of $B - L$ asymmetry converted into a baryon asymmetry by sphalerons in the MSSM. The second fraction is the equilibrium density of singlet neutrinos and sneutrinos, at $T \gg M_1$, divided by the entropy density s . Numerically, it is of order 4×10^{-3} , similar to the non-SUSY case⁴. The ϵ_{α} are the CP asymmetries in each flavor [58]:

$$\begin{aligned} \epsilon_{\alpha} &= \frac{\Gamma(N_1 \rightarrow \ell_{\alpha} H, \tilde{\ell}_{\alpha} h) - \Gamma(N_1 \rightarrow \bar{\ell}_{\alpha} \bar{H}, \bar{\tilde{\ell}}_{\alpha} \bar{h})}{\Gamma(N_1 \rightarrow \ell H, \tilde{\ell} h) + \Gamma(N_1 \rightarrow \bar{\ell} \bar{H}, \bar{\tilde{\ell}} \bar{h})} \\ &\simeq \frac{3M_1}{8\pi v_u^2 [\lambda^\dagger \lambda]_{11}} \text{Im} \{ [\lambda]_{\alpha 1} [m_{\nu}^\dagger \lambda]_{\alpha 1} \}, \end{aligned} \quad (4.16)$$

so that $\alpha = \tau, o$ or $\alpha = \tau, \mu, e$ in the two- or three-flavor regimes respectively (see section 2.2.3). At temperatures $T > \tan^2 \beta 10^{12}$ GeV, the charged lepton yukawa interactions are out of equilibrium ($\Gamma_{\ell_{\alpha}} \ll H$) and there are no flavor effects, so leptogenesis can be studied in one-flavor case. As the temperature drops, the τ interactions come into equilibrium. In the range $\tan^2 \beta 10^9 \lesssim T \lesssim \tan^2 \beta 10^{12}$ GeV, we have an intermediate two-flavor regime.

Finally, the factors η_{α} in Eq. (4.15) are the efficiency factors which take into account that these CP asymmetries are partially erased by inverse decays and scattering processes. We use the following efficiency factors [62, 63, 64]:

$$\eta_{\alpha} \simeq \left[\left(\frac{m_*}{2|A_{\alpha\alpha}| \tilde{m}_{\alpha\alpha}} \right)^{-1.16} + \left(\frac{|A_{\alpha\alpha}| \tilde{m}_{\alpha\alpha}}{2m_*} \right)^{-1} \right]^{-1}, \quad (4.17)$$

where we neglect A -matrix [87] factors in our numerical analysis. We remind the reader the definition of the rescaled N_1 decay rate:

$$\tilde{m} = \sum_{\alpha} \tilde{m}_{\alpha\alpha} = \sum_{\alpha} \frac{|\lambda_{\alpha 1}|^2}{M_1} v_u^2, \quad (4.18)$$

⁴The addition of the \tilde{N} s is compensated by the approximate doubling of the degrees of freedom in the plasma : $g_* = 228.75$ for the MSSM.

and in supersymmetry $m_*^{MSSM} = m_*^{SM}/\sqrt{2} = 4\pi v_u^2 H_1/M_1^2 \simeq 0.78 \times 10^{-3} \text{ eV}$ ⁵, where H_1 is the Hubble expansion rate at $T = M_1$.

Combining all the above equations we can write the BAU as:

$$Y_B = -\frac{10}{31} \frac{135 M_1}{4\pi^5 g_* v_u^2} \sum_{\alpha} \eta_{\alpha} \text{Im}\{\hat{\lambda}_{\alpha}[m_{\nu}^{\dagger} \cdot \hat{\lambda}]_{\alpha}\}, \quad (4.19)$$

where $\hat{\lambda}_{\alpha} = [\lambda]_{\alpha 1}/\sqrt{[\lambda^{\dagger}\lambda]_{11}}$. Y_B is roughly a factor of $\sqrt{2}$ larger than in the SM, in the limit where $\tilde{m}_{\alpha\alpha} > m_*$ for all flavors.

Supersymmetric thermal leptogenesis suffers from the so called gravitino problem [70], which we have already mentioned in section 2.2.3. We showed there that a reheat temperature $\gtrsim 10^9 \text{ GeV}$ is difficult but not impossible in supersymmetry. So for the purposes of this paper, we will allow $M_1 < 10^{11} \text{ GeV}$.

4.4 Reconstructing leptogenesis from low energy observables

In order to search for a connection between the low-energy observables and leptogenesis, we need a parametrization in which we can input the low energy observables, and then compute the BAU. Ideally we want to express the high-energy parameters in terms of observables [21]. Therefore, we write the seesaw parameters in terms of operators acting on the left-handed space, potentially more accessible: so we chose D_{ν} , D_{λ} and V_L (that appears in the combination $\lambda\lambda^{\dagger}$) and the PMNS matrix U . We use the standard parametrization for U , Eq. (1.2). Within this bottom-up approach, the CP violation is now encoded in the three, still unknown, low energy phases of the PMNS matrix U , and in the three unknown phases in V_L . We then reconstruct the right-handed neutrino parameters in terms of those inputs.

The matrices D_{ν} and U_{PMNS} can be determined in low-energy experiments. Through neutrino oscillation experiments we can extract the two neutrino mass differences, the PMNS matrix mixing angles and, in the future, the Dirac phase [110] (if Nature is kind with us). Furthermore, we have an upper bound on light neutrino masses that comes from cosmological evaluations [111], Tritium beta decay [112], and neutrino-less double beta decay [113]. Observing this last process could prove the Majorana nature of neutrinos and put some constraints on the combination of Majorana phases.

We have seen that in MSUGRA there is an enhancement of lepton flavor violating processes due to the neutrino Yukawa couplings. Assuming that these processes can be measured in the near future constrains the coefficients $[C]_{\alpha\beta}$, see Eq. (4.8),

⁵There are factors of 2 for SUSY: defining Γ_D to be the total N decay rate, we have $\Gamma_D^{SUSY} = 2\Gamma_D^{SM}$. So with the definition of eq. (4.18) for \tilde{m} , we have $\tilde{m} = 4\pi v_u^2 \Gamma_D^{MSSM}/M_1^2$ as opposed to $\tilde{m} = 8\pi v_u^2 \Gamma_D^{SM}/M_1^2$. So $m_*^{SUSY} = m_*^{SM}/\sqrt{2}$, where m_* is the value of \tilde{m} that would give $\Gamma_D = H_1$ at $T = M_1$, and the factor of $\sqrt{2}$ is because there are approximately twice as many degrees of freedom in the plasma.

which depend on D_λ and V_L . We parametrize the V_L matrix as the product of three rotations along the three axes, with a phase associated to each rotation:

$$V_L^\dagger = \begin{pmatrix} c_{13}^L c_{12}^L & c_{13}^L s_{12}^L e^{-i\rho} & s_{13}^L e^{-i\sigma} \\ -c_{23}^L s_{12}^L e^{i\rho} - s_{23}^L e^{-i\omega} s_{13}^L c_{12}^L e^{i\sigma} & c_{23}^L c_{12}^L - s_{23}^L e^{-i\omega} s_{13}^L s_{12}^L e^{-i\rho} e^{i\sigma} & c_{13}^L s_{23}^L e^{-i\omega} \\ s_{23}^L e^{i\omega} s_{12}^L e^{i\rho} - s_{13}^L c_{23}^L c_{12}^L e^{i\sigma} & -s_{23}^L e^{i\omega} c_{12}^L - s_{13}^L s_{12}^L c_{23}^L e^{-i\rho} e^{i\sigma} & c_{23}^L c_{13}^L \end{pmatrix} \quad (4.20)$$

From the bottom-up parameters defined above and using the Eq. (3.4), we are now able to reconstruct the right handed neutrino mass matrix and the V_R matrix appearing in the baryon asymmetry:

$$M^{-1} = V_R D_M^{-1} V_R^T = D_\lambda^{-1} V_L U D_\nu U^T V_L^T D_\lambda^{-1} v_u^{-2}. \quad (4.21)$$

In leptogenesis *without* flavor effects, the BAU is controlled only by the phases of V_R , which also contribute to the U_{PMNS} in the parametrization we use. However, as demonstrated in the R matrix parametrization [22], it is always possible to choose V_L such that the lepton asymmetry ϵ has any value for any value of PMNS phases [78]. So for Y_B in its observed range, the PMNS phases can be anything, and if we measure values of the PMNS phases, Y_B can still vanish. In flavored leptogenesis, the BAU can be written as a function of PMNS phases and unmeasurables, but it was shown in [1] that for the Standard Model seesaw, Y_B is insensitive to the PMNS phases. Relations between low energy CP violation and leptogenesis can be obtained by imposing restrictions on the high-scale theory, for instance that there are no right-handed phases [80].

In the case of MSUGRA, we assume that we will have two more measurable quantities in the near future, $\mu \rightarrow e\gamma$ and either of $\tau \rightarrow \ell\gamma$. Naively, we do not expect LFV rates to add more information on the CP violating phases, because the rates can be used to fix two (real) parameters in D_λ and V_L . The question is whether the remaining phases and real parameters, can always be arranged to generate a large enough BAU. We find the answer to be yes. For instance, in the limit of taking only the largest neutrino Yukawa coupling in D_λ , the matrices $C^{(n)}$ become proportional to H , and using the parametrization of the V_L matrix given in Eq. (4.20) one can easily see that the CP violating phases of the V_L matrix disappear from the LFV branching ratios.

Besides the LFV processes, the neutrino Yukawa couplings can also contribute to the CP violating electric dipole moments. These contributions are expected to be below the sensitivity of current experiments [95, 114]. See [114] for a discussion of the impact of EDMs on seesaw reconstruction. In our framework with hierarchical Yukawas we expect some suppression on this contributions to the EDMs. As we have seen in Section 4.2.1, for low $\tan\beta$ the main contribution is proportional to the commutator of the matrices $C^{(1)}$ and H , see eq. (4.11). Thus in the limit of taking only the largest Yukawa, which implies $C^{(1)} \propto H$, the commutator is equal to zero. Regarding the large $\tan\beta$ regime, although the contribution to the EDMs has a different dependence, given in eq. (4.13), it can be shown that it also vanishes in this limit. This means that a non-zero contribution will be suppressed by mixing angles and a smaller eigenvalue of H .

4.5 Analytic Estimates

If a parametrization existed, in which one could input the light neutrino mass matrix, the neutrino Yukawa couplings that control lepton flavor violation, *and* the baryon asymmetry, then it would be clear that the BAU, and other observables, are all insensitive to each other. In this section, we argue that at the minimum values of M_1 where leptogenesis works, such a parametrization “approximately” exists.

We analytically construct a point in parameter space that satisfies our criteria (large enough BAU, LFV observable soon), and where the baryon asymmetry is insensitive to the PMNS phases. To find the point, we parametrize the seesaw with the parameters of the effective Lagrangian relevant to N_1 decay. Since the observed light neutrino mass matrix is not an input in this parametrization, one must check that the correct low energy observables are obtained. This should occur, in the region of parameter space considered⁶, because the contribution of N_1 to the light neutrino mass matrix can be neglected. We construct the point for the normal hierarchy and small $\tan\beta$; similar constructions are possible for the other cases.

The effective Lagrangian for N_1 and \tilde{N}_1 , at scale $M_1 \lesssim \Lambda \ll M_2$, arises from the superpotential:

$$W_{N_1} = \lambda_{\alpha 1} L_L^\alpha H_u N_1^c + \frac{M_1}{2} N_1^c N_1^c + \kappa_{\alpha\beta} (L_L^\alpha H_u) (L_L^\beta H_u) \quad (4.22)$$

where $\kappa_{\alpha\beta}$ is obtained by integrating out N_2 and N_3 . It is known [116] that the smallest M_1 for which leptogenesis (with hierarchical N_i) works, occurs at $m_* \lesssim \tilde{m} \lesssim m_{sol}$. So we assume that

$$\frac{\lambda_{\alpha 1} \lambda_{\beta 1}}{M_1} v_u^2 \ll m_{\alpha\beta}, \quad (4.23)$$

implying that N_1 makes negligible contribution to light neutrino observables. We are therefore free to tune the $\lambda_{\alpha 1}$ s to maximize the baryon asymmetry.

To obtain a baryon asymmetry $Y_B \simeq 10^{-3} \sum_\alpha \epsilon_\alpha \eta_\alpha \simeq 8 \times 10^{-11}$, we require:

$$\sum_\alpha \epsilon_\alpha \eta_\alpha \simeq 8 \times 10^{-8}. \quad (4.24)$$

For $\tan\beta \simeq 2$, it is unclear whether the ℓ_μ is distinct for leptogenesis purposes. For simplicity we assume not, and use two flavors o and τ . The efficiency factors η_α are maximized to $\eta_\alpha \simeq 1/4$ for $\tilde{m}_{\alpha\alpha} = |\lambda_{\alpha 1}|^2 v_u^2 / M_1 \simeq \sqrt{2} m_*$. Since $\tilde{m} \simeq 3m_*$, this is barely in the strong washout regime, and (4.17) should be an acceptable approximation.

We would therefore like to find a point in parameter space, such that $M_1 \sim 10^9$ GeV, $\epsilon_o \simeq \epsilon_\tau \simeq 1.6 \times 10^{-7}$. Defining $\hat{\lambda}_\alpha = \lambda_{\alpha 1} / \sqrt{\sum_\alpha |\lambda_{\alpha 1}|^2}$, Eq. (4.16) implies that we need, for $\alpha = o$ and $\alpha = \tau$:

$$\text{Im} \left\{ \hat{\lambda}_{\alpha 1} \frac{[m^\dagger \hat{\lambda}]_{\alpha 1}}{m_3} \right\} \gtrsim \frac{10^9 \text{ GeV}}{M_1}. \quad (4.25)$$

⁶This area of parameter space was also found in [115] using a left-handed parametrization inputting $W = V_L U$ instead of V_L . See also [59].

This means that $\hat{\lambda}_1$ needs a component along \hat{u}_3 (the eigenvector of m_3), and, since it should also generate m_1 , it needs a component along \hat{u}_1 . It can always be written as:

$$\vec{\lambda}_1 = \lambda_{11}\hat{u}_1 + \lambda_{21}\hat{u}_2 + \lambda_{31}\hat{u}_3 \quad , \quad (4.26)$$

where $\{1, 2, 3\}$ indices indicate the light neutrino mass basis. In the following we take $\lambda_{21} = 0$, $\lambda_{31} = |\lambda_{31}|e^{i\zeta}$, $|\lambda_{31}| \gg |\lambda_{11}|$. With Eq. (3.3),

$$\begin{aligned} \text{Im}\left\{\hat{\lambda}_{\alpha 1}\frac{[m^\dagger\hat{\lambda}]_{\alpha 1}}{m_3}\right\} &= \frac{1}{|\lambda_{11}|^2 + |\lambda_{31}|^2}\text{Im}\left\{(\lambda_{11}\lambda_{31}U_{\alpha 1} + \lambda_{31}^2U_{\alpha 3})U_{\alpha 3}^*\right\} \\ &\rightarrow \frac{1}{|\lambda_{11}|^2 + |\lambda_{31}|^2}\text{Im}\left\{\frac{\lambda_{31}^2}{2}\right\} \end{aligned}$$

(no sum on α). In the last formula, we drop the terms $\propto \lambda_{11}$, which may contain asymmetries that cancel in the sum $\epsilon_o + \epsilon_\tau$. These are not useful to us, because we aim for $\eta_o \simeq \eta_\tau \simeq 1/4$. For $\text{Im}\{\lambda_{31}^2\}/(|\lambda_{31}|^2 + |\lambda_{11}|^2) \gtrsim 1/2$, Eq. (4.25) implies that a large enough BAU could be produced for $M_1 \sim 3 \times 10^9$ GeV.

We now check that we obtain the observed light neutrino mass matrix, even with ζ , the phase of λ_{31} , of order $\pi/4$. The light neutrino mass matrix is:

$$[m]_{\alpha\beta} = \frac{\lambda_{\alpha 1}\lambda_{\beta 1}}{M_1}v_u^2 + \kappa_{\alpha\beta}v_u^2 = v_u^2\left[\frac{\lambda_{11}^2}{M_1}\hat{u}_1\hat{u}_1^T + \kappa_2\hat{u}_2\hat{u}_2^T + \left(\frac{\lambda_{31}^2}{M_1} + \kappa_3\right)\hat{u}_3\hat{u}_3^T\right]_{\alpha\beta} \quad (4.27)$$

where κ_2 and κ_3 are the eigenvalues of κ . By convention there is no phase on m_3 , so in the 2 right-handed neutrino (2RHN) model that generates κ , we should put a phase on the larger eigenvalue κ_3 . Since $\lambda_{31}^2v_u^2/M_1 \simeq e^{i2\zeta} \times 10^{-3}$ eV, the phase on κ_3 is very small and we neglect it in the following discussion of lepton flavor violation. It is well known [117] that the seesaw mechanism with 2 right-handed neutrinos can reproduce the observed light neutrino mass matrix, with $m_1 = 0$. In our case, we assume that N_2 and N_3 give the observed m_2 , and m_3 up to (negligible) corrections due to N_1 of order 10^{-3} eV. m_1 arises due to N_1 .

In the 2RHN model, there is less freedom to tune the LFV branching ratios [118] than in the seesaw with three N_i . So as a last step, we check that we can obtain LFV branching ratios just below the current sensitivity. The 2RHN model can be conveniently parametrized with \hat{D}_κ , the 3×2 \hat{U}_{PMNS} matrix, the 2×2 unitary matrix $\hat{W} = \hat{V}_L\hat{U}$, and the eigenvalues Λ_2 and Λ_3 of $\hat{\Lambda}$ (matrices in the 2RHN subspace are denoted by hats). $\hat{\Lambda}$ is a 2×2 sub-matrix of λ , obtained by expressing the 3×3 Yukawa matrix in the eigenbases of the heavy and light neutrinos, and dropping the first row and column, corresponding to ν_1 and N_1 . It is straightforward to verify that $[\hat{V}_L]_{3e} \sim 10^{-3}$ can be obtained by taking $\tan\hat{\theta}_W \simeq s_{13}/(c_{13}s_{12})$, where $\hat{\theta}_W$ is the rotation angle in \hat{W} and θ_{ij} are from U_{PMNS} . Choosing Λ_2 , the smaller eigenvalue of Λ , to be $\sim .06$, ensures that $BR(\mu \rightarrow e\gamma)$ is small enough. We can simultaneously take $\Lambda_3 \sim 1$ and obtain $[V_L]_{3\tau} \sim [V_L]_{3\mu} \sim 1$, which allows $BR(\tau \rightarrow \mu\gamma) \sim 10^{-8}$. The resulting masses of N_2, N_3 are $\sim 10^{12}, 10^{15}$ GeV.

Our MCMC has some difficulties in finding the analytic points. We imagine this to be because they are ‘‘fine-tuned’’ in the parametrization used by the MCMC. The

amount of tuning required in the angles of V_L , to obtain the desired $\{\lambda_{j1}\}$, can be estimated by taking logarithmic derivatives.

4.6 MCMC

In this section we describe our numerical analysis. In order to verify if the baryon asymmetry of the universe is sensitive to the low energy PMNS phases, we perform a scan over the neutrino sector parameters aiming for those points compatible with the measured baryon asymmetry and the bound on the reheating temperature, that have large enough LFV branching ratios to be seen in the next experiments.

Using the bottom-up parametrization of the seesaw defined by the V_L , D_λ , D_ν and U matrices, our parameter space consists of the 14 variables displayed in Table 4.4. We take as an experimental input the best fit values of the light neutrino mass differences and of the solar and atmospheric mixing angles, Eq. (1.4). With respect to the SUSY parameters, we choose two different regimes for $\tan\beta$, equal to 2 or 50, while the m_{SUSY} scale is deduced from the data on the anomalous magnetic moment, see section 4.2.1.

Due to the large number of parameters it would be prohibitive to consider a usual grid scan. Thus, we choose to explore our parameter space by a Markov Chain Monte Carlo that behaves much more efficiently, and has been already successfully employed in other analysis [119].

4.6.1 Bayesian inference

Given a model with free parameters $X = \{x_1, \dots, x_n\}$ and a set of derived parameters $\xi(X)$, for an experimental data set d , the central quantity to be estimated is the *posterior distribution* $P(X|d)$, which defines the probability associated to a specific model, given the data set d . Following the Bayes theorem, it can be written as:

$$P(X|d) = \frac{\mathcal{L}(d|\xi(X))\pi(X)}{P(d)}, \quad (4.28)$$

where $\mathcal{L}(d|X)$ is the well known likelihood, that is the probability of reproducing the data set d from a given model X , $\pi(X)$ is the prior density function, which encodes our knowledge about the model, and $P(d) = \int \mathcal{L}(d|\xi(X))\pi(X)dX$ is an overall normalization neglected in the following. In the case of flat priors:

$$\pi(X) = \begin{cases} \frac{1}{X_{max}-X_{min}} & \text{if } X \in [X_{min}, X_{max}] \\ 0 & \text{otherwise} \end{cases} \quad (4.29)$$

the posterior distribution reduces to the likelihood distribution in the allowed parameter space.

The main feature of the Markov chains is that they are able to reproduce a specific target distribution we are interested in, in our case the posterior distribution, through a fast random walk over the parameter space. The Markov chain is an

ordered sequence of points X_i with a *transition probability* $W(X_{i+1}|X_i)$ from the i -th point to the next one. The first point X_0 is randomly chosen with prior probability $\pi(X)$. Then a new point is proposed by a *proposal distribution* $Q(X_{i+1}|X_i)$ and accepted with probability $\mathcal{A}(X_{i+1}|X_i)$. The transition probability assigned to each point is then given by $W(X_{i+1}|X_i) = Q(X_{i+1}|X_i)\mathcal{A}(X_{i+1}|X_i)$. Given a *target distribution* $P(X)$, if the following *detailed balance condition*:

$$W(X_k|X_j)P(X_j) = W(X_j|X_k)P(X_k) \quad (4.30)$$

is satisfied for any j, k , then the points X_i are distributed according to the target distribution. For a more detailed discussion see [96, 97].

4.6.2 The Metropolis-Hastings algorithm

In order to generate the MCMC with a final posterior distribution (4.28), we use the Metropolis-Hastings algorithm. In the following, we briefly recall how the algorithm behaves, but the discussion is done in terms of the likelihood, instead of the posterior distribution, since we assume flat priors on our parameter space, see eq. (4.29).

Let X be the parameter set we want to scan, and $\mathcal{L}(X)$ our likelihood function, the target distribution. From a given point in the chain X_i with likelihood $\mathcal{L}(X_i)$, a new point X_{new} with likelihood $\mathcal{L}(X_{new})$ is randomly selected by a gaussian proposal distribution $Q(X_{new}, X_i)$ centered in X_i and having width ϵ . This last quantity ϵ controls the *step size* of the random walk. The new point is surely added to the chain if it has a bigger likelihood, otherwise the chain adds the new point with probability $\mathcal{L}(X_{new})/\mathcal{L}(X_i)$. So the value of the next point X_{i+1} in the chain is determined by:

$$X_{i+1} = \begin{cases} X_{new} & \text{with probability } \min[\mathcal{A}(X_{new}, X_i), 1] \\ X_i & \text{with probability } 1 - \min[\mathcal{A}(X_{new}, X_i), 1] \end{cases}, \quad (4.31)$$

where $\mathcal{A}(X_{new}, X_i)$ is the acceptance probability:

$$\mathcal{A}(X_{new}, X_i) = \frac{\mathcal{L}(X_{new})}{\mathcal{L}(X_i)}. \quad (4.32)$$

Given this acceptance distribution and using the symmetry of our proposal distribution $Q(X_l, X_i)$ under the exchange $l \leftrightarrow i$, it is straightforward to see that the detailed balance condition 4.30 is satisfied for the likelihood $\mathcal{L}(X)$ as target distribution. This implies that when the chain has reached the equilibrium, after a sufficiently long run, the sample is independent of the initial point and distributed according to $\mathcal{L}(X)$.

In order to arrive at the equilibrium in a reasonable amount of time, the step scale ϵ of the random walk must be accurately chosen. Indeed, if we define the acceptance rate as the number of points accepted over the number of points proposed, a too big step ϵ implies a too low acceptance rate, so that the Markov Chain never advances, while a too small ϵ and, so, a very large acceptance ratio, implies that the chain needs a very large time to scan all the space. It has been suggested that ϵ must be

Free parameters	Allowed range [X_{min}, X_{max}]	
Yukawas	$\lambda_2/\lambda_1 \simeq \lambda_3/\lambda_2 \simeq 30$	$\lambda_2/\lambda_1 \simeq 100, \lambda_3/\lambda_2 \simeq 50$
$\log_{10} \lambda_3$	$[-0.3, 0.3]$	$[-0.5, 0.5]$
$\log_{10} \lambda_2$	$[-1.77, -1.17]$	$[-2.2, -1.2]$
$\log_{10} \lambda_1$	$[-3.25, -2.65]$	$[-4.2, -3.2]$
V_L		
$\log_{10}(m_0/\text{eV})$	$[-6, -3]$	
$\log_{10} \theta_{ij}^{VL}$	$[-4, \log_{10} \pi]$	
ρ, ω, σ	$[0, \pi]$	
PMNS U		
θ_{13}	$[0., 0.2]$	
$\delta, \alpha_{13}, \alpha_{23}$	$[0, \pi]$	

Table 4.4: Allowed parameter space, so that the uniform prior on each parameter is defined as in eq.(4.29).

chosen according to an optimal acceptance rate between 20% and 50%. However, in order to ensure the detailed balance condition, ϵ cannot change during the run of the chain, thus, in our program it is set in a burn-in period.

4.6.3 Convergence

A valid statistical inference from the numerical sample relies on the assumption that the points are distributed according to the target distribution. The first points of the chain are arbitrarily chosen and the chain needs a burn-in period to reach the target distribution. The length of the burn-in strongly depends on the intrinsic properties of the chain and cannot be set *a priori*. It changes according to the complexity of the model, to the target distribution, and the efficiency of the proposal distribution employed. Once the chain has reached the equilibrium the first burn-in points are discarded to ensure the independence of the chain from the initial conditions. The question we want to answer in this paper does not require a statistical analysis of the sample. Here we only aim to show that, for any value of the low energy phases, the unmeasurable high energy parameters can be rearranged to obtain the right baryon asymmetry. Therefore a careful diagnostic of the convergence is not a priority. Nevertheless, we briefly discuss it in this section since it is an important issue that can help the reader to have a better overview on our results.

A simple way to check convergence is to run different chains starting from different values and compare the behaviour of the parameters, once the chains have converged the parameters should move around the same limiting values. However, this method does not allow to detect lack of convergence in case of *poor mixing*, i.e. when the chains are trapped in a region of low probability relative to the maximum of the target distribution. This happens in models with strongly correlated vari-

ables, when the proposal distribution does not efficiently escape this region. This can be an issue for our numerical analysis, when, as mentioned in section 4.5, we look for a fine-tuned region with a large baryon asymmetry and low M_1 . We can understand the poor mixing situation if we imagine a landscape on the parameter space corresponding to the target distribution, with some broad hills and a tall but very thin peak at the maximum of the target distribution. In that case, the step of the chain can be optimized to efficiently scan all the space but, if its size is larger than the width of the peak it easily misses it.

In case of strongly correlated variables it can also happen that the region to be scanned is mainly a plane, that is with almost null likelihoods. And if a gaussian-like proposal distribution is employed, the choice of the starting point becomes important to allow the chain to advance. Indeed, if the starting point is surrounded by points with null likelihood (and so null acceptance rate) and its distance from the interesting region is much larger than the step of the random walk, the chain cannot move from this point, since it always finds points with null likelihood. On the other side, if the chain starts in a region which is a reasonable fit to the data, it advances. However, if this region is well separated from another interesting region, the chain has almost null probability to find the second one. In literature many studies exist on convergence criterion that help to check the mixing of the sample and are based on the similarity of the resulting sampling densities of input parameters from different chains. An example can be found in [120] and [121].

4.6.4 The seesaw sample

In our work the free variables X are given by the 14 seesaw parameters, with uniform priors, Eq. 4.29, on the allowed range of parameter space (see Table 4.4). The choice of a logarithmic scale on some unknown parameters allows us to scan with the same probability different orders of magnitude. We analyze models with two different hierarchies in the neutrino Yukawas, so that, for a $\lambda_3 \sim 1$ we impose $\lambda_2/\lambda_1 \sim \lambda_3/\lambda_2 \sim 30$ or $\lambda_2/\lambda_1 \sim 100$ and $\lambda_3/\lambda_2 \sim 50$. The lightest neutrino mass is allowed to vary between three orders of magnitude $10^{-6} < m_0 < 10^{-3} eV$ and the θ_{13} mixing angle within its 3σ range, $0 < \theta_{13} < 0.2$ rad. The V_L mixing angles can vary over 4 orders of magnitude, with maximum value π . All the CP violating phases, those of the V_L matrix indicated by ρ , ω and σ and the Dirac and Majorana phases δ , α_{13} and α_{23} , are allowed to vary on all their definition range: $[0, \pi]$ (this avoids degeneracies).

The idea is, now, to generate a sample of points in our parameter space that provide enough BAU, give LFV rates big enough to be seen in the next generation of experiments, and also have an M_1 light enough to avoid the gravitino problem. We then define our set of derived parameters $\xi(X)$ as in Table 4.5 and we associate to them a multivariate gaussian likelihood with uncorrelated errors:

$$\mathcal{L}(\xi_{exp}|\xi) = \frac{1}{(2\pi)^{1/2}\mathcal{R}^{m/2}} \exp\left\{-\frac{1}{2}(\xi - \xi_{exp})^t \mathcal{R}^{-1}(\xi - \xi_{exp})\right\}. \quad (4.33)$$

Derived parameters $\xi(X)$	$\xi_{exp} \pm \sigma$
Y_B	$(8.75 \pm 0.23) 10^{-11}$
$\log_{10} BR(\mu- > e\gamma)$	-13 ± 0.1
$\log_{10} BR(\tau- > l\gamma)$	-9 ± 0.1
$\log_{10}(M_1/GeV)$	-9 ± 0.1

Table 4.5: Best values and errors for the derived parameters $\xi(X)$ we want to maximize.

Where $m = 4$ is the dimension of the derived parameter set. The centre values ξ_{exp} are the best fit values and \mathcal{R} is an $m \times m$ error matrix, in this case diagonal, since we assume no correlation between the errors. As we can see in Table 4.5, the bau is set to its experimental value, while the LFV rates are set to be one order of magnitude below the present bounds, and the expected value of lightest heavy neutrino mass $M_1 \sim 10^9$ GeV is set to escape the gravitino problem. The branching ratio of LFV τ decays is given in terms of the combination $BR(\tau \rightarrow e\gamma) + BR(\tau \rightarrow \mu\gamma) \equiv BR_{\tau\alpha}$, since one of them is suppressed to respect the stringent bound from $BR(\mu \rightarrow e\gamma)$ (we assume hierarchical yukawas).

For each point X_i of the chain, the lepton flavor violating branching ratios are estimated with equation Eq. (4.10), while Y_B is computed after the reconstruction of the right neutrino mass, see Eq. (4.21), using Eq. (4.19) in the flavor regime is in act at the temperatures we consider. We recall that the temperature at which leptogenesis takes place is of the same order of the reconstructed right-handed neutrino mass. Depending on the value of $\tan\beta$, the range of temperatures at which the flavor regimes have a role changes. For small $\tan\beta$, in the temperature range 10^9 GeV $< T < 10^{12}$ GeV the τ flavor is in equilibrium and the two flavor regime is in order; while for $T < 10^9$ GeV μ are also in equilibrium and the three flavors are distinguishable. Since we aim for values of $M_1 \sim 10^9$ GeV if we consider a small value of $\tan\beta$ our program takes into account that the BAU can be produced in both two or three flavor regimes. For very large $\tan\beta$, instead, already for $T < 10^{12}$ GeV τ and μ are in equilibrium, thus the three flavor regime always takes place.

In the case of steeper yukawa hierarchy, in agreement with our analytical estimate, we enlarge our set of derived parameters and maximize the rescaled N_1 decay rate to $\tilde{m} \sim 10^{-3}$ eV and the heaviest right-handed neutrino masses to $M_2 \sim 10^{12}$ GeV and $M_3 \sim 3 \cdot 10^{14}$ GeV.

All the points that do not respect the present bounds on LFV, do not have large enough baryon asymmetry or have $M_1 > 10^{11}$ GeV, have a null likelihood. We assume that the largest uncertainty on the baryon asymmetry comes from our calculation, so we allow Y_B to be as small as $4 \cdot 10^{-11}$. Those points having one of the RH neutrino masses above the $M_{GUT} \sim 3 \cdot 10^{16}$ GeV scale have a null likelihood too, since in that case the equations we use for the evaluation of LFV processes do not apply.

4.6.5 Run details

In this subsection we explain the details of our MCMC run. The parameter space we scan is very large if compared to the derived variables and, in addition, we expect a strong correlation between the evaluated baryon asymmetry and lightest right-handed neutrino mass, see Eq. (4.19). Thus, since we expect a sample with poor mixing, as discussed in section 4.6.3, we first look for an initial point which is a reasonable fit to our observables. This procedure is done running previous shorter chains without imposing null likelihoods to the not interesting points. Once a wide enough set of interesting starting points is found we start running the chains.

As explained before, during the first burn-in iterations the scale of the random walk ϵ is varied until the acceptance rate of points is between the optimal range 20% and 50%. This usually takes much less than $3 \cdot 10^3$ iterations. When the optimal acceptance rate is reached, the scale ϵ is fixed during the rest of the run. We always discard the first 10^5 points of the chain, in order to give enough time for the chain to converge. This procedure should eliminate any dependence on the initial point inside the interesting region.

All the simulations we present are performed by running 5 chains with 10^6 points each. These chains are then added together after having excluded the points corresponding to the burn-in period. We run simulations for both normal and inverted hierarchy, in the two cases of small and large $\tan\beta$.

4.7 Discussion

4.7.1 Assumptions

We assume a three generation type I seesaw with a hierarchical neutrino Yukawa matrix. We require that this model produces the baryon asymmetry via flavored thermal leptogenesis, and induces the observed light neutrino mass matrix (thus we get hierarchical singlet neutrino masses). This model has a hierarchy problem, so we include supersymmetry.

We make a number of approximations and assumptions in supersymmetrizing the seesaw. First, we use real and universal soft terms at some high scale, above the masses M_i of the singlet neutrinos. In this restrictive model, the only contributions to flavor off-diagonal elements of the slepton mass² matrix $\equiv [\tilde{m}^2]_{\alpha\beta}$, arise due to Renormalization Group running. Second, we use simple leading log estimates for the off-diagonals $[\tilde{m}^2]_{\alpha\beta}$. Third, we estimate the SUSY contributions to the dimension five dipole operator (see Eq. (4.7)) using simple formulae of dimensional analysis (see Eqs. (4.10,4.11,4.13)). This operator induces flavor diagonal electric and magnetic dipole moments, and the flavor changing decays $\ell_\alpha \rightarrow \ell_\beta\gamma$. We assume the $(g-2)_\mu$ anomaly is due to supersymmetry, and use it to “normalize” the dipole operator. This implies that our SUSY masses scale with $\tan\beta$: $m_{SUSY}^2 = \frac{\tan\beta}{2}(200 \text{ GeV})^2$. We imagine that there is an uncertainty ~ 10 in our estimates of electric dipole moments and $\ell_\alpha \rightarrow \ell_\beta\gamma$ decays rates, due to mixing angles and sparticle mass differences.

Our first approximation, of universal soft terms, seems contrary to our phenomenological perspective: the RG-induced contributions to $[\tilde{m}^2]_{\alpha\beta}$ can be interpreted as lower bounds on the mass² matrix elements. However, we neglect other contributions, and require that the RG induced flavor-violating mass terms are $\propto C_{e\mu}^{(1)}$ (see Eq. (4.6)), give detectable rates for $\mu \rightarrow e\gamma$ and $\tau \rightarrow \ell\gamma$ in upcoming experiments. Realistically, measuring $\mu \rightarrow e\gamma$ mediated by sleptons might allow to determine $\tilde{m}_{e\mu}^2$, but does not determine the seesaw model parameters $C_{e\mu}^{(1)}$. This model dependence is compatible with our phenomenological approach, because our result is negative: we say that *even if* we could determine $C_{e\mu}^{(1)}$, the baryon asymmetry is insensitive to the PMNS phases.

4.7.2 Method

We explore the seesaw parameter space with a Monte Carlo Markov Chain, for two reasons. First, an MCMC is more efficient than a grid scan for multi-dimensional parameter space. It is essentially a programme for exploring hilltops in the dark. Since the programme always steps up and is reluctant to step down, it takes most of its steps in the most probable areas of parameter space.

The second potential advantage of a MCMC, is that it could make the results less dependent on the priors, that is, the choice of seesaw parametrization, and of the distribution of points. The predictions of theoretical models are often presented as scatter plots, and it is difficult to not interpret the point distribution as probability. However, the density of points in the scatter plots depends not only on what the model predicts, but also on the distribution of input points⁷. We had hoped that a MCMC could improve this, because a converged MCMC distributes points in parameter space according to a likelihood function. However, in practice there are various difficulties.

The prior on the seesaw model parameter space matters, because the MCMC takes steps of some size in each parameter: broad hilltops are easier to find than sharp peaks. As discussed in [121], this can be addressed by describing the model with parameters that match closely to physical observables. For this reason we parametrize the seesaw in terms of the diagonal singlet mass matrix D_M , the light neutrino mass matrix $m_\nu = UD_mU^T$, and the neutrino Yukawa matrix $\lambda\lambda^\dagger = V_L^\dagger D_\lambda^2 V_L$. These are related to low energy observables, because $\lambda\lambda^\dagger$ controls the RG contributions to the slepton mass matrix. We take the priors for our inputs as given in Table 4.4. However, the baryon asymmetry and the mass M_1 belong to the “right-handed” sector, so are complicated function of the “left-handed” input parameters. The bridge between the LH and RH sector is the Yukawa matrix, whose hierarchies may strongly distort the MCMC step size. To obtain a large enough baryon asymmetry for $M_1 \sim 10^9$ GeV requires careful tuning in the “right-handed”

⁷For example, if a model parameter such as a Yukawa can vary between 0 and 1, the results will be different depending on whether the Yukawa is $\mathcal{O}(1)$ (take points uniformly distributed between 0 and 1) or can vary by orders of magnitude (take the exponential of a variable uniformly distributed between $-n$ and 0).

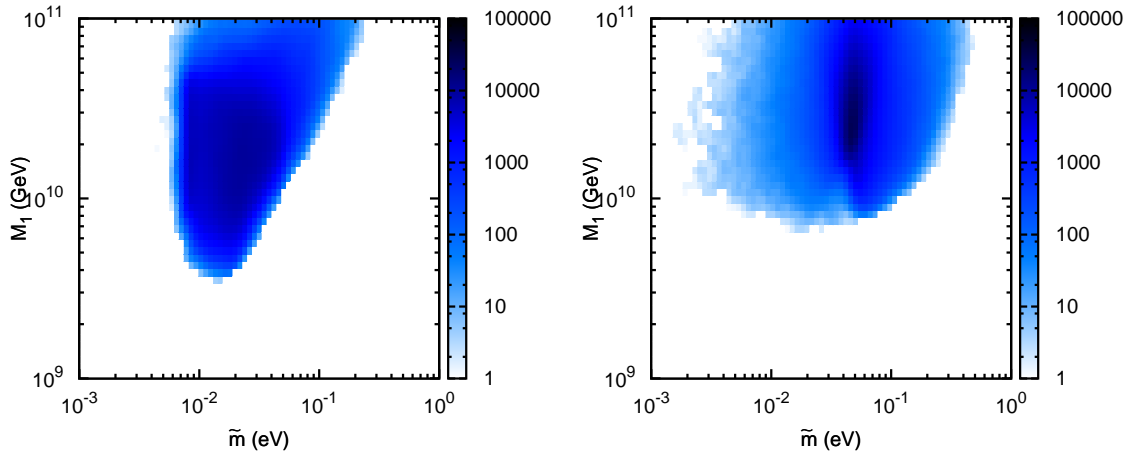


Figure 4.1: Correlation between the lightest right-handed neutrino mass M_1 and rescaled decay rate \tilde{m} , assuming $\lambda_3 \sim 1$ and $\lambda_2/\lambda_1 \sim \lambda_3/\lambda_2 \sim 30$, for two different simulations: NH and $\tan\beta = 50$ (left), and IH and $\tan\beta = 2$ (right).

space, and our MCMC has difficulty to find these points. This is related to a second, practical problem, that there are many more parameters than observables, so the space to explore is big, but the peaks with enough baryon asymmetry and small enough M_1 are rare. We therefore encounter some of the difficulties discussed in [120].

The parametrization used in section 4.5 avoids the above problems. It can be used if N_1 makes a negligible contribution, at low energy, to the dimension five neutrino mass operator. In the area of parameter space where this is the case, the dimension five operator at M_1 , generated by N_2 and N_3 , can be approximated as the one we measure (with a zero eigenvalue). So the seesaw model can be conveniently parametrized with the interactions of the effective theory at M_1 . In this parametrization, it is simple to tune the coupling constants to fit the light neutrino mass matrix, LFV rates, and the baryon asymmetry.

4.7.3 Results

The aim of our analysis was to verify if a preferred range of values for PMNS phases δ , α_{13} and α_{23} can be predicted, once low energy neutrino oscillation data, a large enough BAU, and LFV processes within the sensitivity of future experiments are requirements of the model.

In Fig. 4.1, we show the distribution, as a function of the singlet mass M_1 and the (rescaled) decay rate \tilde{m}_1 , of the successful points for a yukawa hierarchy $\lambda_2/\lambda_1 \sim \lambda_3/\lambda_2 \sim 30$, with $\lambda_3 \sim 1$.

With the parametrization described in section 4.6.4, the MCMC easily finds larger values of M_1 and \tilde{m} , than the “tuned” points found analytically in Section 4.5. This preference for larger M_1 is expected, because the baryon asymmetry and

right-handed neutrino masses are strongly correlated, see Fig. (4.2) and Eq. (4.16).

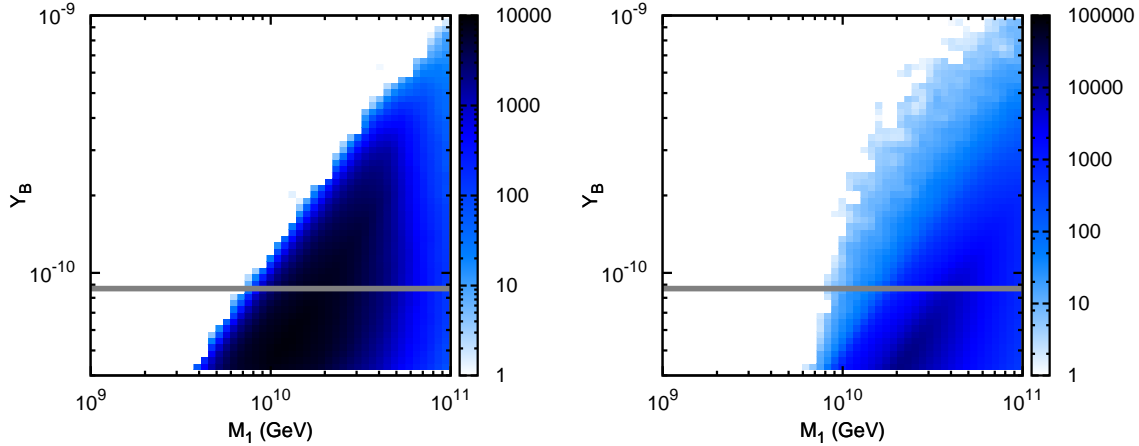


Figure 4.2: Correlation between the baryon asymmetry and the lightest right-handed neutrino mass, assuming $\lambda_3 \sim 1$ and $\lambda_2/\lambda_1 \sim \lambda_3/\lambda_2 \sim 30$, for two different simulations: NH and $\tan\beta = 50$ (left), and IH and $\tan\beta = 2$ (right).

Nonetheless, as illustrated in Fig. (4.3), the MCMC succeeded in finding points at lower M_1 , with a steeper⁸ hierarchy in the yukawas $\lambda_3 \sim 1$, $\lambda_2/\lambda_1 \sim 100$ and $\lambda_3/\lambda_2 \sim 50$. The difficulties of finding these tuned points are discussed in section 4.6.3.

The importance of the ~ 2 decrease in M_1 and \tilde{m} , at the tuned points, is unclear to us: the cosmological bound is on T_{RH} , rather than M_1 . Since in strong washout, an equilibrium population of N_1 can be generated for $T_{RH} \gtrsim M_1/5$, the points found by the MCMC at $M_1 \sim 10^{10}$ GeV, could perhaps generate the BAU at the same T_{RH} as the analytic points. In any case, we see in Fig. (4.2) that the fraction of points with big enough Y_B is very sensitive to M_1 , and therefore to details of the complicated reheating/preheating process.

In Fig. (4.4), we show density plots of the points resulting from our Markov Chains, corresponding to the the yukawa hierarchy $\lambda_2/\lambda_1 \sim \lambda_3/\lambda_2 \sim 30$, with $\lambda_3 \sim 1$, for normal hierarchy (NH) of the light neutrino masses and $\tan\beta = 2$, and for inverse hierarchy (IH) and $\tan\beta = 50$. In Fig. (4.7) (plot on the left) we show a density plot in the $\delta - \alpha_{23}$ plane for $\tan\beta = 2$, NH and the steeper hierarchy $\lambda_2/\lambda_1 \sim 100$, $\lambda_3/\lambda_2 \sim 50$ and $\lambda_3 \sim 1$. From those plots we see that, for any value of the phases δ , α_{13} and α_{23} our conditions are satisfied. The analytic results of Section 4.5 agree with this. Thus, we can conclude that the baryon asymmetry of the universe is *insensitive* to the low energy PMNS phases, even in the “best case” where we see MSUGRA-mediated lepton flavor violating processes. For completeness we also show correlation plots between the generated BAU and the three low energy

⁸the smallest yukawa must be small enough to ensure that the contribution of M_1 to the light neutrino masses is negligible

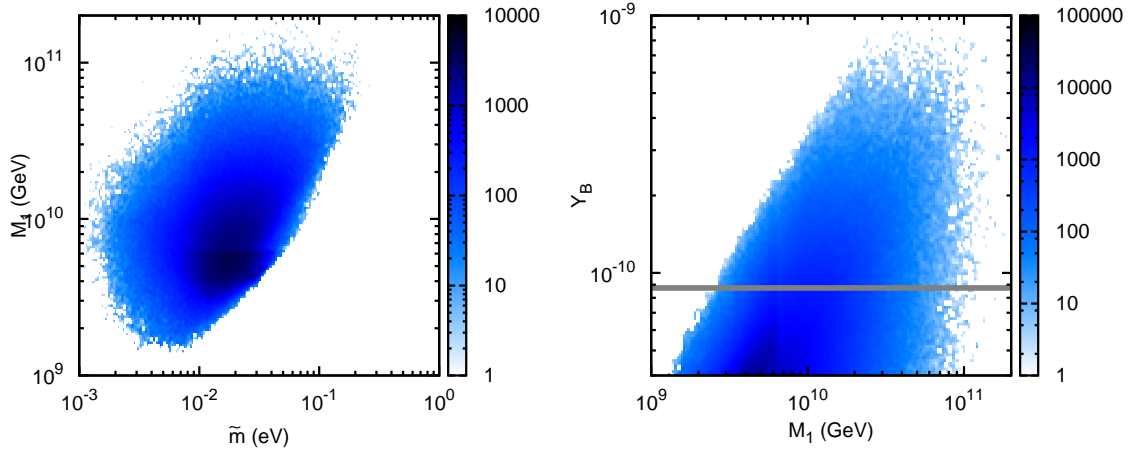


Figure 4.3: Correlation between the lightest right-handed neutrino mass M_1 and rescaled decay rate \tilde{m} , on the left-side, and between the baryon asymmetry and the lightest right-handed neutrino mass, on the right-side. We assume here $\lambda_3 \sim 1$ and $\lambda_2/\lambda_1 \sim 100$ and $\lambda_3/\lambda_2 \sim 50$, for a NH in the light neutrinos and $\tan\beta = 2$.

phases in Fig. (4.5). The low energy observables do not depend on $\tan\beta$, because we assume the $(g-2)_\mu$ discrepancy is due to slepton loops, and we use it to normalize the LFV rates (see Eq. (4.10)). On the contrary, the value of $\tan\beta$ is relevant in leptogenesis because it changes the number of distinguishable flavors. However, as we can see comparing plots for small/large $\tan\beta$, the value of $\tan\beta$ does not change our conclusions.

In Figs. (4.6,4.7) (plot on the right), we plot the contribution to the electric dipole moment of the electron, arising in the MSUGRA seesaw with real soft parameters at the high scale. For both low and large $\tan\beta$, points from our MCMC generate an electron EDM $\lesssim 10^{-30}$ ecm. This agrees with the results of [26, 95, 108].

4.8 Summary

The aim of this work was to study whether the baryon asymmetry produced by thermal leptogenesis was sensitive to the “low energy” phases present in the leptonic mixing matrix U_{PMNS} . We considered the three generation type-I supersymmetric seesaw model, in the framework of MSUGRA with real soft parameters at the GUT scale, and require that it reproduces low energy neutrino oscillation data, generates a large enough baryon asymmetry of the Universe via flavored leptogenesis and induces lepton flavor violating rates within a few orders of magnitude of current bounds. We then enquire whether a preferred range for the low energy PMNS phases δ , α_{13} and α_{23} can be predicted.

Our parameter space scan is performed by a Monte Carlo Markov Chain (MCMC), which allows to efficiently explore high-dimensional spaces. We use a “left-handed”

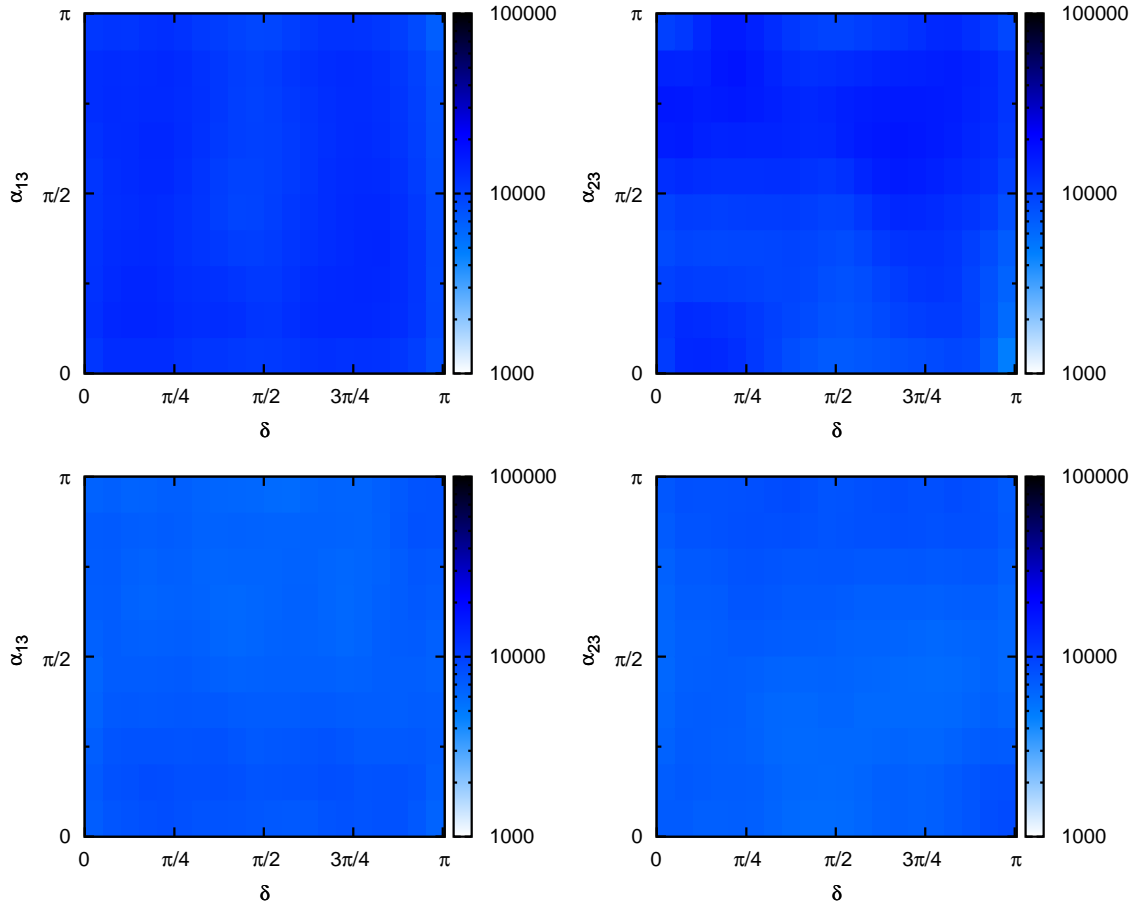


Figure 4.4: Density plots in the plane of the low energy phases $\delta - \alpha_{13}$ and $\delta - \alpha_{23}$ in models with $\lambda_3 \sim 1$ and $\lambda_2/\lambda_1 \sim \lambda_3/\lambda_2 \sim 30$. Upper plots correspond to a simulation with NH and $\tan\beta = 50$, and lower plots to IH and $\tan\beta = 2$. We remind the reader that all the points in our simulations generate a BAU bigger than $4 \cdot 10^{-11}$.

bottom-up parametrization of the seesaw, and our MCMC can find successful points with a small N_1 only with an accurate choice of the random walk step size. For this area of parameter space, we can also show analytically that the baryon asymmetry is insensitive to the PMNS phases.

We have checked that there is no correlation between successful leptogenesis and the low energy CP phases. That is: for any value of the low energy phases, the unmeasurable high energy parameters can be arranged in order to have successful leptogenesis and LFV rates in the next round of experiments. Finally, we have estimated, for each point in our chains, the contribution of the complex neutrino Yukawa couplings to the electric dipole moment of the electron. As expected, we find it to be $\lesssim 10^{-30} ecm$, just beyond the reach of next generation experiments.

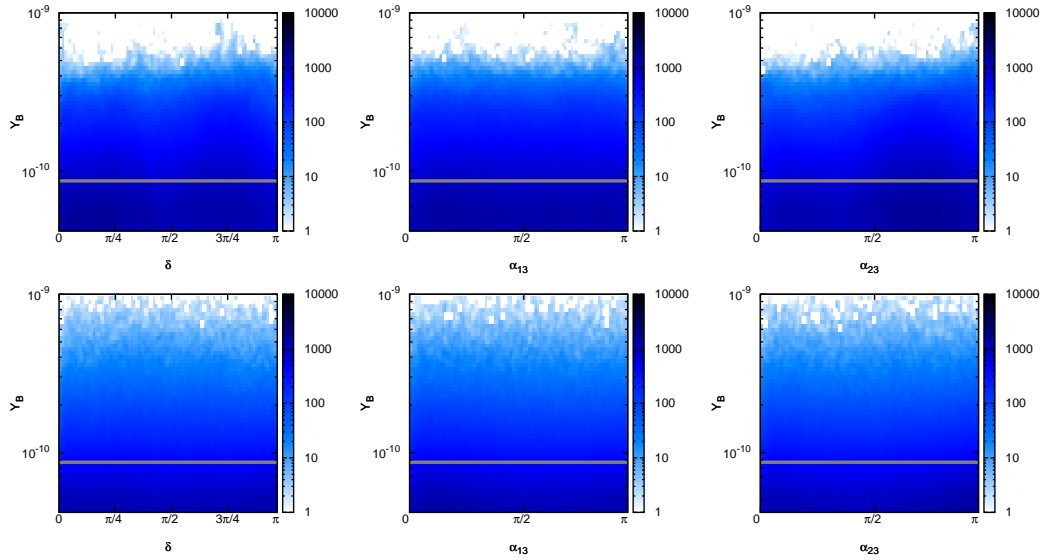


Figure 4.5: Correlation plots between the BAU and the low energy phases in models with $\lambda_3 \sim 1$ and $\lambda_2/\lambda_1 \sim \lambda_3/\lambda_2 \sim 30$. Upper plots correspond to a simulation with NH (and $\tan \beta = 50$), and the others to IH (and $\tan \beta = 2$).

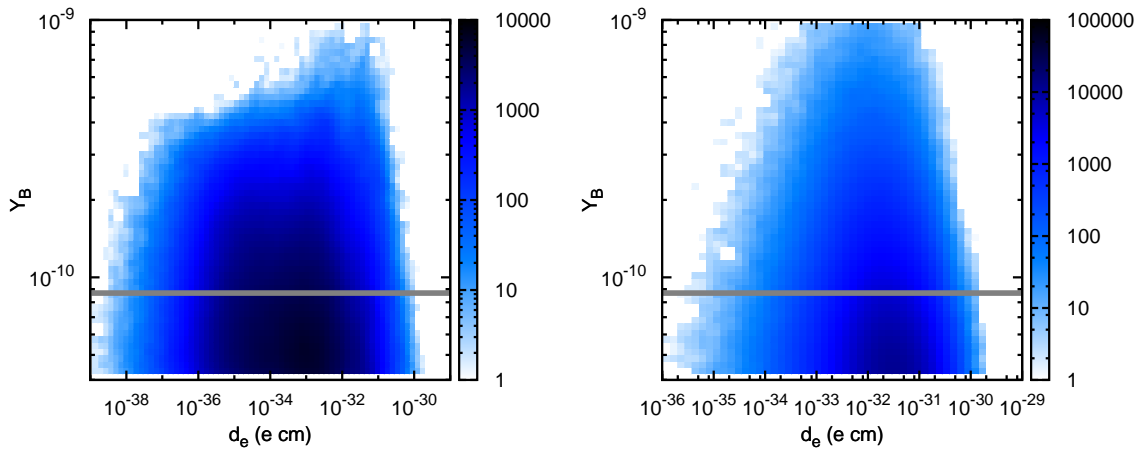


Figure 4.6: Correlation plots between the baryon asymmetry and the electron EDM generated by neutrino yukawas in models with $\lambda_3 \sim 1$ and $\lambda_2/\lambda_1 \sim \lambda_3/\lambda_2 \sim 30$. Upper plots correspond to a simulation with NH (and $\tan \beta = 50$), and the others to IH (and $\tan \beta = 2$).

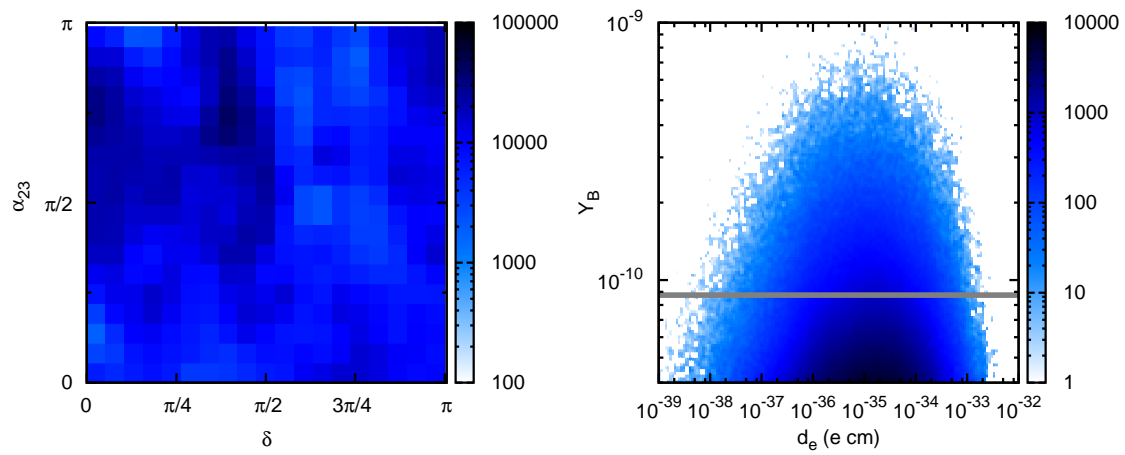


Figure 4.7: Density plot in δ - α_{23} plane and correlation between the baryon asymmetry and the electron EDM generated by neutrino yukawas. We assume here $\lambda_3 \sim 1$, $\lambda_2/\lambda_1 \sim 100$ and $\lambda_3/\lambda_2 \sim 50$, for a NH in the light neutrinos and $\tan \beta = 2$.

Chapter 5

Soft Leptogenesis in the Inverse Seesaw Model

5.1 Introduction

The Baryon Asymmetry of the Universe can be generated within the standard type I seesaw model via Leptogenesis. For a hierarchical spectrum of right-handed neutrinos, successful leptogenesis requires generically quite heavy singlet neutrino masses [69], of order $M > 2.4(0.4) \times 10^9$ GeV for vanishing (thermal) initial neutrino densities [69, 122, 94], although flavor effects [62, 63, 64] and/or extended scenarios [123] may affect this limit¹. The stability of the hierarchy between this new scale and the electroweak one is natural in low-energy supersymmetry, but in the supersymmetric seesaw scenario there is some conflict between the gravitino bound on the reheat temperature and the thermal production of right-handed neutrinos, as described in section 2.2.3. This is so because in a high temperature plasma, gravitinos are copiously produced, and their late decay could modify the light nuclei abundances, contrary to observation. This sets an upper bound on the reheat temperature after inflation, $T_{RH} < 10^{8-10}$ GeV, which may be too low for the right-handed neutrinos to be thermally produced.

Once supersymmetry has been introduced, leptogenesis is induced also in singlet sneutrino decays. If supersymmetry is not broken, the order of magnitude of the asymmetry and the basic mechanism are the same as in the non-supersymmetric case. However, as shown in Refs. [74, 75, 76], supersymmetry breaking terms can play an important role in the lepton asymmetry generated in sneutrino decays because they induce effects which are essentially different from the neutrino ones. The new sources of lepton flavor and CP violation from soft supersymmetry breaking terms can be large enough to generate the baryon asymmetry. In particular the asymmetry is large for a right-handed neutrino mass scale relatively low, in the

¹This bound applies when the lepton asymmetry is generated in the decay of the lightest right-handed neutrino. The possibility to evade the bound producing the asymmetry from the second lightest right-handed neutrino has been considered in [124], and flavor effects have been analyzed for this case in [59].

range $10^5 - 10^8$ GeV, well below the reheat temperature limits, what solves the cosmological gravitino problem.

In this work [3] we want to explore soft leptogenesis in the framework of an alternative mechanism to generate small neutrino masses, namely the inverse seesaw scheme [28]. This scheme is characterized by a *small* lepton number violating Majorana mass term μ , while the effective light neutrino mass is $m_\nu \propto \mu$. Small values of μ are technically natural, given that when $\mu \rightarrow 0$ a larger symmetry is realized [125]: lepton number is conserved and neutrinos become massless. In the inverse seesaw scheme lepton flavor and CP violation can arise even in the limit where lepton number is strictly conserved and the light neutrinos are massless [126], due to the mixing of the $SU(2)$ doublet neutrinos with new $SU(2) \times U(1)$ singlet leptons.

As opposite to the standard seesaw case, these singlet leptons do not need to be very heavy [127], and, as a result, lepton flavor and CP violating processes are highly enhanced [126]. In Ref. [128] it was studied the possibility that the baryon asymmetry is generated in this type of models during the electroweak phase transition, in the limit $\mu = 0$. A suppression was found due to the experimental constraints on the mixing angles of the neutrinos [129]. Therefore we consider here the supersymmetric version of the model and the soft leptogenesis mechanism, since (i) in this case we expect that a CP asymmetry will be generated in sneutrino decays even with a single-generation and no suppression due to the mixing angles is expected, and (ii) this scheme provides a more natural framework for the relatively low right-handed neutrino mass scale.

5.2 Inverse Seesaw Mechanism

We consider the supersymmetric version of the inverse seesaw model, whose main features were described in section 1.3.1. In this model the lepton sector is extended with two electroweak singlet leptons per generation, N_i and S_i . The superpotential that generates the lagrangian in Eq. (1.17) and the neutral lepton mass matrix Eq. (1.18) is:

$$W = Y_{ij} N_i L_j H + \frac{1}{2} \mu_{ij} S_i S_j + M_{ij} S_i N_j , \quad (5.1)$$

where $i, j = 1, 2, 3$ are flavor indices, H, L_i, N_i, S_i are the superfields corresponding to the $SU(2)$ up-Higgs and lepton doublets, and the new neutral singlets N_i^c and S_i , respectively, and Y_{ij} denote the neutrino Yukawa couplings. We assign lepton number $L = 1$ to the neutral singlets (N, S), so that the coupling μ leads to lepton number violation. In the limit $\mu \rightarrow 0$, lepton number conservation is restored. The light neutrino masses are given by, Eq. (1.19):

$$m_\nu = m_D^T M^{T-1} \mu M^{-1} m_D , \quad (5.2)$$

The relevant soft supersymmetry breaking terms are the bilinear and trilinear scalar couplings involving the singlet sneutrino fields, that provide new sources of

lepton number and CP violation. From now on we consider a simplified one generation of (N, S) model because a single generation of singlet sneutrinos is sufficient to generate the CP asymmetry. Indeed in the three-generation case, the relevant out of equilibrium decays are usually those of the lightest heavy singlet states while the decay of the heavier (if heavier enough) give no effect. Thus with our simplified single generation model we refer to the lightest of the three heavy singlet sneutrinos which we number as 1. Consequently we label $M = M_{11}$ and $\mu = \mu_{11}$. Also, for simplicity, we will assume proportionality of the soft trilinear terms.

$$-L_{soft} = AY_{1i}\tilde{L}_i\tilde{N}H + \tilde{m}_S^2\tilde{S}\tilde{S}^\dagger + \tilde{m}_N^2\tilde{N}\tilde{N}^\dagger + \tilde{m}_{SN}^2\tilde{S}\tilde{N}^\dagger + B_S\tilde{S}\tilde{S} + B_{SN}\tilde{S}\tilde{N} + h.c. \quad (5.3)$$

With our lepton number assignments, the soft SUSY breaking terms which violate L are \tilde{m}_{SN}^2 and B_S . The sneutrino interaction Lagrangian is then:

$$\begin{aligned} -L = & (Y_{1i}L_iNH + Y_{1i}L_i\tilde{N}h + Y_{1i}\tilde{L}_iNh + h.c.) + \\ & + (Y_{1i}M^*\tilde{L}_i\tilde{S}^\dagger H + AY_{1i}\tilde{L}_i\tilde{N}H + h.c.) + \\ & + (\mu SS + MSN + h.c.) + \\ & + (|\mu|^2 + \tilde{m}_S^2 + |M|^2)\tilde{S}^\dagger\tilde{S} + (\tilde{m}_N^2 + |M|^2)\tilde{N}\tilde{N}^\dagger + (\mu M^* + \tilde{m}_{SN}^2)\tilde{S}\tilde{N}^\dagger + h.c.) + \\ & + (B_S\tilde{S}\tilde{S} + B_{SN}\tilde{S}\tilde{N} + h.c.) \end{aligned} \quad (5.4)$$

In this expression \tilde{f} represent sfermions, H is the up-Higgs doublet, and h its supersymmetric partner, the higgsino. This Lagrangian has three independent physical CP violating phases: ϕ_B which can be assigned to B_{SN} , ϕ_A which is common to the three terms with AY_{1i} , and ϕ_{MY} which is common to the three terms with MY_{1i}^* , and are given by:

$$\begin{aligned} \phi_B &= \arg(B_{SN}B_S^*\tilde{M}_{SN}^2) \\ \phi_A &= \arg(AB_S^*M^2\mu^*(\tilde{M}_{SN}^2)^2) \\ \phi_{MY} &= \arg(\tilde{M}_{SN}^2M^*\mu) , \end{aligned} \quad (5.5)$$

where we have defined $\tilde{M}_{SN}^2 \equiv \mu M^* + \tilde{m}_{SN}^2$. These phases provide the CP violation necessary to generate dynamically a lepton asymmetry, even with a single generation of sneutrinos. They can also contribute to lepton electric dipole moments [130].

From the Lagrangian in Eq. (5.4) we obtain the sneutrino mass matrix in the interaction basis ($\tilde{F}_i \equiv \tilde{N}, \tilde{N}^\dagger, \tilde{S}, \tilde{S}^\dagger$):

$$\begin{pmatrix} \tilde{m}_N^2 + |M|^2 & 0 & \tilde{M}_{SN}^{2*} & B_{SN} \\ 0 & \tilde{m}_N^2 + |M|^2 & B_{SN}^* & \tilde{M}_{SN}^2 \\ \tilde{M}_{SN}^2 & B_{SN} & |\mu|^2 + \tilde{m}_S^2 + |M|^2 & 2B_S \\ B_{SN}^* & \tilde{M}_{SN}^{2*} & 2B_S^* & |\mu|^2 + \tilde{m}_S^2 + |M|^2 \end{pmatrix} \quad (5.6)$$

Notice that in the most general case it is not possible to remove all CP phases from the sneutrino mass matrix. With our choice of basis, B_{SN} is the only complex parameter, $B_{SN} = |B_{SN}|e^{i\phi_B}$.

Although one can easily obtain the analytic expressions for the corresponding mass eigenvalues and eigenvectors, for the general case they are lengthy and we do not give them here. Under the assumption that all the entries are real, i.e., $\phi_B = 0$, we obtain the following mass eigenvalues:

$$\begin{aligned}
M_1^2 &= M'^2 + B_S - \frac{1}{2}\sqrt{4(B_{SN} + \widetilde{M}_{SN}^2)^2 + (2B_S - \widetilde{m}_N^2 + \widetilde{m}_S^2 + |\mu|^2)^2} \\
M_2^2 &= M'^2 - B_S + \frac{1}{2}\sqrt{4(B_{SN} - \widetilde{M}_{SN}^2)^2 + (2B_S + \widetilde{m}_N^2 - \widetilde{m}_S^2 - |\mu|^2)^2} \\
M_3^2 &= M'^2 - B_S - \frac{1}{2}\sqrt{4(B_{SN} - \widetilde{M}_{SN}^2)^2 + (2B_S + \widetilde{m}_N^2 - \widetilde{m}_S^2 - |\mu|^2)^2} \\
M_4^2 &= M'^2 + B_S + \frac{1}{2}\sqrt{4(B_{SN} + \widetilde{M}_{SN}^2)^2 + (2B_S - \widetilde{m}_N^2 + \widetilde{m}_S^2 + |\mu|^2)^2}, \quad (5.7)
\end{aligned}$$

where we have defined $M'^2 \equiv |M|^2 + \widetilde{m}_N^2 + \widetilde{m}_S^2 + |\mu|^2$.

Furthermore, if we assume conservative values of the soft breaking terms:

$$\begin{aligned}
A &\sim \mathcal{O}(m_{SUSY}) \\
\widetilde{m}_N &\sim \widetilde{m}_S \sim \widetilde{m}_{SN} \sim \mathcal{O}(m_{SUSY}) \\
B_S &\sim \mathcal{O}(m_{SUSY}\mu) \\
B_{SN} &\sim \mathcal{O}(m_{SUSY}M)
\end{aligned} \quad (5.8)$$

with both, $\mu, m_{SUSY} \ll M$, we see that $B_S, \widetilde{m}_N^2, \widetilde{m}_S^2, \widetilde{m}_{SN}^2 \ll B_{SN}$ and $\widetilde{M}_{SN}^2 \sim \mu M^*$. Neglecting these small soft terms, there is still one physical CP violating phase,

$$\phi = \phi_A - \phi_B = \arg(AB_{SN}^*M). \quad (5.9)$$

In this limit, we choose for simplicity a basis where $A = |A|e^{i\phi}$ is the only complex parameter. Then we diagonalize to first order in two expansion parameters,

$$\epsilon = \frac{|\mu|}{2|M|}, \quad \tilde{\epsilon} = \frac{|B_{SN}|}{2|M|^2} \sim \mathcal{O}(m_{SUSY}/M) \quad (5.10)$$

To this order the mass eigenvalues are:

$$\begin{aligned}
M_1^2 &= M^2 - M\mu - B_{SN} \\
M_2^2 &= M^2 - M\mu + B_{SN} \\
M_3^2 &= M^2 + M\mu - B_{SN} \\
M_4^2 &= M^2 + M\mu + B_{SN}
\end{aligned} \quad (5.11)$$

and the eigenvectors:

$$\begin{aligned}
\widetilde{N}_1 &= \frac{1}{2}(\widetilde{S}^\dagger - \widetilde{N}^\dagger) + \frac{1}{2}(\widetilde{S} - \widetilde{N}) \\
\widetilde{N}_2 &= \frac{i}{2}(\widetilde{S}^\dagger - \widetilde{N}^\dagger) - \frac{i}{2}(\widetilde{S} - \widetilde{N}) \\
\widetilde{N}_3 &= \frac{i}{2}(\widetilde{S}^\dagger + \widetilde{N}^\dagger) - \frac{i}{2}(\widetilde{S} + \widetilde{N}) \\
\widetilde{N}_4 &= \frac{1}{2}(\widetilde{S}^\dagger + \widetilde{N}^\dagger) + \frac{1}{2}(\widetilde{S} + \widetilde{N})
\end{aligned} \quad (5.12)$$

Note that in this limit the mass degeneracy among the four sneutrino states is removed by both the L -violating mass μ and L -conserving supersymmetry breaking term B_{SN} . Together with the trilinear A term they also provide a source of CP violation, and the mixing among the four sneutrino states leads to a CP asymmetry in their decay.

Another interesting limit is to diagonalize the sneutrino mass matrix (5.6) neglecting only the B_S entry, which may be appropriate if $\mu \ll m_{SUSY}$ and the order of magnitude of the soft breaking terms is as given by (5.8). In this limit the mass matrix can also be taken real and the mass eigenvalues can be read from Eq. (5.7), just setting $B_S = 0$. Now there are two non zero CP violating phases, ϕ_{YM} and $\phi'_A = \arg(AB_{SN}^* M^2 \mu^* \widetilde{M}_{SN}^2)$. However the combination that is relevant for the CP asymmetry in sneutrino decays is the same as in the previous case, $\phi = \phi_{YM} + \phi'_A = \arg(AB_{SN}^* M)$.

As we will see in Sec. 5.6, the total CP asymmetry in the singlet sneutrino decays turns out to be sizable for very small values of the soft term $B_{SN} \ll M m_{SUSY}$. Neglecting the B_{SN} term in the Lagrangian there are still two CP violating phases, ϕ_{MY} and ϕ_A , but again the sneutrino mass matrix can be taken real, so that the mass eigenvalues are as given by Eq. (5.7) with $B_{SN} = 0$. The phase relevant for the CP asymmetry in the singlet sneutrino decays is now $\phi' = \phi_{YM} + \phi_A = \arg(AB_S^* M \widetilde{M}_{SN}^2)$.

Finally, neglecting supersymmetry breaking effects, the total singlet sneutrino decay width is given by:

$$\Gamma = \frac{\sum_i |M| |Y_{1i}|^2}{8\pi} . \quad (5.13)$$

5.3 The CP Asymmetry

In this section we compute the CP asymmetry in the singlet sneutrino decays. As discussed in Ref.[76], when $\Gamma \gg \Delta M_{ij} \equiv M_i - M_j$, the four singlet sneutrino states are not well-separated particles. In this case, the result for the asymmetry depends on how the initial state is prepared. In what follows we will assume that the sneutrinos are in a thermal bath with a thermalization time Γ^{-1} shorter than the typical oscillation times, ΔM_{ij}^{-1} , therefore coherence is lost and it is appropriate to compute the CP asymmetry in terms of the mass eigenstates Eq. (5.12).

The CP asymmetry produced in the decay of the state \widetilde{N}_i is given by (see section 5.5):

$$\epsilon_i = \frac{\sum_f \Gamma(\widetilde{N}_i \rightarrow f) - \Gamma(\widetilde{N}_i \rightarrow \bar{f})}{\sum_f \Gamma(\widetilde{N}_i \rightarrow f) + \Gamma(\widetilde{N}_i \rightarrow \bar{f})} , \quad (5.14)$$

where $f = \widetilde{L}_k H, L_k h$. We also define the fermionic and scalar CP asymmetries in

the decay of each \tilde{N}_i as:

$$\epsilon_{s_i} = \frac{\sum_k |\hat{A}_i(\tilde{N}_i \rightarrow \tilde{L}_k H)|^2 - |\hat{A}_i(\tilde{N}_i \rightarrow \tilde{L}_k^\dagger H^\dagger)|^2}{\sum_k |\hat{A}_i(\tilde{N}_i \rightarrow \tilde{L}_k H)|^2 + |\hat{A}_i(\tilde{N}_i \rightarrow \tilde{L}_k^\dagger H^\dagger)|^2} \quad (5.15)$$

$$\epsilon_{f_i} = \frac{\sum_k |\hat{A}_i(\tilde{N}_i \rightarrow L_k h)|^2 - |\hat{A}_i(\tilde{N}_i \rightarrow \bar{L}_k \bar{h})|^2}{\sum_k |\hat{A}_i(\tilde{N}_i \rightarrow L_k h)|^2 + |\hat{A}_i(\tilde{N}_i \rightarrow \bar{L}_k \bar{h})|^2}. \quad (5.16)$$

Notice that ϵ_{s_i} and ϵ_{f_i} are defined in terms of decay amplitudes, without the phase-space factors which, as we will see, are crucial to obtain a non-vanishing CP asymmetry, much as in the standard seesaw case [74, 75, 76]. The total asymmetry ϵ_i generated in the decay of the singlet sneutrino \tilde{N}_i can then be written as:

$$\epsilon_i = \frac{\epsilon_{s_i} c_s + \epsilon_{f_i} c_f}{c_s + c_f}, \quad (5.17)$$

where c_s, c_f are the phase-space factors of the scalar and fermionic channels, respectively.

Since the scale of lepton number and supersymmetry breaking are $\mu, m_{SUSY} \ll M$, there is an enhancement of the CP violation in mixing (wave-function diagrams), so we only include this leading effect and neglect direct CP violation in the decay (vertex diagrams).

We compute the CP asymmetry following the effective field theory approach described in [131], which takes into account the CP violation due to mixing of nearly degenerate states by using resummed propagators for unstable (mass eigenstate) particles. The decay amplitude \hat{A}_i^f of the unstable external state \tilde{N}_i defined in Eq. (5.12) into a final state f is described by a superposition of amplitudes with stable final states:

$$\hat{A}_i(\tilde{N}_i \rightarrow f) = A_i^f - \sum_{j \neq i} A_j^f \frac{i\Pi_{ij}}{M_i^2 - M_j^2 + i\Pi_{jj}}, \quad (5.18)$$

where A_i^f are the tree level decay amplitudes and Π_{ij} are the absorptive parts of the two-point functions for $i, j = 1, 2, 3, 4$. The amplitude for the decay into the conjugate final state is obtained from (5.18) by the replacement $A_i^f \rightarrow A_i^{f*}$.

The decay amplitudes can be read off from the interaction Lagrangian (5.4), after performing the change from the current to the mass eigenstate basis:

$$\begin{aligned} \mathcal{L} &= \frac{1}{2} \tilde{N}_1 [-Y_{1k} L_k h + (Y_{1k} M^* - AY_{1k}) \tilde{L}_k H] + \\ &+ \frac{i}{2} \tilde{N}_2 [-Y_{1k} L_k h - (Y_{1k} M^* + AY_{1k}) \tilde{L}_k H] + \\ &+ \frac{i}{2} \tilde{N}_3 [Y_{1k} L_k h - (Y_{1k} M^* - AY_{1k}) \tilde{L}_k H] + \\ &+ \frac{1}{2} \tilde{N}_4 [Y_{1k} L_k h + (Y_{1k} M^* + AY_{1k}) \tilde{L}_k H] + h.c. \end{aligned} \quad (5.19)$$

Neglecting supersymmetry breaking in vertices, up to an overall normalization we obtain that the decay amplitudes into scalars, $A_i^{sk} = A(\tilde{N}_i \rightarrow \tilde{L}_k H)$, verify $A_2^{sk} = A_3^{sk} = iA_1^{sk} = iA_4^s$. Correspondingly the decay amplitudes into fermions $A_i^{fk} = A(\tilde{N}_i \rightarrow L_k h)$, verify $A_2^{fk} = -A_3^{fk} = -iA_1^{fk} = iA_4^{fk}$.

Keeping only the lowest order contribution in the soft terms,

$$\Pi_{ii} = M \Gamma \quad i = 1, \dots, 4 \quad (5.20)$$

$$\Pi_{12} = \Pi_{21} = -\Pi_{34} = -\Pi_{43} = |A| \Gamma \sin \phi \quad (5.21)$$

Altogether we can then write the fermionic and scalar CP asymmetries as:

$$\epsilon_{s_i} = \sum_{j \neq i} \frac{2(M_i^2 - M_j^2) \Pi_{ji} \sum_k \text{Im}(A_i^{sk*} A_j^{sk})}{[(M_i^2 - M_j^2)^2 + \Pi_{jj}^2] \sum_k |A_i^{sk}|^2} \quad (5.22)$$

$$\epsilon_{f_i} = \sum_{j \neq i} \frac{2(M_i^2 - M_j^2) \Pi_{ji} \sum_k \text{Im}(A_i^{fk*} A_j^{fk})}{[(M_i^2 - M_j^2)^2 + \Pi_{jj}^2] \sum_k |A_i^{fk}|^2} \quad (5.23)$$

Inserting the values of the amplitudes A_i^f and the absorptive parts of the two-point functions (5.20) we obtain the final expression for the scalar and fermionic CP asymmetries at $T = 0$:

$$\epsilon_{s_i} = -\epsilon_{f_i} = \bar{\epsilon}_i = -\frac{4 |B_{SN} A| \Gamma}{4 |B_{SN}|^2 + |M|^2 \Gamma^2} \sin \phi \quad (5.24)$$

and the total CP asymmetry generated in the decay of the sneutrino \tilde{N}_i is then:

$$\epsilon_i(T) = \bar{\epsilon}_i \frac{c_s - c_f}{c_s + c_f}. \quad (5.25)$$

As long as we neglect the zero temperature lepton and slepton masses and small Yukawa couplings, the phase-space factors of the final states are flavor independent. After including finite temperature effects they are given by:

$$c_f = (1 - x_L - x_h) \lambda(1, x_L, x_h) [1 - f_L^{eq}] [1 - f_h^{eq}] \quad (5.26)$$

$$c_s = \lambda(1, x_H, x_{\tilde{L}}) [1 + f_H^{eq}] [1 + f_{\tilde{L}}^{eq}] \quad (5.27)$$

where

$$f_{H, \tilde{L}}^{eq} = \frac{1}{\exp[E_{H, \tilde{L}}/T] - 1} \quad (5.28)$$

$$f_{h, L}^{eq} = \frac{1}{\exp[E_{h, L}/T] + 1} \quad (5.29)$$

are the Bose-Einstein and Fermi-Dirac equilibrium distributions, respectively, and,

$$E_{L,h} = \frac{M}{2}(1 + x_{L,h} - x_{h,L}), \quad E_{H,\tilde{L}} = \frac{M}{2}(1 + x_{H,\tilde{L}} - x_{\tilde{L},H}) \quad (5.30)$$

$$\lambda(1, x, y) = \sqrt{(1 + x - y)^2 - 4x}, \quad x_a \equiv \frac{m_a(T)^2}{M^2}. \quad (5.31)$$

The thermal masses for the relevant supersymmetric degrees of freedom are [77]:

$$m_H^2(T) = 2m_h^2(T) = \left(\frac{3}{8}g_2^2 + \frac{1}{8}g_Y^2 + \frac{3}{4}\lambda_t^2 \right) T^2, \quad (5.32)$$

$$m_{\tilde{L}}^2(T) = 2m_L^2(T) = \left(\frac{3}{8}g_2^2 + \frac{1}{8}g_Y^2 \right) T^2. \quad (5.33)$$

Here g_2 and g_Y are gauge couplings and λ_t is the top Yukawa, renormalized at the appropriate high-energy scale.

As we will see in the next section, from Eq. (5.104), if the initial distributions of all four states \tilde{N}_i are equal, their total contribution to the total lepton number can be factorized as:

$$\epsilon(T) \equiv \sum_i \frac{\sum_f \Gamma(\tilde{N}_i \rightarrow f) - \Gamma(\tilde{N}_i \rightarrow \bar{f})}{\sum_f \Gamma(\tilde{N}_i \rightarrow f) + \Gamma(\tilde{N}_i \rightarrow \bar{f})}. \quad (5.34)$$

Several comments are in order. We find that this leptogenesis scenario presents many features analogous to soft leptogenesis in seesaw models [74, 75, 76, 132]: (i) The CP asymmetry Eq. (5.25) vanishes if $c_s = c_f$, because then there is an exact cancellation between the asymmetry in the fermionic and bosonic channels. Finite temperature effects break supersymmetry and make the fermion and boson phase-spaces different $c_s \neq c_f$, mainly because of the final state Fermi blocking and Bose stimulation factors. (ii) It also displays a resonance behaviour: the maximum value of the asymmetry is obtained for $2B_{SN}/M \sim \Gamma$. (iii) The CP asymmetry is due to the presence of supersymmetry breaking and irremovable CP violating phases, thus it is proportional to $|B_{SN} A| \sin \phi$.

As seen from Eq. (5.24) we obtain that the CP asymmetry is not suppressed by the lepton number violating scale μ . This may seem counterintuitive. However if $\mu = 0$ the four sneutrino states are pair degenerate, and we can choose a lepton number conserving mass basis, made of the ($L = 1$) states:

$$\begin{aligned} \tilde{N}'_1 &= \frac{1}{\sqrt{2}} (\tilde{S}^\dagger - \tilde{N}) \\ \tilde{N}'_2 &= \frac{1}{\sqrt{2}} (\tilde{S}^\dagger + \tilde{N}), \end{aligned} \quad (5.35)$$

and their hermitian conjugates, with $L = -1$, $\tilde{N}'_1{}^\dagger, \tilde{N}'_2{}^\dagger$. Although there is a CP asymmetry in the decay of these sneutrinos, it is not a lepton number asymmetry (since in the limit $\mu = 0$ total lepton number is conserved) but just a redistribution

of the lepton number stored in heavy sneutrinos and light lepton and slepton $SU(2)$ doublets. At very low temperatures, $T \ll M$, when no heavy sneutrinos remain in the thermal bath, all lepton number is in the light species and obviously if we started in a symmetric Universe with no lepton number asymmetry it will not be generated.

In other words, the total lepton number generated for the case with no lepton number violation is zero but it cannot be recovered by taking the limit $\mu \rightarrow 0$ of Eq. (5.24) because in the derivation of Eq. (5.24) it is assumed implicitly that the four singlet sneutrino states are non-degenerate and consequently it is only valid if μ (or some of the other L violating parameters) is non zero.

In section 5.4 we recompute the asymmetry using a quantum mechanics approach, based on an effective (non hermitic) Hamiltonian [74, 75, 76], and we get the same parametric dependence of the result, which differs only by numerical factors. Both expressions agree in the limit $\Gamma \ll |B_{SN}/M|$.

As discussed at the end of the previous section there may be other interesting ranges of parameters beyond Eq. (5.10). Thus in order to verify the stability of the results to departures from this expansion we have redone the computation of the CP asymmetry keeping all the entries in the sneutrino mass matrix, and just assuming that it is real. The expressions are too lengthy to be given here but let us simply mention that we have found that, in the general case, the CP asymmetries generated in the decay of each of the four singlet sneutrino states are not equal but they can always be written as:

$$\epsilon_i = -\frac{4|B_{SN}A|\Gamma}{4|B_{SN}|^2 + |M|^2\Gamma^2} \sin\phi + f_i(B_S, \mu, \widetilde{M}_{SN}^2), \quad (5.36)$$

where the functions f_i verify that for $|\mu|^2 \ll |B_{SN}|$ and to any order in $|B_S|$:

$$\sum_i f_i(B_S, \mu, \widetilde{M}_{SN}^2) \propto |B_{SN}|. \quad (5.37)$$

In the limiting case $|B_{SN}| \ll |B_S|, m_{SUSY}^2, |\mu|^2$ the dominant term in the CP asymmetry at leading order in $|B_S| \sim |M|\Gamma \ll |\widetilde{M}_{SN}^2|$ is:

$$\sum_i \epsilon_i = \frac{8|B_S A|\Gamma}{(4|B_S|^2 + |M|^2\Gamma^2)^2} \frac{|\mu|^2 + \widetilde{m}_S^2 - \widetilde{m}_N^2}{|\widetilde{M}_{SN}^2|} (4|B_S|^2 - |M|^2\Gamma^2) \sin\phi'. \quad (5.38)$$

It also exhibits a resonant behaviour, described now by $|B_S|\Gamma/(4|B_S|^2 + |M|^2\Gamma^2)^2$, however the total CP asymmetry in this limit is further suppressed by a factor of order $(|\mu|^2, m_{SUSY}^2)/|\widetilde{M}_{SN}^2|$.

Finally, let's comment that in the previous derivation we have neglected thermal corrections to the CP asymmetry from the loops, i.e., we have computed the imaginary part of the one-loop graphs using Cutkosky cutting rules at $T = 0$. These corrections are the same for scalar and fermion decay channels, since only bosonic loops contribute to the wave-function diagrams in both cases, so they are not expected to introduce significant changes to our results.

5.4 CP Asymmetry in Quantum Mechanics

The four sneutrino system is completely analogous to the $K^0 - \bar{K}^0$ system, so here we compute the CP asymmetry generated in their decay using the same formalism. In order to compare with the effective field theory approach described in Sec. 5.3 we consider only the simplified case $B_S, \tilde{m}_N^2, \tilde{m}_S^2, \tilde{m}_{SN}^2 \ll B_{SN}$ and $\tilde{M}_{SN}^2 \sim \mu M^*$. In this limit, we have chosen for simplicity a basis where $A = |A|e^{i\phi}$ is the only complex parameter with ϕ given in Eq. (5.9).

The evolution of the system is then determined by the effective Hamiltonian,

$$H = \hat{M} - i\frac{\hat{\Gamma}}{2} \quad (5.39)$$

where, in the interaction basis and at leading order in the expansion parameters $\epsilon, \tilde{\epsilon}$ defined in Eq. (5.10),

$$\hat{M} = M \begin{pmatrix} 1 & 0 & \epsilon & \tilde{\epsilon} \\ 0 & 1 & \tilde{\epsilon} & \epsilon \\ \epsilon & \tilde{\epsilon} & 1 & 0 \\ \tilde{\epsilon} & \epsilon & 0 & 1 \end{pmatrix} \quad (5.40)$$

and

$$\hat{\Gamma} = \Gamma \begin{pmatrix} 1 & 0 & 0 & \frac{A}{M} \\ 0 & 1 & \frac{A^*}{M} & 0 \\ 0 & \frac{A}{M} & 1 & 0 \\ \frac{A^*}{M} & 0 & 0 & 1 \end{pmatrix} \quad (5.41)$$

with Γ given in Eq. (5.13).

It is convenient to write the effective Hamiltonian in the mass eigenstate basis Eq. (5.12), because in such basis the four sneutrino system decouples in two subsystems of two sneutrinos, with the resulting width matrix:

$$\Gamma = \Gamma \begin{pmatrix} 1 - \epsilon_A \cos \phi & \epsilon_A \sin \phi & 0 & 0 \\ \epsilon_A \sin \phi & 1 + \epsilon_A \cos \phi & 0 & 0 \\ 0 & 0 & 1 - \epsilon_A \cos \phi & -\epsilon_A \sin \phi \\ 0 & 0 & -\epsilon_A \sin \phi & 1 + \epsilon_A \cos \phi \end{pmatrix} \quad (5.42)$$

where $\epsilon_A = \frac{|A|}{|M|}$.

The eigenvectors of the effective Hamiltonian H are:

$$\begin{aligned} \tilde{N}'_1 &= \frac{1}{\sqrt{2+2\frac{|\epsilon_+|}{|\epsilon_-|}}} \left[e^{i(\phi_- - \phi_+)/4} (\tilde{S}^\dagger - \tilde{N}^\dagger) + \sqrt{\frac{|\epsilon_+|}{|\epsilon_-|}} e^{-i(\phi_- - \phi_+)/4} (\tilde{S} - \tilde{N}) \right] \\ \tilde{N}'_2 &= \frac{i}{\sqrt{2+2\frac{|\epsilon_+|}{|\epsilon_-|}}} \left[e^{i(\phi_- - \phi_+)/4} (\tilde{S}^\dagger - \tilde{N}^\dagger) - \sqrt{\frac{|\epsilon_+|}{|\epsilon_-|}} e^{-i(\phi_- - \phi_+)/4} (\tilde{S} - \tilde{N}) \right] \\ \tilde{N}'_3 &= \frac{i}{\sqrt{2+2\frac{|\epsilon_+|}{|\epsilon_-|}}} \left[e^{i(\phi_- - \phi_+)/4} (\tilde{S}^\dagger + \tilde{N}^\dagger) - \sqrt{\frac{|\epsilon_+|}{|\epsilon_-|}} e^{-i(\phi_- - \phi_+)/4} (\tilde{S} + \tilde{N}) \right] \\ \tilde{N}'_4 &= \frac{1}{\sqrt{2+2\frac{|\epsilon_+|}{|\epsilon_-|}}} \left[e^{i(\phi_- - \phi_+)/4} (\tilde{S}^\dagger + \tilde{N}^\dagger) + \sqrt{\frac{|\epsilon_+|}{|\epsilon_-|}} e^{-i(\phi_- - \phi_+)/4} (\tilde{S} + \tilde{N}) \right] \end{aligned}$$

and the eigenvalues

$$\begin{aligned}
\nu_1 &= |M| - |\mu|/2 - i\Gamma/2 - e^{i(\phi_- + \phi_+)/2} \sqrt{|\epsilon_+|} \sqrt{|\epsilon_-|} \\
\nu_2 &= |M| - |\mu|/2 - i\Gamma/2 + e^{i(\phi_- + \phi_+)/2} \sqrt{|\epsilon_+|} \sqrt{|\epsilon_-|} \\
\nu_3 &= |M| + |\mu|/2 - i\Gamma/2 - e^{i(\phi_- + \phi_+)/2} \sqrt{|\epsilon_+|} \sqrt{|\epsilon_-|} \\
\nu_4 &= |M| + |\mu|/2 - i\Gamma/2 + e^{i(\phi_- + \phi_+)/2} \sqrt{|\epsilon_+|} \sqrt{|\epsilon_-|}
\end{aligned}$$

where

$$\begin{aligned}
\epsilon_- &= |\epsilon_-| e^{i\phi_-} = |B_{SN}/(2M)| - i\Gamma\epsilon_A/2 \\
\epsilon_+ &= |\epsilon_+| e^{i\phi_+} = |B_{SN}/(2M)| - i\Gamma\epsilon_A^*/2
\end{aligned}$$

We consider an initial state at $t = 0$ with equal number densities of the four sneutrino interaction states \tilde{F}_i . Using that the time evolution for the hamiltonian eigenstates Eq. (5.43) is trivially $|\tilde{N}'_i(t)\rangle = e^{-i\nu_i t} |\tilde{N}'_i\rangle$, we obtain that at time t the interaction states are the following:

$$\begin{aligned}
|\tilde{N}(t)\rangle &= \\
&= \frac{g_{1+}(t) + g_{2+}(t)}{4} |\tilde{N}\rangle + \sqrt{\frac{|\epsilon_-|}{|\epsilon_+|}} e^{i(\phi_- - \phi_+)/2} \frac{g_{1-}(t) - g_{2-}(t)}{4} |\tilde{N}^\dagger\rangle - \\
&- \frac{g_{1+}(t) - g_{2+}(t)}{4} |\tilde{S}\rangle - \sqrt{\frac{|\epsilon_-|}{|\epsilon_+|}} e^{i(\phi_- - \phi_+)/2} \frac{g_{1-}(t) + g_{2-}(t)}{4} |\tilde{S}^\dagger\rangle \\
|\tilde{N}^\dagger(t)\rangle &= \\
&= \sqrt{\frac{|\epsilon_+|}{|\epsilon_-|}} e^{-i(\phi_- - \phi_+)/2} \frac{g_{1-}(t) - g_{2-}(t)}{4} |\tilde{N}\rangle + \frac{g_{1+}(t) + g_{2+}(t)}{4} |\tilde{N}^\dagger\rangle - \\
&- \sqrt{\frac{|\epsilon_+|}{|\epsilon_-|}} e^{-i(\phi_- - \phi_+)/2} \frac{g_{1-}(t) + g_{2-}(t)}{4} |\tilde{S}\rangle - \frac{g_{1+}(t) - g_{2+}(t)}{4} |\tilde{S}^\dagger\rangle \\
|\tilde{S}(t)\rangle &= \\
&= -\frac{g_{1+}(t) - g_{2+}(t)}{4} |\tilde{N}\rangle - \sqrt{\frac{|\epsilon_-|}{|\epsilon_+|}} e^{i(\phi_- - \phi_+)/2} \frac{g_{1-}(t) + g_{2-}(t)}{4} |\tilde{N}^\dagger\rangle + \\
&+ \frac{g_{1+}(t) + g_{2+}(t)}{4} |\tilde{S}\rangle + \sqrt{\frac{|\epsilon_-|}{|\epsilon_+|}} e^{i(\phi_- - \phi_+)/2} \frac{g_{1-}(t) - g_{2-}(t)}{4} |\tilde{S}^\dagger\rangle \quad (5.43) \\
|\tilde{S}^\dagger(t)\rangle &= \\
&= -\sqrt{\frac{|\epsilon_+|}{|\epsilon_-|}} e^{-i(\phi_- - \phi_+)/2} \frac{g_{1-}(t) + g_{2-}(t)}{4} |\tilde{N}\rangle - \frac{g_{1+}(t) - g_{2+}(t)}{4} |\tilde{N}^\dagger\rangle + \\
&+ \sqrt{\frac{|\epsilon_+|}{|\epsilon_-|}} e^{-i(\phi_- - \phi_+)/2} \frac{g_{1-}(t) - g_{2-}(t)}{4} |\tilde{S}\rangle + \frac{g_{1+}(t) + g_{2+}(t)}{4} |\tilde{S}^\dagger\rangle
\end{aligned}$$

The functions $g_{1\pm}(t)$ and $g_{2\pm}(t)$ containing the time dependence are given by:

$$g_{1\pm}(t) = e^{-i(|M| - \frac{|\mu|}{2} - i\frac{\Gamma}{2})t} [e^{i\Delta\nu t} \pm e^{-i\Delta\nu t}] , \quad (5.44)$$

$$g_{2\pm}(t) = e^{-i(|M| + \frac{|\mu|}{2} - i\frac{\Gamma}{2})t} [e^{i\Delta\nu t} \pm e^{-i\Delta\nu t}] , \quad (5.45)$$

with,

$$\Delta\nu = e^{i(\frac{\phi_- + \phi_+}{2})} \sqrt{|\epsilon_-|} \sqrt{|\epsilon_+|} . \quad (5.46)$$

We neglect soft supersymmetry-breaking terms, so that \tilde{S} only decay to scalars, and \tilde{N} to antifermions:

$$\begin{aligned} |A[\tilde{S} \rightarrow \tilde{L}_k H]|^2 &= |A[\tilde{S}^\dagger \rightarrow \tilde{L}_k^\dagger H^\dagger]|^2 = |Y_{1k} M|^2 \equiv |A_{\tilde{L}_k}|^2 \\ |A[\tilde{N} \rightarrow L_k^\dagger h^\dagger]|^2 &= |A[\tilde{N}^\dagger \rightarrow L_k h]|^2 = |Y_{1k}|^2 (s - m_L^2 - m_h^2) \equiv |A_{L_k}|^2 \end{aligned} \quad (5.47)$$

We next write the time dependent decay amplitudes in terms of $|A_{\tilde{L}_k}|^2$ and $|A_{L_k}|^2$:

$$|A[\tilde{N}(t) \rightarrow \tilde{L}_k H]|^2 = |A[\tilde{N}^\dagger(t) \rightarrow \tilde{L}_k^\dagger H^\dagger]|^2 = \frac{|g_{1+} - g_{2+}|^2}{16} |A_{\tilde{L}_k}|^2 \quad (5.48)$$

$$|A[\tilde{S}(t) \rightarrow \tilde{L}_k H]|^2 = |A[\tilde{S}^\dagger(t) \rightarrow \tilde{L}_k^\dagger H^\dagger]|^2 = \frac{|g_{1+} + g_{2+}|^2}{16} |A_{\tilde{L}_k}|^2 \quad (5.49)$$

$$|A[\tilde{N}(t) \rightarrow L_k^\dagger h^\dagger]|^2 = |A[\tilde{N}^\dagger(t) \rightarrow L_k h]|^2 = \frac{|g_{1+} + g_{2+}|^2}{16} |A_{L_k}|^2 \quad (5.50)$$

$$|A[\tilde{S}(t) \rightarrow L_k^\dagger h^\dagger]|^2 = |A[\tilde{S}^\dagger(t) \rightarrow L_k h]|^2 = \frac{|g_{1+} - g_{2+}|^2}{16} |A_{L_k}|^2 \quad (5.51)$$

$$\begin{aligned} |A[\tilde{N}(t) \rightarrow \tilde{L}_k^\dagger H^\dagger]|^2 &= \left(\frac{|\epsilon_-|}{|\epsilon_+|} \right)^2 |A[\tilde{N}^\dagger(t) \rightarrow \tilde{L}_k H]|^2 = \\ &= \frac{|\epsilon_-|}{|\epsilon_+|} \frac{|g_{1-} + g_{2-}|^2}{16} |A_{\tilde{L}_k}|^2 \end{aligned} \quad (5.52)$$

$$\begin{aligned} |A[\tilde{S}(t) \rightarrow \tilde{L}_k^\dagger H^\dagger]|^2 &= \left(\frac{|\epsilon_-|}{|\epsilon_+|} \right)^2 |A[\tilde{S}^\dagger(t) \rightarrow \tilde{L}_k H]|^2 = \\ &= \frac{|\epsilon_-|}{|\epsilon_+|} \frac{|g_{1-} - g_{2-}|^2}{16} |A_{\tilde{L}_k}|^2 \end{aligned} \quad (5.53)$$

$$\begin{aligned} |A[\tilde{N}(t) \rightarrow L_k h]|^2 &= \left(\frac{|\epsilon_-|}{|\epsilon_+|} \right)^2 |A[\tilde{N}^\dagger(t) \rightarrow L_k^\dagger h^\dagger]|^2 = \\ &= \frac{|\epsilon_-|}{|\epsilon_+|} \frac{|g_{1-} - g_{2-}|^2}{16} |A_{L_k}|^2 \end{aligned} \quad (5.54)$$

$$\begin{aligned} |A[\tilde{S}(t) \rightarrow L_k h]|^2 &= \left(\frac{|\epsilon_-|}{|\epsilon_+|} \right)^2 |A[\tilde{S}^\dagger(t) \rightarrow L_k^\dagger h^\dagger]|^2 = \\ &= \frac{|\epsilon_-|}{|\epsilon_+|} \frac{|g_{1-} + g_{2-}|^2}{16} |A_{L_k}|^2 \end{aligned} \quad (5.55)$$

We define the integrated CP asymmetries for the fermionic and scalar channels as:

$$\begin{aligned}\epsilon_f &= \frac{\int dt \sum_{i,k} \left[|A[\tilde{F}_i(t) \rightarrow L_k + X]|^2 - |A[\tilde{F}_i(t) \rightarrow L_k^\dagger + X]|^2 \right]}{\int dt \sum_{i,k} \left[|A[\tilde{F}_i(t) \rightarrow L_k + X]|^2 + |A[\tilde{F}_i(t) \rightarrow L_k^\dagger + X]|^2 \right]} \\ \epsilon_s &= \frac{\int dt \sum_{i,k} \left[|A[\tilde{F}_i(t) \rightarrow \tilde{L}_k + X]|^2 - |A[\tilde{F}_i(t) \rightarrow \tilde{L}_k^\dagger + X]|^2 \right]}{\int dt \sum_{i,k} \left[|A[\tilde{F}_i(t) \rightarrow \tilde{L}_k + X]|^2 + |A[\tilde{F}_i(t) \rightarrow \tilde{L}_k^\dagger + X]|^2 \right]}\end{aligned}\quad (5.56)$$

Using the time-dependent amplitudes from Eq. (5.4), the time integrated asymmetries are:

$$\epsilon_s = -\epsilon_f = \bar{\epsilon} = -\frac{1}{2} \left(\frac{|\epsilon_-|}{|\epsilon_+|} - \frac{|\epsilon_+|}{|\epsilon_-|} \right) \chi, \quad (5.57)$$

where the factor $\frac{|\epsilon_-|}{|\epsilon_+|} - \frac{|\epsilon_+|}{|\epsilon_-|}$ vanishes if CP is conserved, and for $\epsilon_A \ll 1$ is given by:

$$\frac{|\epsilon_-|}{|\epsilon_+|} - \frac{|\epsilon_+|}{|\epsilon_-|} \simeq \frac{4M\Gamma|\epsilon_A|}{B_{SN}} \sin \phi = \frac{4\Gamma A}{B_{SN}} \sin \phi \quad (5.58)$$

The time dependence is encoded in χ :

$$\chi = \frac{\int_0^\infty dt [|g_{1-}(t)|^2 + |g_{2-}(t)|^2]}{\int_0^\infty dt [|g_{1+}(t)|^2 + |g_{2+}(t)|^2 + |g_{1-}(t)|^2 + |g_{2-}(t)|^2]}. \quad (5.59)$$

In the limit $\epsilon_A \ll 1$ the time integrals are :

$$\int_0^\infty dt [|g_{1-}|^2 + |g_{2-}|^2] \simeq 4 \frac{|B_{SN}|^2/\Gamma|M|^2}{\Gamma^2 + |B_{SN}|^2/|M|^2}, \quad (5.60)$$

$$\int_0^\infty dt [|g_{1+}|^2 + |g_{2+}|^2 + |g_{1-}(t)|^2 + |g_{2-}(t)|^2] \simeq \frac{8}{\Gamma}; \quad (5.61)$$

$$\epsilon_s = -\epsilon_f = \bar{\epsilon} = -\frac{\Gamma |B_{SN}| |A|}{\Gamma^2 |M|^2 + |B_{SN}|^2} \sin \phi \quad (5.62)$$

The comparison between the asymmetry in Eq. (5.24) and Eq. (5.62) is in full analogy to the corresponding comparison in the standard see-saw case discussed in [74]. The asymmetry computed in the quantum mechanics approach, based on an effective (non hermitic) Hamiltonian, Eq. (5.62), agrees with the one obtained using a field-theoretical approach, Eq. (5.24) in the limit $\Gamma \ll B_{SN}/M$. When $\Gamma \gg B_{SN}/M$, the four sneutrino states become two pairs of not well-separated particles. In this case the result for the asymmetry can depend on how the initial state is prepared. If one assumes that the singlet sneutrinos are in a thermal bath with a thermalization time Γ^{-1} shorter than the typical oscillation times, ΔM_{ij}^{-1} ,

coherence is lost and it is appropriate to compute the CP asymmetry in terms of the mass eigenstates Eq. (5.12) as done in Sec. 5.3 and one obtains Eq. (5.24). If, on the contrary, one assumed that the \tilde{N}, \tilde{S} states are produced in interaction eigenstates and coherence is not lost in their evolution, then it is appropriate to compute the CP asymmetry in terms of the interaction eigenstates Eq. (5.43) as done in this appendix and one obtains Eq. (5.62).

5.5 Boltzmann Equations

We next write the relevant Boltzmann equations describing the decay, inverse decay and scattering processes involving the sneutrino states.

As mentioned above we assume that the sneutrinos are in a thermal bath with a thermalization time shorter than the oscillation time. Under this assumption the initial states can be taken as being the mass eigenstates in Eq. (5.12) and we write the corresponding equations for those states and the scalar and fermion lepton numbers. The CP fermionic and scalar asymmetries for each \tilde{N}_i defined at $T = 0$ are those given in Eq. (5.24).

Let's notice that the CP asymmetries as defined in Eq. (5.24) verify $\epsilon_{s_i} = -\epsilon_{f_i} \equiv \bar{\epsilon}_i$. However in order to better trace the evolution of the scalar and fermion lepton numbers separately we will keep them as two different quantities in writing the equations.

Using CPT invariance and the above definitions for the CP asymmetries and including all the multiplicative factors we have:

$$\begin{aligned}
\sum_k |\hat{A}(\tilde{N}_i \rightarrow \tilde{L}_k H)|^2 &= \sum_k |\hat{A}(\tilde{L}_k^\dagger H^\dagger \rightarrow \tilde{N}_i)|^2 \simeq \frac{1 + \epsilon_{s_i}}{2} \sum_k |A_i^{s_k}|^2, \\
\sum_k |\hat{A}(\tilde{N}_i \rightarrow \tilde{L}_k^\dagger H^\dagger)|^2 &= \sum_k |\hat{A}(\tilde{L}_k H \rightarrow \tilde{N}_i)|^2 \simeq \frac{1 - \epsilon_{s_i}}{2} \sum_k |A_i^{s_k}|^2, \\
\sum_k |\hat{A}(\tilde{N}_i \rightarrow L_k h)|^2 &= \sum_k |\hat{A}(\bar{L}_k \bar{h} \rightarrow \tilde{N}_i)|^2 \simeq \frac{1 + \epsilon_{f_i}}{2} \sum_k |A_i^{f_k}|^2, \\
\sum_k |\hat{A}(\tilde{N}_i \rightarrow \bar{L}_k \bar{h})|^2 &= \sum_k |\hat{A}(L_k h \rightarrow \tilde{N}_i)|^2 \simeq \frac{1 - \epsilon_{f_i}}{2} \sum_k |A_i^{f_k}|^2.
\end{aligned} \tag{5.63}$$

where:

$$\begin{aligned}
\sum_k |A_i^{s_k}|^2 &= \sum_k \frac{|Y_{1k} M|^2}{4}, \\
\sum_k |A_i^{f_k}|^2 &= \sum_k \frac{|Y_{1k} M|^2 M_i^2}{4 M^2}.
\end{aligned} \tag{5.64}$$

The Boltzmann equations describe the evolution of the number density of particles

in the plasma, Eq. (2.10):

$$\begin{aligned} \frac{dn_X}{dt} + 3Hn_X &= \sum_{j,l,m} \Lambda_{lm\dots}^{Xj\dots} [f_l f_m \dots (1 \pm f_X)(1 \pm f_j) \dots W(lm\dots \rightarrow Xj\dots) - \\ &- f_X f_j \dots (1 \pm f_l)(1 \pm f_m) \dots W(Xj\dots \rightarrow lm\dots)] \end{aligned}$$

where,

$$\Lambda_{lm\dots}^{Xj\dots} = \int \frac{d^3 p_X}{(2\pi)^3 2E_X} \int \frac{d^3 p_j}{(2\pi)^3 2E_j} \cdots \int \frac{d^3 p_l}{(2\pi)^3 2E_l} \int \frac{d^3 p_m}{(2\pi)^3 2E_m} \cdots,$$

and $W(lm\dots \rightarrow Xj\dots)$ is the squared transition amplitude summed over initial and final spins. In what follows we will use the notation of Ref.[65] and we will assume that the Higgs and higgsino fields are in thermal equilibrium with distributions given in Eqs. (5.28) and (5.29) respectively, while the leptons and sleptons are in kinetic equilibrium and we introduce a chemical potential for the leptons, μ_f , and sleptons, μ_s :

$$\begin{aligned} f_L &= \frac{1}{\exp[(E_L + \mu_f)/T] + 1}, \\ f_{\bar{L}} &= \frac{1}{\exp[(E_L - \mu_f)/T] + 1}, \\ f_{\tilde{L}} &= \frac{1}{\exp[(E_{\tilde{L}} + \mu_s)/T] - 1}, \\ f_{\tilde{L}^\dagger} &= \frac{1}{\exp[(E_{\tilde{L}} - \mu_s)/T] - 1}. \end{aligned} \tag{5.65}$$

Furthermore in order to eliminate the dependence in the expansion of the Universe we write the equations in terms of the abundances Y_X , where $Y_X = n_X/s$.

We are interested in the evolution of sneutrinos $Y_{\tilde{N}_i}$, and the fermionic $Y_{\mathcal{L}}$ and scalar $Y_{\tilde{\mathcal{L}}}$ lepton number, defined as $Y_{\mathcal{L}} = (Y_L - Y_{\bar{L}})/2$, $Y_{\tilde{\mathcal{L}}} = (Y_{\tilde{L}} - Y_{\tilde{L}^\dagger})/2$. Here we assume that the distinguishable states in the plasma are given by Eq. (5.12), i.e., $\mu > H$, so we don't find a μ suppression of the resulting baryon asymmetry. However, in the limit $\mu \rightarrow 0$ this is not longer true. Then, one should write the Boltzmann equations for the lepton number conserving states in Eq. (5.35) and their hermitian conjugates, considering μ as a mixing term between the $L = 1$ and $L = -1$ heavy sneutrino distributions. In this case, we expect a μ suppression of the final lepton asymmetry, because when lepton number is exactly conserved ($\mu = 0$), the $L = 1$ and $L = -1$ heavy sneutrino distributions are decoupled and the final lepton asymmetry vanishes, as we discussed previously.

The number density of sneutrinos is regulated through its decays and inverse decays, defined in the decay $D - terms$, while to compute the evolution of the fermionic and scalar lepton number we also need to consider the scatterings where leptons and sleptons are involved. The scattering terms are defined in the scattering

S – terms.

$$\frac{dY_{\tilde{N}_i}}{dt} = -D_i - \bar{D}_i - \tilde{D}_i - \tilde{D}_i^\dagger \quad (5.66)$$

$$\frac{dY_{\mathcal{L}}}{dt} = \sum_i (D_i - \bar{D}_i) - 2S - S_{L\tilde{L}^\dagger} + \bar{S}_{L\tilde{L}^\dagger} - S_{L\tilde{L}} + \bar{S}_{L\tilde{L}} \quad (5.67)$$

$$\frac{dY_{\tilde{\mathcal{L}}}}{dt} = \sum_i (\tilde{D}_i - \tilde{D}_i^\dagger) - 2\tilde{S} - S_{L\tilde{L}^\dagger} + \bar{S}_{L\tilde{L}^\dagger} + S_{L\tilde{L}} - \bar{S}_{L\tilde{L}} \quad (5.68)$$

where:

$$sD_i = \Lambda_{\tilde{N}_i}^{12} \left[f_{\tilde{N}_i} (1 - f_L) (1 - f_h^{eq}) \sum_k |\hat{A}(\tilde{N}_i \rightarrow L_k h)|^2 - f_L f_h^{eq} (1 + f_{\tilde{N}_i}) \sum_k |\hat{A}(L_k h \rightarrow \tilde{N}_i)|^2 \right], \quad (5.69)$$

$$s\bar{D}_i = \Lambda_{\tilde{N}_i}^{12} \left[f_{\tilde{N}_i} (1 - f_{\bar{L}}) (1 - f_h^{eq}) \sum_k |\hat{A}(\tilde{N}_i \rightarrow \bar{L}_k \bar{h})|^2 - f_{\bar{L}} f_h^{eq} (1 + f_{\tilde{N}_i}) \sum_k |\hat{A}(\bar{L}_k \bar{h} \rightarrow \tilde{N}_i)|^2 \right], \quad (5.70)$$

$$s\tilde{D}_i = \Lambda_{\tilde{N}_i}^{12} \left[f_{\tilde{N}_i} (1 + f_{\tilde{L}}) (1 + f_H^{eq}) \sum_k |\hat{A}(\tilde{N}_i \rightarrow \tilde{L}_k H)|^2 - f_{\tilde{L}} f_H^{eq} (1 + f_{\tilde{N}_i}) \sum_k |\hat{A}(\tilde{L}_k H \rightarrow \tilde{N}_i)|^2 \right], \quad (5.71)$$

$$s\tilde{D}_i^\dagger = \Lambda_{\tilde{N}_i}^{12} \left[f_{\tilde{N}_i} (1 + f_{\tilde{L}^\dagger}) (1 + f_H^{eq}) \sum_k |\hat{A}(\tilde{N}_i \rightarrow \tilde{L}_k^\dagger H^\dagger)|^2 - f_{\tilde{L}^\dagger} f_H^{eq} (1 + f_{\tilde{N}_i}) \sum_k |\hat{A}(\tilde{L}_k^\dagger H^\dagger \rightarrow \tilde{N}_i)|^2 \right], \quad (5.72)$$

and

$$sS = \Lambda_{34}^{12} \left[f_L f_h^{eq} (1 - f_{\bar{L}}) (1 - f_h^{eq}) \sum_{k,k'} |M_{sub}(L_k h \rightarrow \bar{L}_{k'} \bar{h})|^2 - f_{\bar{L}} f_h^{eq} (1 - f_L) (1 - f_h^{eq}) \sum_{k,k'} |M_{sub}(\bar{L}_k \bar{h} \rightarrow L_{k'} h)|^2 \right], \quad (5.73)$$

$$\begin{aligned}
s\tilde{S} = & \Lambda_{34}^{12} \left[f_{\tilde{L}} f_H^{eq} (1 + f_{\tilde{L}^\dagger}) (1 + f_H^{eq}) \sum_{k,k'} |M_{sub}(\tilde{L}_k H \rightarrow \tilde{L}_{k'}^\dagger H^\dagger)|^2 - \right. \\
& \left. - f_{\tilde{L}^\dagger} f_H^{eq} (1 + f_{\tilde{L}}) (1 + f_H^{eq}) \sum_{k,k'} |M_{sub}(\tilde{L}_k^\dagger H^\dagger \rightarrow \tilde{L}_{k'} H)|^2 \right], \quad (5.74)
\end{aligned}$$

$$\begin{aligned}
sS_{L\tilde{L}^\dagger} = & \Lambda_{34}^{12} \left[f_L f_h^{eq} (1 + f_{\tilde{L}^\dagger}) (1 + f_{H^\dagger}) \sum_{k,k'} |M_{sub}(L_k h \rightarrow \tilde{L}_{k'}^\dagger H^\dagger)|^2 - \right. \\
& \left. - f_{\tilde{L}^\dagger} f_H^{eq} (1 - f_L) (1 - f_h^{eq}) \sum_{k,k'} |M_{sub}(\tilde{L}_k^\dagger H^\dagger \rightarrow L_{k'} h)|^2 \right], \quad (5.75)
\end{aligned}$$

$$\begin{aligned}
s\bar{S}_{L\tilde{L}^\dagger} = & \Lambda_{34}^{12} \left[f_{\bar{L}} f_h^{eq} (1 + f_{\tilde{L}}) (1 + f_H^{eq}) \sum_{k,k'} |M_{sub}(\bar{L}_k \bar{h} \rightarrow \tilde{L}_{k'} H)|^2 - \right. \\
& \left. - f_{\tilde{L}} f_H^{eq} (1 - f_{\bar{L}}) (1 - f_h^{eq}) \sum_{k,k'} |M_{sub}(\tilde{L}_k H \rightarrow \bar{L}_{k'} \bar{h})|^2 \right], \quad (5.76)
\end{aligned}$$

$$\begin{aligned}
sS_{L\tilde{L}} = & \Lambda_{34}^{12} \left[f_L f_h^{eq} (1 + f_{\tilde{L}}) (1 + f_H^{eq}) \sum_{k,k'} |M_{sub}(L_k h \rightarrow \tilde{L}_{k'} H)|^2 - \right. \\
& \left. - f_{\tilde{L}} f_H^{eq} (1 - f_L) (1 - f_h^{eq}) \sum_{k,k'} |M_{sub}(\tilde{L}_k H \rightarrow L_{k'} h)|^2 \right], \quad (5.77)
\end{aligned}$$

$$\begin{aligned}
s\bar{S}_{L\tilde{L}} = & \Lambda_{34}^{12} \left[f_{\bar{L}} f_h^{eq} (1 + f_{\tilde{L}^\dagger}) (1 + f_H^{eq}) \sum_{k,k'} |M_{sub}(\bar{L}_k \bar{h} \rightarrow \tilde{L}_{k'}^\dagger H^\dagger)|^2 - \right. \\
& \left. - f_{\tilde{L}^\dagger} f_H^{eq} (1 - f_{\bar{L}}) (1 - f_h^{eq}) \sum_{k,k'} |M_{sub}(\tilde{L}_k^\dagger H^\dagger \rightarrow \bar{L}_{k'} \bar{h})|^2 \right]. \quad (5.78)
\end{aligned}$$

The scattering terms are defined in terms of subtracted amplitudes, since the on-shell contribution is already taken into account through the decays and inverse decays in the decay terms. So for example:

$$|M_{sub}(L_k h \rightarrow \bar{L}_{k'} \bar{h})|^2 = |M(L_k h \rightarrow \bar{L}_{k'} \bar{h})|^2 - |M_{os}(L_k h \rightarrow \bar{L}_{k'} \bar{h})|^2, \quad (5.79)$$

where,

$$|M_{os}(L_k h \rightarrow \bar{L}_{k'} \bar{h})|^2 = \left| \hat{A}(L_k h \rightarrow \tilde{N}_i) \right|^2 \frac{\pi \delta(s - m_{\tilde{N}_i}^2)}{m_{\tilde{N}_i} \Gamma_{\tilde{N}_i}} \left| \hat{A}(\tilde{N}_i \rightarrow \bar{L}_{k'} \bar{h}) \right|^2. \quad (5.80)$$

In writing Eqs. (5.66)–(5.68) we have not included the $\Delta L = 1$ processes. They do not contribute to the out of equilibrium condition. However they can lead to a dilution of the generated \mathcal{L}_{total} . Therefore they are relevant in the exact computation of the κ factor defined in Eq. (5.106).

In order to compute the decay terms, we use the following relation between the equilibrium densities:

$$\begin{aligned} f_{\tilde{L}} f_h^{eq} (1 + f_{\tilde{N}_i}^{eq}) &= f_{\tilde{N}_i}^{eq} (1 - f_{\tilde{L}}) (1 - f_h^{eq}) e^{\mp \mu_f/T} \simeq \\ &\simeq f_{\tilde{N}_i}^{eq} (1 - f_L^{eq}) (1 - f_h^{eq}) (1 \mp Y_{\mathcal{L}}), \end{aligned} \quad (5.81)$$

$$\begin{aligned} f_{\tilde{L}^{(\dagger)}} f_H^{eq} (1 + f_{\tilde{N}_i}^{eq}) &= f_{\tilde{N}_i}^{eq} (1 + f_{\tilde{L}^{(\dagger)}}) (1 + f_H^{eq}) e^{\mp \mu_s/T} \simeq \\ &\simeq f_{\tilde{N}_i}^{eq} (1 + f_{\tilde{L}}^{eq}) (1 + f_H^{eq}) (1 \mp Y_{\tilde{L}}), \end{aligned} \quad (5.82)$$

with:

$$f_{\tilde{N}_i}^{eq} = \frac{1}{\exp[E_{\tilde{N}_i}/T] - 1}. \quad (5.83)$$

One gets:

$$\begin{aligned} D_i + \bar{D}_i &= \frac{1}{s} \Lambda_{\tilde{N}_i}^{12} \left[f_{\tilde{N}_i} (1 - f_L^{eq}) (1 - f_h^{eq}) \left(\frac{1 + \epsilon_{f_i}}{2} + \frac{1 - \epsilon_{f_i}}{2} \right) \sum_k |A_i^{f_k}|^2 - \right. \\ &\quad \left. - f_{\tilde{N}_i}^{eq} \frac{1 + f_{\tilde{N}_i}}{1 + f_{\tilde{N}_i}^{eq}} (1 - f_L^{eq}) (1 - f_h^{eq}) \times \right. \\ &\quad \left. \times \left[(1 - Y_{\mathcal{L}}) \frac{1 - \epsilon_{f_i}}{2} + (1 + Y_{\mathcal{L}}) \frac{1 + \epsilon_{f_i}}{2} \right] \sum_k |A_i^{f_k}|^2 \right] = \\ &= \left(Y_{\tilde{N}_i} \langle \Gamma_{\tilde{N}_i}^f \rangle - Y_{\tilde{N}_i}^{eq} \langle \tilde{\Gamma}_{\tilde{N}_i}^f \rangle \right) + Y_{\tilde{N}_i}^{eq} Y_{\mathcal{L}} \epsilon_{f_i} \langle \tilde{\Gamma}_{\tilde{N}_i}^f \rangle, \end{aligned}$$

where in order to write the equations in the closest to the standard notation we have defined the following average widths:

$$n_{\tilde{N}_i}^{eq} \langle \Gamma_{\tilde{N}_i}^{f, eq} \rangle = \Lambda_{\tilde{N}_i}^{12} f_{\tilde{N}_i}^{eq} (1 - f_L^{eq}) (1 - f_h^{eq}) \sum_k |A_i^{f_k}|^2 \quad (5.84)$$

$$n_{\tilde{N}_i} \langle \Gamma_{\tilde{N}_i}^f \rangle = \Lambda_{\tilde{N}_i}^{12} f_{\tilde{N}_i} (1 - f_L^{eq}) (1 - f_h^{eq}) \sum_k |A_i^{f_k}|^2 \quad (5.85)$$

$$n_{\tilde{N}_i}^{eq} \langle \tilde{\Gamma}_{\tilde{N}_i}^f \rangle = \Lambda_{\tilde{N}_i}^{12} f_{\tilde{N}_i}^{eq} \frac{(1 + f_{\tilde{N}_i})}{(1 + f_{\tilde{N}_i}^{eq})} (1 - f_L^{eq}) (1 - f_h^{eq}) \sum_k |A_i^{f_k}|^2 \quad (5.86)$$

$$n_{\tilde{N}_i}^{eq} \langle \Gamma_{\tilde{N}_i}^{s, eq} \rangle = \Lambda_{\tilde{N}_i}^{12} f_{\tilde{N}_i}^{eq} (1 + f_{\tilde{L}}^{eq}) (1 + f_H^{eq}) \sum_k |A_i^{s_k}|^2 \quad (5.87)$$

$$n_{\tilde{N}_i} \langle \Gamma_{\tilde{N}_i}^s \rangle = \Lambda_{\tilde{N}_i}^{12} f_{\tilde{N}_i} (1 + f_L^{eq}) (1 + f_H^{eq}) \sum_k |A_i^{s_k}|^2 \quad (5.88)$$

$$n_{\tilde{N}_i}^{eq} \langle \tilde{\Gamma}_{\tilde{N}_i}^s \rangle = \Lambda_{\tilde{N}_i}^{12} f_{\tilde{N}_i}^{eq} \frac{(1 + f_{\tilde{N}_i})}{(1 + f_{\tilde{N}_i}^{eq})} (1 + f_{\tilde{L}}^{eq}) (1 + f_H^{eq}) \sum_k |A_i^{s_k}|^2 \quad (5.89)$$

which verify that in equilibrium:

$$\langle \Gamma_{\tilde{N}_i}^{f(s)} \rangle = \langle \Gamma_{\tilde{N}_i^{eq}}^{f(s)} \rangle = \langle \tilde{\Gamma}_{\tilde{N}_i}^{f(s)} \rangle \quad (5.90)$$

Equivalently for the rest of terms :

$$D_i + \bar{D}_i = \left(Y_{\tilde{N}_i} \langle \Gamma_{\tilde{N}_i}^f \rangle - Y_{\tilde{N}_i}^{eq} \langle \tilde{\Gamma}_{\tilde{N}_i}^f \rangle \right) + Y_{\tilde{N}_i}^{eq} Y_{\mathcal{L}} \epsilon_{f_i} \langle \tilde{\Gamma}_{\tilde{N}_i}^f \rangle \quad (5.91)$$

$$D_i - \bar{D}_i = \epsilon_{f_i} \left(Y_{\tilde{N}_i} \langle \Gamma_{\tilde{N}_i}^f \rangle + Y_{\tilde{N}_i}^{eq} \langle \tilde{\Gamma}_{\tilde{N}_i}^f \rangle \right) + Y_{\tilde{N}_i}^{eq} Y_{\mathcal{L}} \langle \tilde{\Gamma}_{\tilde{N}_i}^f \rangle \quad (5.92)$$

$$\tilde{D}_i + \tilde{D}_i^\dagger = \left(Y_{\tilde{N}_i} \langle \Gamma_{\tilde{N}_i}^s \rangle - Y_{\tilde{N}_i}^{eq} \langle \tilde{\Gamma}_{\tilde{N}_i}^s \rangle \right) + Y_{\tilde{N}_i}^{eq} Y_{\tilde{\mathcal{L}}} \epsilon_{s_i} \langle \tilde{\Gamma}_{\tilde{N}_i}^s \rangle \quad (5.93)$$

$$\tilde{D}_i - \tilde{D}_i^\dagger = \epsilon_{s_i} \left(Y_{\tilde{N}_i} \langle \Gamma_{\tilde{N}_i}^s \rangle + Y_{\tilde{N}_i}^{eq} \langle \tilde{\Gamma}_{\tilde{N}_i}^s \rangle \right) + Y_{\tilde{N}_i}^{eq} Y_{\tilde{\mathcal{L}}} \langle \tilde{\Gamma}_{\tilde{N}_i}^s \rangle \quad (5.94)$$

Concerning scattering terms, in order to evaluate, for example, the on-shell contribution $|M_{os}(L_k h \rightarrow \bar{L}_{k'} \bar{h})|^2$ we use the following relation between the equilibrium densities:

$$(1 - f_L^{eq})(1 - f_h^{eq}) = f_{\tilde{N}_i}^{eq} e^{E_N/T} [(1 - f_L^{eq})(1 - f_h^{eq}) - f_L^{eq} f_h^{eq}] , \quad (5.95)$$

and the identity,

$$1 = \int d^4 p_N \delta^4(p_{\tilde{N}_i} - p_L - p_h) . \quad (5.96)$$

They allow us to write the on-shell contribution to the scattering terms at the required order in ϵ as:

$$\begin{aligned} \Lambda_{12}^{34} f_L f_h^{eq} (1 - f_L)(1 - f_h^{eq}) \sum_k |\hat{A}(L_k h \rightarrow \tilde{N}_i)|^2 \frac{\pi \delta(s - m_{\tilde{N}_i})}{m_{\tilde{N}_i} \Gamma_{\tilde{N}_i}^{th}} \sum_{k'} |\hat{A}(\tilde{N}_i \rightarrow \bar{L}_{k'} \bar{h})|^2 = \\ = \int \frac{d^3 p_L}{(2\pi)^3 2E_L} \frac{d^3 p_h}{(2\pi)^3 2E_h} (2\pi)^4 \delta^4(p_{\tilde{N}_i} - p_L - p_h) f_L^{av} f_h^{eq} \left(\frac{1 - \epsilon_{f_i}}{2} \right)^2 \sum_k |A_i^{fk}|^2 \times \\ \int \frac{d^4 p_{\tilde{N}_i}}{(2\pi)^4} \frac{2\pi \delta(s - m_{\tilde{N}_i})}{2m_{\tilde{N}_i} \Gamma_{\tilde{N}_i}^{th}} \int \frac{d^3 p_L}{(2\pi)^3 2E_L} \frac{d^3 p_h}{(2\pi)^3 2E_h} (2\pi)^4 \delta^4(p_{\tilde{N}_i} - p_L - p_h) \times \\ f_{\tilde{N}_i}^{eq} e^{E_N/T} [(1 - f_L^{eq})(1 - f_h^{eq}) - f_L^{eq} f_h^{eq}] \sum_{k'} |A_i^{fk'}|^2 \end{aligned} \quad (5.97)$$

Now we define the thermal width into fermion and scalars as:

$$\begin{aligned} \Gamma_{\tilde{N}_i}^{th,f} &= \frac{1}{2m_{\tilde{N}_i}} \int \frac{d^3 p_L}{(2\pi)^3 2E_L} \frac{d^3 p_h}{(2\pi)^3 2E_L} (2\pi)^4 \delta^4(p_{\tilde{N}_i} - p_L - p_h) \\ &\quad [(1 - f_L^{eq})(1 - f_h^{eq}) - f_L^{eq} f_h^{eq}] \sum_k |A_i^{fk}|^2 , \\ \Gamma_{\tilde{N}_i}^{th,s} &= \frac{1}{2m_{\tilde{N}_i}} \int \frac{d^3 p_{\tilde{L}}}{(2\pi)^3 2E_{\tilde{L}}} \frac{d^3 p_H}{(2\pi)^3 2E_H} (2\pi)^4 \delta^4(p_{\tilde{N}_i} - p_{\tilde{L}} - p_H) \\ &\quad \left[(1 + f_{\tilde{L}}^{eq})(1 + f_H^{eq}) - f_{\tilde{L}}^{eq} f_H^{eq} \right] \sum_k |A_i^{sk}|^2 . \end{aligned} \quad (5.98)$$

so that the thermal width of sneutrinos is $\Gamma_{\tilde{N}_i}^{th} = \Gamma_{\tilde{N}_i}^{th,f} + \Gamma_{\tilde{N}_i}^{th,s}$.

Using that $\int \frac{d^4 p_{\tilde{N}_i}}{(2\pi)^4} 2\pi\delta(p_{\tilde{N}_i}^2 - m_{\tilde{N}_i}^2) = \int \frac{d^3 p_{\tilde{N}_i}}{(2\pi)^3 2E_{\tilde{N}_i}}$ we can write Eq. (5.97) as:

$$\Lambda_{\tilde{N}_i}^{12} f_{\tilde{N}_i}^{eq} (1 - f_L^{eq})(1 - f_h^{eq}) \left(\frac{1 - \epsilon_{f_i}}{2} \right)^2 \sum_k |A_i^{fk}|^2 \frac{\Gamma_{\tilde{N}_i}^{th,f}}{\Gamma_{\tilde{N}_i}^{th}} = n_{\tilde{N}_i}^{eq} \frac{(1 - \epsilon_{f_i})^2}{4} \langle \Gamma_{\tilde{N}_i}^f \rangle \frac{\Gamma_{\tilde{N}_i}^{th,f}}{\Gamma_{\tilde{N}_i}^{th}}.$$

Altogether we find that:

$$S = \sum_{k,k'} \langle \sigma(L_k h \rightarrow \bar{L}_{k'} \bar{h}) - \sigma(\bar{L}_{k'} \bar{h} \rightarrow L_k h) \rangle + Y_{\tilde{N}_i}^{eq} \epsilon_{f_i} \langle \Gamma_{\tilde{N}_i}^f \rangle \frac{\Gamma_{\tilde{N}_i}^{th,f}}{\Gamma_{\tilde{N}_i}^{th}}. \quad (5.99)$$

The rest of on-shell contributions can be evaluated similarly:

$$\begin{aligned} \tilde{S} &= \sum_{k,k'} \langle \sigma(\tilde{L}_k H \rightarrow \tilde{L}_{k'}^\dagger H^\dagger) - \sigma(\tilde{L}_{k'}^\dagger H^\dagger \rightarrow \tilde{L}_k H) \rangle + Y_{\tilde{N}_i}^{eq} \epsilon_{s_i} \langle \Gamma_{\tilde{N}_i}^s \rangle \frac{\Gamma_{\tilde{N}_i}^{th,s}}{\Gamma_{\tilde{N}_i}^{th}} \\ S_{L\tilde{L}^\dagger} &= \sum_{k,k'} \langle \sigma(L_k h \rightarrow \tilde{L}_{k'}^\dagger H^\dagger) - \sigma(\tilde{L}_{k'}^\dagger H^\dagger \rightarrow L_k h) \rangle + Y_{\tilde{N}_i}^{eq} \frac{\epsilon_{f_i} + \epsilon_{s_i}}{2} \langle \Gamma_{\tilde{N}_i}^f \rangle \frac{\Gamma_{\tilde{N}_i}^{th,s}}{\Gamma_{\tilde{N}_i}^{th}} = \\ &= \sum_{k,k'} \langle \sigma(L_k h \rightarrow \tilde{L}_{k'}^\dagger H^\dagger) - \sigma(\tilde{L}_{k'}^\dagger H^\dagger \rightarrow L_k h) \rangle + Y_{\tilde{N}_i}^{eq} \frac{\epsilon_{f_i} + \epsilon_{s_i}}{2} \langle \Gamma_{\tilde{N}_i}^s \rangle \frac{\Gamma_{\tilde{N}_i}^{th,f}}{\Gamma_{\tilde{N}_i}^{th}} \\ \bar{S}_{L\tilde{L}^\dagger} &= \sum_{k,k'} \langle \sigma(\bar{L}_k \bar{h} \rightarrow \tilde{L}_{k'} H) - \sigma(\tilde{L}_{k'} H \rightarrow \bar{L}_k \bar{h}) \rangle - Y_{\tilde{N}_i}^{eq} \frac{\epsilon_{f_i} + \epsilon_{s_i}}{2} \langle \Gamma_{\tilde{N}_i}^f \rangle \frac{\Gamma_{\tilde{N}_i}^{th,s}}{\Gamma_{\tilde{N}_i}^{th}} = \\ &= \sum_{k,k'} \langle \sigma(\bar{L}_k \bar{h} \rightarrow \tilde{L}_{k'} H) - \sigma(\tilde{L}_{k'} H \rightarrow \bar{L}_k \bar{h}) \rangle - Y_{\tilde{N}_i}^{eq} \frac{\epsilon_{f_i} + \epsilon_{s_i}}{2} \langle \Gamma_{\tilde{N}_i}^s \rangle \frac{\Gamma_{\tilde{N}_i}^{th,f}}{\Gamma_{\tilde{N}_i}^{th}} \\ S_{L\tilde{L}} &= \sum_{k,k'} \langle \sigma(L_k h \rightarrow \tilde{L}_{k'} H) - \sigma(\tilde{L}_{k'} H \rightarrow L_k h) \rangle + Y_{\tilde{N}_i}^{eq} \frac{\epsilon_{f_i} - \epsilon_{s_i}}{2} \langle \Gamma_{\tilde{N}_i}^f \rangle \frac{\Gamma_{\tilde{N}_i}^{th,s}}{\Gamma_{\tilde{N}_i}^{th}} = \\ &= \sum_{k,k'} \langle \sigma(L_k h \rightarrow \tilde{L}_{k'} H) - \sigma(\tilde{L}_{k'} H \rightarrow L_k h) \rangle - Y_{\tilde{N}_i}^{eq} \frac{\epsilon_{f_i} - \epsilon_{s_i}}{2} \langle \Gamma_{\tilde{N}_i}^s \rangle \frac{\Gamma_{\tilde{N}_i}^{th,f}}{\Gamma_{\tilde{N}_i}^{th}} \\ \bar{S}_{L\tilde{L}} &= \sum_{k,k'} \langle \sigma(\bar{L}_k \bar{h} \rightarrow \tilde{L}_{k'}^\dagger H^\dagger) - \sigma(\tilde{L}_{k'}^\dagger H^\dagger \rightarrow \bar{L}_k \bar{h}) \rangle - Y_{\tilde{N}_i}^{eq} \frac{\epsilon_{f_i} - \epsilon_{s_i}}{2} \langle \Gamma_{\tilde{N}_i}^f \rangle \frac{\Gamma_{\tilde{N}_i}^{th,s}}{\Gamma_{\tilde{N}_i}^{th}} = \\ &= \sum_{k,k'} \langle \sigma(\bar{L}_k \bar{h} \rightarrow \tilde{L}_{k'}^\dagger H^\dagger) - \sigma(\tilde{L}_{k'}^\dagger H^\dagger \rightarrow \bar{L}_k \bar{h}) \rangle - Y_{\tilde{N}_i}^{eq} \frac{\epsilon_{f_i} - \epsilon_{s_i}}{2} \langle \Gamma_{\tilde{N}_i}^s \rangle \frac{\Gamma_{\tilde{N}_i}^{th,f}}{\Gamma_{\tilde{N}_i}^{th}} \end{aligned}$$

Altogether we can write the Boltzmann equations for the sneutrinos and leptonic numbers ²:

$$\begin{aligned} \frac{dY_{\tilde{N}_i}}{dt} = & -Y_{\tilde{N}_i} \left(\langle \Gamma_{\tilde{N}_i}^f \rangle + \langle \Gamma_{\tilde{N}_i}^s \rangle \right) + Y_{\tilde{N}_i}^{eq} \left(\langle \tilde{\Gamma}_{\tilde{N}_i}^f \rangle + \langle \tilde{\Gamma}_{\tilde{N}_i}^s \rangle \right) - \\ & -Y_{\tilde{N}_i}^{eq} \left(Y_{\mathcal{L}} \epsilon_{f_i} \langle \tilde{\Gamma}_{\tilde{N}_i}^f \rangle + Y_{\tilde{\mathcal{L}}} \epsilon_{s_i} \langle \tilde{\Gamma}_{\tilde{N}_i}^s \rangle \right) \end{aligned} \quad (5.100)$$

$$\begin{aligned} \frac{dY_{\mathcal{L}}}{dt} = & \sum_i \left[\epsilon_{f_i} \left(Y_{\tilde{N}_i} \langle \Gamma_{\tilde{N}_i}^f \rangle + Y_{\tilde{N}_i}^{eq} \langle \tilde{\Gamma}_{\tilde{N}_i}^f \rangle - 2Y_{\tilde{N}_i}^{eq} \langle \Gamma_{\tilde{N}_i}^f \rangle \right) + Y_{\tilde{N}_i}^{eq} Y_{\mathcal{L}} \langle \tilde{\Gamma}_{\tilde{N}_i}^f \rangle \right] - \\ & - \langle 2\sigma(Lh \rightarrow \bar{L}\bar{h}) + \sigma(Lh \rightarrow \tilde{L}^\dagger H^\dagger) + \sigma(Lh \rightarrow \tilde{L}H) \rangle + \\ & + \langle 2\sigma(\bar{L}\bar{h} \rightarrow Lh) + \sigma(\bar{L}\bar{h} \rightarrow \tilde{L}H) + \sigma(\bar{L}\bar{h} \rightarrow \tilde{L}^\dagger H^\dagger) \rangle - \\ & - \langle \sigma(\tilde{L}H \rightarrow \bar{L}\bar{h}) - \sigma(\tilde{L}H \rightarrow Lh) \rangle + \\ & + \langle \sigma(\tilde{L}^\dagger H^\dagger \rightarrow Lh) - \sigma(\tilde{L}^\dagger H^\dagger \rightarrow \bar{L}\bar{h}) \rangle \end{aligned} \quad (5.101)$$

$$\begin{aligned} \frac{dY_{\tilde{\mathcal{L}}}}{dt} = & \sum_i \left[\epsilon_{s_i} \left(Y_{\tilde{N}_i} \langle \Gamma_{\tilde{N}_i}^s \rangle + Y_{\tilde{N}_i}^{eq} \langle \tilde{\Gamma}_{\tilde{N}_i}^s \rangle - 2Y_{\tilde{N}_i}^{eq} \langle \Gamma_{\tilde{N}_i}^s \rangle \right) + Y_{\tilde{N}_i}^{eq} Y_{\tilde{\mathcal{L}}} \langle \tilde{\Gamma}_{\tilde{N}_i}^s \rangle \right] - \\ & - \langle 2\sigma(\tilde{L}H \rightarrow \tilde{L}^\dagger H^\dagger) + \sigma(\tilde{L}H \rightarrow \bar{L}\bar{h}) + \sigma(\tilde{L}H \rightarrow Lh) \rangle + \\ & + \langle 2\sigma(\tilde{L}^\dagger H^\dagger \rightarrow \tilde{L}H) + \sigma(\tilde{L}^\dagger H^\dagger \rightarrow Lh) + \sigma(\tilde{L}^\dagger H^\dagger \rightarrow \bar{L}\bar{h}) \rangle - \\ & - \langle \sigma(Lh \rightarrow \tilde{L}^\dagger H^\dagger) - \sigma(Lh \rightarrow \tilde{L}H) \rangle + \\ & + \langle \sigma(\bar{L}\bar{h} \rightarrow \tilde{L}H) - \sigma(\bar{L}\bar{h} \rightarrow \tilde{L}^\dagger H^\dagger) \rangle \end{aligned} \quad (5.102)$$

The out of equilibrium condition is verified since using Eq. (5.90) the first term of Eq. (5.100) and the ϵ terms of Eqs. (5.101) and (5.102) cancel out in thermal equilibrium.

The Boltzmann equation for the total lepton number can be written as (here we use $\epsilon_{s_i} = -\epsilon_{f_i} = \bar{\epsilon}_i$):

$$\begin{aligned} \frac{dY_{\mathcal{L}_{total}}}{dt} = & \sum_i \bar{\epsilon}_i \left[Y_{\tilde{N}_i} \left(\langle \Gamma_{\tilde{N}_i}^s \rangle - \langle \Gamma_{\tilde{N}_i}^f \rangle \right) + Y_{\tilde{N}_i}^{eq} \left(\langle \tilde{\Gamma}_{\tilde{N}_i}^s \rangle - \langle \tilde{\Gamma}_{\tilde{N}_i}^f \rangle \right) - \right. \\ & - 2Y_{\tilde{N}_i}^{eq} \left(\langle \Gamma_{\tilde{N}_i}^s \rangle - \langle \Gamma_{\tilde{N}_i}^f \rangle \right) + Y_{\tilde{N}_i}^{eq} \left(Y_{\mathcal{L}} \tilde{\Gamma}_{\tilde{N}_i}^f + Y_{\tilde{\mathcal{L}}} \tilde{\Gamma}_{\tilde{N}_i}^s \right) \left. \right] + \\ & + \text{scattering terms} \\ \simeq & \sum_i \left[\langle \Gamma_{\tilde{N}_i}^s \rangle \left(Y_{\tilde{N}_i} - Y_{\tilde{N}_i}^{eq} \right) \epsilon_i^{eff}(T) + Y_{\tilde{N}_i}^{eq} \left(Y_{\mathcal{L}} \tilde{\Gamma}_{\tilde{N}_i}^f + Y_{\tilde{\mathcal{L}}} \tilde{\Gamma}_{\tilde{N}_i}^s \right) \right] + s. t. \end{aligned} \quad (5.103)$$

with $\langle \Gamma_{\tilde{N}_i}^s \rangle = \langle \Gamma_{\tilde{N}_i}^f \rangle + \langle \Gamma_{\tilde{N}_i}^s \rangle$.

²Here we have suppressed flavor indices in the two body $\Delta L = 2$ scattering terms for the sake of simplicity, but a sum over all flavors in initial and final states should be understood.

In the last line we have used that at $\mathcal{O}(\epsilon)$ we can neglect the difference between $f_{\tilde{N}_i}$ and $f_{\tilde{N}_i}^{eq}$ in the definitions of the thermal average widths and we have defined the effective T dependent total asymmetry:

$$\epsilon_i^{eff}(T) = \bar{\epsilon}_i \frac{\langle \Gamma_{\tilde{N}_i}^s \rangle - \langle \Gamma_{\tilde{N}_i}^f \rangle}{\langle \Gamma_{\tilde{N}_i}^f \rangle + \langle \Gamma_{\tilde{N}_i}^s \rangle}, \quad (5.104)$$

which in the approximate decay at rest takes the form Ref.[74, 75, 76]:

$$\epsilon_i(T) = \bar{\epsilon}_i \frac{c_s - c_f}{c_s + c_f}. \quad (5.105)$$

5.6 Results

We now quantify the conditions on the parameters which can be responsible for a successful leptogenesis.

The final amount of $\mathcal{B} - \mathcal{L}$ asymmetry $Y_{\mathcal{B}-\mathcal{L}} = n_{\mathcal{B}-\mathcal{L}}/s$ generated by the decay of the four light singlet sneutrino states \tilde{N}_i assuming no pre-existing asymmetry and thermal initial sneutrino densities can be parametrized as:

$$Y_{\mathcal{B}-\mathcal{L}} = -\kappa \sum_i \epsilon_i(T_d) Y_{\tilde{N}_i}^{eq}(T \gg M_i). \quad (5.106)$$

$\epsilon_i(T)$ is given in Eq. (5.25) and T_d is the temperature at the time of decay defined by the condition that the decay width is equal to the expansion rate of the universe: $\Gamma = H(T_d)$, where the Hubble parameter $H = 1.66 g_*^{1/2} \frac{T^2}{m_{pl}}$, $m_{pl} = 1.22 \cdot 10^{19}$ GeV is the Planck mass and g_* counts the effective number of spin-degrees of freedom in thermal equilibrium, $g_* = 228.75$ in the MSSM. Furthermore $Y_{\tilde{N}_i}^{eq}(T \gg M_i) = 90\zeta(3)/(4\pi^4 g_*)$.

In Eq. (5.106) $\kappa \lesssim 1$ is a dilution factor which takes into account the possible inefficiency in the production of the singlet sneutrinos, the erasure of the generated asymmetry by L -violating scattering processes and the temperature dependence of the CP asymmetry $\epsilon_i(T)$. The precise value of κ can only be obtained from numerical solution of the Boltzmann equations. Moreover, in general, the result depends on how the lepton asymmetry is distributed in the three lepton flavors [62, 63, 64]. For simplicity we will ignore flavor issues. Furthermore, in what follows we will use an approximate constant value $\kappa = 0.2$.

After conversion by the sphaleron transitions, the final baryon asymmetry is related to the $\mathcal{B} - \mathcal{L}$ asymmetry by:

$$Y_{\mathcal{B}} = \frac{24 + 4n_H}{66 + 13n_H} Y_{\mathcal{B}-\mathcal{L}}, \quad (5.107)$$

where n_H is the number of Higgs doublets. For the MSSM:

$$Y_{\mathcal{B}} = -8.4 \times 10^{-4} \kappa \sum_i \epsilon_i(T_d) \quad (5.108)$$

This has to be compared with the WMAP measurements [52]: $Y_B = (8.7_{-0.4}^{+0.3}) \times 10^{-11}$.

Altogether we find that (for maximal CP violating phase $\sin \phi = 1$):

$$\frac{4 |B_{SN} A| \Gamma}{4 |B_{SN}|^2 + |M|^2 \Gamma^2} \frac{c_s(T_d) - c_f(T_d)}{c_s(T_d) + c_f(T_d)} \gtrsim 2.6 \times 10^{-7}. \quad (5.109)$$

Further constraints arise from the timing of the decay. First, successful leptogenesis requires the singlet sneutrinos to decay out of equilibrium: its decay width must be smaller than the expansion rate of the Universe $\Gamma < H|_{T=M}$, with Γ given in Eq. (5.13),

$$\frac{M \sum_k |Y_{1k}|^2}{8\pi} < 1.66 g_*^{1/2} \frac{M^2}{m_{pl}}. \quad (5.110)$$

This condition gives an upper bound:

$$\sum_k |Y_{1k}|^2 \left(\frac{10^8 \text{ GeV}}{M} \right) < 5 \times 10^{-9}. \quad (5.111)$$

Second, in order for the generated lepton asymmetry to be converted into a baryon asymmetry via the B-L violating sphaleron processes, the singlet sneutrino decay should occur before the electroweak phase transition:

$$\Gamma > H(T \sim 100 \text{ GeV}) \Rightarrow M \sum_k |Y_{1k}|^2 \geq 2.6 \times 10^{-13} \text{ GeV}. \quad (5.112)$$

The combination of Eqs. (5.111) and (5.112) determines a range for the possible values of $\sum |Y_{1k}|^2$ for a given M :

$$2.6 \times 10^{-21} \left(\frac{10^8 \text{ GeV}}{M} \right) < \sum_k |Y_{1k}|^2 < 5 \times 10^{-9} \left(\frac{M}{10^8 \text{ GeV}} \right). \quad (5.113)$$

We now turn to the consequences that these constraints may have for the neutrino mass predictions in this scenario. Without loss of generality one can work in the basis in which M_{ij} is diagonal. In that basis the light neutrino masses, Eq. (5.2), are:

$$m_{\nu ij} = 3 \times 10^{-3} \text{ eV} \left(\frac{v}{175 \text{ GeV}} \right)^2 \sum_{kl} Y_{li} \frac{10^8 \text{ GeV}}{M_l} \frac{10^8 \text{ GeV}}{M_k} \frac{\mu_{kl}}{\text{GeV}} Y_{kj}, \quad (5.114)$$

where $v = \langle H \rangle$ is the Higgs vev.

It is clear from Eq. (5.114) that the out of equilibrium condition, Eq. (5.111), implies that the contribution of the lightest pseudo-Dirac singlet neutrino generation to the neutrino mass is negligible. Consequently, to reproduce the observed mass differences Δm_{21}^2 and Δm_{31}^2 , the dominant contribution to the neutrino masses must arise from the exchange of the heavier singlet neutrino states.

This can be easily achieved, for example, in the single right-handed neutrino dominance mechanism (SRHND) [133]. These models naturally explain the strong hierarchy in the masses and the large mixing angle present in the light neutrino sector. In particular, in the simple case in which the matrix μ and M are simultaneously diagonalizable, the results in Ref. [133] imply that for the inverse see-saw model with three generations of singlet neutrinos, the SRHND condition is attained if there is a strong hierarchy:

$$\mu_3 \frac{Y_{3k} Y_{3k'}}{M_3} \gg \mu_2 \frac{Y_{2l} Y_{2l'}}{M_2} \gg \mu_1 \frac{Y_{1l} Y_{1l'}}{M_1}. \quad (5.115)$$

Generically this means that the out of equilibrium condition requires the neutrino mass spectrum to be strongly hierarchical, $m_1 \ll m_2 < m_3$.

Conversely this implies that the measured neutrino masses do not impose any constraint on the combination of Yukawa couplings and sneutrino masses which is relevant for the generation of the lepton asymmetry which can be taken as an independent parameter in the evaluation of the asymmetry.

Finally we plot in Fig. 5.1 the range of parameters $\sum |Y_{1k}|^2$ and B_{SN} for which enough asymmetry is generated, Eq. (5.109), and the out of equilibrium and pre-electroweak phase transition decay conditions, Eq. (5.113) are verified. We show the ranges for three values of M and for the characteristic value of $A = m_{SUSY} = 10^3$ GeV.

From the figure we see that this mechanism works for relatively small values of M ($< 10^9$ GeV). The smaller is M , the smaller are the yukawas $\sum |Y_{1k}|^2$. Also, in total analogy with the standard seesaw [74, 75, 76], the value of the soft supersymmetry-breaking bilinear B_{SN} , is well below the expected value Mm_{SUSY} . The reason is that, in order to generate an asymmetry large enough $B_{SN} \sim M\Gamma$, but Γ is very small if the sneutrinos decay out of equilibrium, $\Gamma \leq 1$ GeV $\left(\frac{M}{10^9 \text{ GeV}}\right)^2$. A small B term with large CP phase can be realized naturally for example within the framework of gauge mediated supersymmetry breaking [134] or in warped extra dimensions [135].

Given the small required values of B_{SN} one can question the expansion in the small parameters in Eq. (5.10). As described at the end of Sec. 5.3 in order to verify the stability of the results we have redone the computation of the CP asymmetry keeping all the entries in the sneutrino mass matrix, and just assuming that it is real. We have found that as long as $|B_{SN}| \gg |B_S|, |\mu|^2$ the total CP asymmetry is always proportional to B_{SN} , and presents the same resonant behaviour, so that it is still significant only for $B_{SN} \ll Mm_{SUSY}$.

In summary in this work we have studied the conditions for successful soft leptogenesis in the context of the supersymmetric inverse seesaw mechanism. In this model the lepton sector is extended with two electroweak singlet superfields to which opposite lepton number can be assigned. This scheme is characterized by a small lepton number violating Majorana mass term μ with the effective light neutrino mass being $m_\nu \propto \mu$. The scalar sector contains four single sneutrino states per generation and, after supersymmetry breaking, their interaction lagrangian contains both L -conserving and L -violating soft supersymmetry-breaking bilinear B -terms

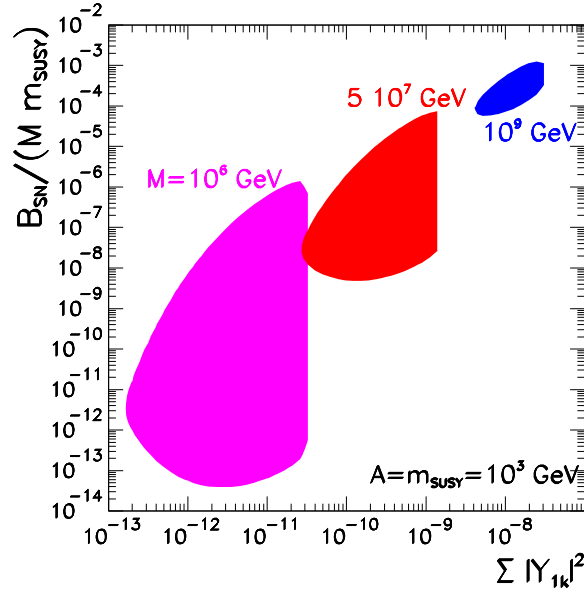


Figure 5.1: $\sum_k |Y_{1k}|^2 - B_{SN}$ regions in which enough CP asymmetry can be generated (Eq. (5.109)) and the non-equilibrium condition in the sneutrino decay, Eq. (5.110) and decay before the electroweak phase transition, Eq. (5.112) are verified. We take $A = m_{SUSY} = 10^3$ GeV. The regions correspond to $M = 10^6$, 5×10^7 , and 10^9 GeV, from left to right.

which together with the μ parameter give a small mass splitting between the four singlet sneutrino states of a single generation. In combination with the trilinear soft supersymmetry breaking terms they also provide new CP violating phases needed to generate a lepton asymmetry in the singlet sneutrino decays.

We have computed the relevant lepton asymmetry and we find in that, as long as the L -conserving B -term, B_{SN} , is not much smaller than the L -violating couplings, the asymmetry is proportional to B_{SN} and it is not suppressed by any L -violating parameter. As in the standard see-saw case, the asymmetry displays a resonance behaviour with the maximum value of the asymmetry being obtained when the largest mass splitting, $2B_{SN}/M$, is of the order of the singlet sneutrinos decay width, Γ . Consequently we find that this mechanism can lead to successful leptogenesis only for relatively small values of B_{SN} . The right-handed neutrino masses are low enough to elude the gravitino problem. Also, the out of equilibrium decay condition implies that the Yukawa couplings involving the lightest of the right-handed neutrinos are constrained to be very small which, for the naturally small values of the L -violating parameter μ , implies that the neutrino mass spectrum has to be strongly hierarchical.

Chapter 6

Neutrino mass hierarchy and Majorana CP phases within the Higgs Triplet Model at LHC

6.1 Introduction

In this chapter, where we show the results obtained in work [4], we consider that the source of neutrino masses is a scalar triplet $\Delta = (\Delta^{\pm\pm}, \Delta^\pm, \Delta^0)$. As we described in section 1.3.2, when the neutral component of the triplet acquires a vacuum expectation value v_T , a Majorana mass term for neutrinos is generated at tree level, proportional to v_T :

$$\mathcal{L}_\Delta = -\lambda_{\alpha\beta} l_{L_\alpha}^T C^{-1} i\tau_2 \Delta l_{L_\beta} + \text{h.c.} \rightarrow -\frac{1}{2} \nu_{L_\alpha}^T C^{-1} m_{\nu_{\alpha\beta}} \nu_{L_\beta} + \text{h.c.} , \quad (6.1)$$

with:

$$m_{\nu_{\alpha\beta}} = \sqrt{2} v_T \lambda_{\alpha\beta} . \quad (6.2)$$

We assume that the triplet states have masses not too far from the electroweak scale. A Higgs triplet slightly below the TeV scale is the generic situation in Little Higgs theories [34], see [35] for a discussion of neutrino masses in this framework. Other examples for models with TeV scale triplets responsible for neutrino masses can be found, e.g., in [136, 137, 138]. Our phenomenological analysis does not rely on a specific model realization, apart from the assumption that neutrino masses arise from a triplet with masses in the TeV range.

The hypothesis of such a Higgs triplet can be tested at collider experiments. In particular, if kinematically accessible, the doubly charged component of the triplet Δ^{++} will be produced in high energy collisions, and its decay into two equally charged leptons provides a rather spectacular signature, basically free of any Standard Model background. This process has been studied extensively in the literature (see [139, 140, 141, 142, 143, 144, 145, 40, 41] for an incomplete list), and has been used to look for doubly charged scalars at LEP [146] and Tevatron [147]. These

searches resulted in lower bounds for the mass of the order $M_{\Delta^{++}} \gtrsim 130$ GeV. Therefore, we will consider in the following masses in the range $130 \text{ GeV} \lesssim M_{\Delta^{++}} \lesssim 1 \text{ TeV}$, above the present bound but still in reach for LHC.

If the Higgs triplet is responsible for the neutrino mass the decay rate for $\Delta^{++} \rightarrow \ell_\alpha^+ \ell_\beta^+$ is proportional to the modulus of the corresponding element of the neutrino mass matrix $|m_{\nu_{\alpha\beta}}|^2$. This opens a phenomenologically very interesting link between neutrino and collider physics¹, and by the observation of like-sign lepton events at LHC a direct test of the neutrino mass matrix becomes possible. In our work we assume that a doubly charged Higgs is indeed discovered at LHC, and we use the information from the decays $\Delta^{++} \rightarrow \ell_\alpha^+ \ell_\beta^+$ to learn something about neutrinos, under the hypothesis that the neutrino mass matrix is dominantly generated by the triplet VEV.

Current neutrino data leave some ambiguities for the neutrino mass spectrum. The neutrino mass states can be ordered normally or inverted, and the masses can be hierarchical or quasi-degenerate. We show that under the above assumptions actually LHC might play a decisive role in distinguishing these possibilities. Furthermore, we show that it might be possible to determine the Majorana phases [38, 153] in the lepton mixing matrix, which in general is a very difficult task. Implications of the different possibilities of the neutrino mass spectrum for the decay of a doubly charged scalar in the Higgs triplet model have been considered previously in [154], see also [145]. Building upon the results obtained there, we perform a full parameter scan including all complex phases, which—as we will see—play a crucial role for the relevant observables.

6.2 Doubly charged scalars at the LHC

At the LHC the process

$$pp \rightarrow \Delta^{++} \Delta^{--} \rightarrow \ell^+ \ell^+ \ell^- \ell^- \quad (6.3)$$

provides a very spectacular signature, namely two like-sign lepton pairs with the same invariant mass and no missing transverse momentum, which has essentially no Standard Model background. The pair production of the doubly charged scalar occurs by the Drell-Yan process $q\bar{q} \rightarrow \gamma^*, Z^* \rightarrow \Delta^{--} \Delta^{++}$, with a sub-dominant contribution also from two-photon fusion $\gamma\gamma \rightarrow \Delta^{--} \Delta^{++}$. The cross section is not suppressed by any small quantity (such as the Yukawas or the triplet VEV) and depends only on the mass $M_{\Delta^{++}}$, see e.g. [141, 41]. QCD corrections at next-to-leading order have been calculated [143].² The cross section for $\Delta^{--} \Delta^{++}$ pair

¹Such a link exists also in other classes of models, see for example [148, 47, 149, 150, 151, 152, 45]. However, in most cases the connection between collider signals and the neutrino mass matrix is much less direct as in the Higgs triplet model.

²Let us note that—depending on the mass splitting between the double and single charged components of the triplet—also the channel $q\bar{q} \rightarrow \Delta^{\pm\pm} \Delta^\mp$ may significantly contribute to the production of doubly charged scalars, see e.g. [142, 145].

production at the LHC ranges from 100 fb for a Higgs mass $M_{\Delta^{++}} = 200$ GeV to 0.1 fb for $M_{\Delta^{++}} = 900$ GeV [41]. Hence, if the doubly charged scalar is not too heavy a considerable number of them will be produced at LHC assuming an integrated luminosity of order 100 fb^{-1} .

The rate for the decay $\Delta^{++} \rightarrow \ell_\alpha^+ \ell_\beta^+$ is given by

$$\Gamma(\Delta^{++} \rightarrow \ell_\alpha^+ \ell_\beta^+) = \frac{1}{4\pi(1 + \delta_{\alpha\beta})} |\lambda_{\alpha\beta}|^2 M_{\Delta^{++}}, \quad (6.4)$$

with $\delta_{\alpha\beta} = 1$ (0) for $\alpha = \beta$ ($\alpha \neq \beta$). Hence, the rate is proportional to the corresponding element of the neutrino mass matrix $|m_{\nu_{\alpha\beta}}|^2$. This observation is the basis of our analysis. Using Eqs. (6.2,6.4) the branching ratio can be expressed as:

$$\text{BR}_{\alpha\beta} \equiv \text{BR}(\Delta^{++} \rightarrow \ell_\alpha^+ \ell_\beta^+) \equiv \frac{\Gamma(\Delta^{++} \rightarrow \ell_\alpha^+ \ell_\beta^+)}{\sum_{\delta\rho} \Gamma(\Delta^{++} \rightarrow \ell_\delta^+ \ell_\rho^+)} = \frac{2}{(1 + \delta_{\alpha\beta})} \frac{|m_{\nu_{\alpha\beta}}|^2}{\sum_{\delta\rho} |m_{\nu_{\delta\rho}}|^2}, \quad (6.5)$$

where m_0 denotes the lightest neutrino mass eigenstate, $m_0 = m_1$ for Normal Hierarchy (NH) and $m_0 = m_3$ for Inverted Hierarchy (IH). We write the neutrino mass matrix in terms of the PMNS mixing matrix Eq. (1.2), $m_\nu = U \text{diag}(m_1, m_2, m_3) U^T$. Making use of the unitarity of U it follows:

$$\sum_{\delta\rho} |m_{\nu_{\delta\rho}}|^2 = \sum_{i=1}^3 m_i^2 = \begin{cases} 3m_0^2 + \Delta m_{21}^2 + \Delta m_{31}^2 & \text{(NH)} \\ 3m_0^2 + \Delta m_{21}^2 + 2|\Delta m_{31}^2| & \text{(IH)} \end{cases}. \quad (6.6)$$

In addition to the lepton channel the doubly charged Higgs can in principle decay also into the following two-body final states including singly charged Higgses and/or the W :

$$\Delta^{++} \rightarrow \Delta^+ \Delta^+, \quad \Delta^{++} \rightarrow \Delta^+ W^+, \quad \Delta^{++} \rightarrow W^+ W^+. \quad (6.7)$$

The first two decay modes depend on the mass splitting within the triplet. We assume in the following that they are kinematically suppressed. The rate for the WW mode is given by

$$\Gamma(\Delta^{++} \rightarrow W^+ W^+) \approx \frac{v_T^2 M_{\Delta^{++}}^3}{2\pi v^4}, \quad (6.8)$$

where $v = 246$ GeV is the VEV of the Standard Model Higgs doublet, and we have used $M_{\Delta^{++}} \gg M_W$, see e.g. [41] for full expressions and a discussion of possibilities to observe this process at LHC. Hence, the branching ratio between $\ell^+ \ell^+$ and $W^+ W^+$ decays is controlled by the relative magnitude of the triplet Yukawas $\lambda_{\alpha\beta}$ and the VEV v_T . The requirement $\Gamma(\Delta^{++} \rightarrow W^+ W^+) \lesssim \Gamma(\Delta^{++} \rightarrow \ell_\alpha^+ \ell_\beta^+)$, together with the constraint on neutrino masses from cosmology $v_T \lambda_{\alpha\beta} \lesssim 10^{-10}$ GeV implies:

$$\frac{v_T}{v} \lesssim 10^{-6} \left(\frac{100 \text{ GeV}}{M_{\Delta^{++}}} \right)^{1/2}. \quad (6.9)$$

The triplet VEV contributes to the ρ parameter at tree level as [32] $\rho \approx 1 - 2(v_T/v)^2$. The constraint from electroweak precision data $\rho = 1.0002^{+0.0024}_{-0.0009}$ at 2σ [50] translates into $v_T/v < 0.02$, which is savely satisfied by requiring Eq. (6.9).

In this model contributions to lepton flavor violating processes, $g_\mu - 2$, and in principle also to the electron electric dipole moment are expected, see e.g. [154, 155, 42] and references therein. Following Refs. [154, 42], the most stringent constraint on the Yukawa couplings λ_{ab} comes from $\mu \rightarrow eee$, a process which occurs at tree level via Eq. (6.1). The branching ratio for this decay is given by [42]:

$$\text{BR}(\mu \rightarrow eee) = \frac{1}{4G_F^2} \frac{|\lambda_{ee}^* \lambda_{e\mu}|^2}{M_{\Delta^{++}}^4} \approx 20 \left(\frac{M_{\Delta^{++}}}{100 \text{ GeV}} \right)^{-4} |\lambda_{ee}^* \lambda_{e\mu}|^2. \quad (6.10)$$

Hence, the experimental bound $\text{BR}(\mu \rightarrow eee) < 10^{-12}$ [50] constrains the combination $|\lambda_{ee}^* \lambda_{e\mu}| \lesssim 2 \times 10^{-7} (M_{\Delta^{++}}/100 \text{ GeV})^2$. Assuming that all λ_{ab} have roughly the same order of magnitude we obtain an estimate for the interesting range of the Yukawa couplings:

$$4 \times 10^{-7} \left(\frac{M_{\Delta^{++}}}{100 \text{ GeV}} \right)^{1/2} \lesssim \lambda_{ab} \lesssim 5 \times 10^{-4} \left(\frac{M_{\Delta^{++}}}{100 \text{ GeV}} \right), \quad (6.11)$$

where the lower bound emerges from Eq. (6.9) assuming that the cosmological bound is saturated. We see that several orders of magnitude are available for the Yukawa couplings. For $\lambda_{\alpha\beta}$ close to the lower bound of Eq. (6.11) the decay $\Delta^{++} \rightarrow W^+W^+$ will become observable at LHC, whereas close to the upper bound a signal in future searches for lepton flavor violation is expected, where the details depend on the structure of the neutrino mass matrix [154, 42]. The interval for the Yukawas from Eq. (6.11) implies a triplet VEV roughly in the keV to MeV range.

Let us note that in the minimal version of this model the Baryon Asymmetry of the Universe cannot be generated by leptogenesis, and one has to invoke some other mechanism beyond the model. However, in this case lepton number violating decays of the doubly charged scalar of the model might destroy the pre-generated baryon asymmetry.³ To avoid this to happen one has to require that these decays never come into equilibrium before the electroweak phase transition [156]. This translates into a much stronger upper bound on the yukawas than the one given above: $2 \times 10^{-5} \lesssim \lambda_{ab} \lesssim 5 \times 10^{-4}$, for $M_{\Delta^{++}} = 100 \text{ GeV}$.

The basic assumption in our analysis is that a sufficient number of like-sign leptons is observed. If some of the decay modes of Eq. (6.7) are present the number of dilepton events will be reduced according to the branching. If enough events from both types of decay (leptonic and non-leptonic) were observed in principle an order of magnitude estimate for the Yukawa couplings $\lambda_{\alpha\beta}$ and the triplet VEV v_T might be possible [141, 145]. Here we do not consider this case and use only dilepton events, and therefore, we do not obtain any information on the overall scale of the $\lambda_{\alpha\beta}$ in addition to Eq. (6.11).

³We thank Hitoshi Murayama for pointing out this problem to us.

6.3 Numerical analysis and results

6.3.1 Description of the analysis

As mentioned above, we focus in our analysis on the process Eq. (6.3), which provides the clean signal of four leptons, where the like-sign lepton pairs have the same invariant mass, namely the mass of the doubly charged Higgs. Given the fact that the branching $\Delta^{++} \rightarrow \ell_\alpha^+ \ell_\beta^+$ is proportional to the neutrino mass matrix, one expects all possible flavor combinations of the four leptons to occur, including lepton flavor violating ones. In reference [41] simple cuts have been defined for final states consisting of electrons and muons, eliminating essentially any Standard Model background.

In general tau reconstruction is experimentally more difficult because of the missing transverse energy from neutrinos. However, in the case of interest enough kinematic constraints should be available to identify also events involving taus. It turns out that the inclusion of such events significantly increases the sensitivity for neutrino parameters. Therefore, following [40], we assume that events where one of the four leptons is a tau can also be reconstructed.⁴ This should be possible efficiently, despite the complications involving the tau reconstruction, since the invariant mass is known from decays without tau, which can be used as kinematic constraint for events of the type $\ell^\pm \ell^\pm \ell^\mp \tau^\mp$ for $\ell = e$ or μ . Furthermore, one can adopt the assumption that the neutrinos carrying away the missing energy are aligned with the tau.

In principle it is difficult to distinguish a primary electron or muon from the ones originating from leptonic tau decays. Since here we are interested in investigating the flavor structure of the decays, leptonically decaying taus might be a “background” for the Higgs decays into electrons and muons, and vice versa. However, due to the energy carried away by the two neutrinos from the leptonic tau decay, a cut on the invariant mass of the like-sign leptons should eliminate such a confusion very efficiently. It is beyond the scope of our work to perform a detailed simulation and event reconstruction study. The above arguments suggest that our assumptions are suitable to estimate the sensitivity of the Higgs decays for neutrino parameters by the procedure outlined in the following.

We define as our five observables the number of like-sign lepton pairs with the flavor combinations

$$x = (ee), (e\mu), (\mu\mu), (e\tau), (\mu\tau). \quad (6.12)$$

Note that these five branchings contain the full information, since $\text{BR}_{\tau\tau}$, which we do not use explicitly, is fixed by $\text{BR}_{\tau\tau} = 1 - \sum_x \text{BR}_x$. Taking into account the number of occurrences of the combinations in Eq. (6.12) in four leptons where at

⁴To be conservative we do not include events with more than one tau, since already the inclusion of events with one tau provides enough information for our purposes.

most one tau is allowed, the number of events in each channel is obtained as:

$$\begin{aligned}
 N_{\alpha\beta} &= 2N_{2\Delta} \epsilon \text{BR}_{\alpha\beta} \sum_x \text{BR}_x & \text{for } (\alpha\beta) &= (ee), (e\mu), (\mu\mu), \\
 N_{\alpha\beta} &= 2N_{2\Delta} \epsilon \text{BR}_{\alpha\beta} (\text{BR}_{ee} + \text{BR}_{e\mu} + \text{BR}_{\mu\mu}) & \text{for } (\alpha\beta) &= (e\tau), (\mu\tau),
 \end{aligned} \tag{6.13}$$

where $N_{2\Delta}$ is the total number of doubly charged scalar pairs decaying into four leptons, and ϵ is the detection efficiency for the four lepton events. For simplicity we assume here a flavor independent efficiency. The branching ratios are given in Eq. (6.5). To illustrate the sensitivity to neutrino parameters we will use $\epsilon N_{2\Delta} = 10^3$ or $\epsilon N_{2\Delta} = 10^2$ events. For an integrated luminosity of 100 fb^{-1} at LHC these event numbers will be roughly obtained for $M_{\Delta^{++}} \simeq 350 \text{ GeV}$ and $M_{\Delta^{++}} \simeq 600 \text{ GeV}$, respectively [41].

To carry out the analysis we define a χ^2 function from the observables in Eq. (6.13). For given $\epsilon N_{2\Delta}$ they depend only on neutrino parameters (see section 1.1.1). We consider five continuous parameters: the lightest neutrino mass m_0 , s_{13} , the Dirac phase δ , and the two Majorana phases $\alpha_{12} = \alpha_1 - \alpha_2$ and $\alpha_{32} = \alpha_3 - \alpha_2$, plus the discrete parameter $h = \text{NH}$ or IH describing the mass ordering. The remaining neutrino parameters, the two mass-squared differences and the mixing angles s_{12} and s_{23} , are fixed to their experimental best fit values given in Eq. (1.4). The χ^2 is constructed as:

$$\begin{aligned}
 \chi^2(m_0, s_{13}, \delta, \alpha_{12}, \alpha_{32}, h) &= \sum_{xy} V_x S_{xy}^{-1} V_y + \left(\frac{s_{13}^2}{\sigma_{s_{13}^2}} \right)^2 & \text{with} \\
 V_x &= N_x^{\text{pred}}(m_0, s_{13}, \delta, \alpha_{12}, \alpha_{32}, h) - N_x^{\text{exp}}
 \end{aligned} \tag{6.14}$$

where x and y run over the five combinations given in Eq. (6.12). For the ‘‘data’’ N_x^{exp} we use the prediction for N_x at some assumed ‘‘true values’’ of the parameters, $(m_0, s_{13}, \delta, \alpha_{12}, \alpha_{32}, h)^{\text{true}}$. Then the statistical analysis tells us the ability to reconstruct these true values from the data. For the covariance matrix S we assume the following form:

$$S_{xy} = N_x^{\text{exp}} \delta_{xy} + \sigma_{\text{norm}}^2 N_x^{\text{pred}} N_y^{\text{pred}} + S_{xy}^{\text{osc}}. \tag{6.15}$$

It includes statistical errors, a fully correlated normalization error σ_{norm} , and the uncertainty introduced from the errors on the oscillation parameters S^{osc} . The normalization error σ_{norm} arises from the uncertainty on the luminosity and the efficiency. Moreover, the possibility that the non-leptonic decays of Δ^{++} of Eq. (6.7) might occur at a sub-leading level and are not observed introduces an uncertainty in the number of leptonic decays. We adopt a value of $\sigma_{\text{norm}} = 20\%$. We have checked that even an analysis with free normalization (i.e., $\sigma_{\text{norm}} \rightarrow \infty$) leads to very similar results. This means that the information is fully captured by the ratios of branchings.⁵

⁵This is true as long as all branchings from Eq. (6.12) are used; if the events containing taus are omitted our results depend to some degree on the value adopted for σ_{norm} .

Via the covariance matrix S^{osc} we account for the fact that the parameters Δm_{21}^2 , $|\Delta m_{31}^2|$, s_{12} and s_{23} have a finite uncertainty. We include the errors from Eq. (1.4) and take into account the correlations which they introduce between the observables N_x . The last term in Eq. (6.14) takes into account the constraint on s_{13} from present data according to Eq. (1.5). Let us note that within the time scale of a few years the errors on oscillation parameters are likely to decrease. In particular, also the bound on s_{13} will be strengthened or eventually a finite value could be discovered by upcoming reactor or accelerator experiments, see for example [157]. To be conservative we included only present information, although at the time of the analysis better constraints might be available. We have checked that the precise value of s_{13} within the current limits as well as its uncertainty have a very small impact on our results, and a better determination may lead at most to a marginal improvement of the sensitivities.

6.3.2 Branching ratios

In Fig.(6.1) we show the branching ratios for NH and IH as a function of the lightest neutrino mass m_0 . For fixed m_0 , the interval for the branching emerges due to the dependence on the phases $\alpha_{12}, \alpha_{32}, \delta$, and also the uncertainty on solar and atmospheric oscillation parameters contributes to the interval. In the plots one can identify the regions of hierarchical neutrino masses, $m_0 < 10^{-3}$ eV, and QD masses, $m_0 > 0.1$ eV, where NH and IH become indistinguishable. In the limiting cases $m_0 = 0$ and $m_0 \rightarrow \infty$ the analytic expressions for the branchings are rather simple. For NH and $m_0 = 0$ one finds to leading order in the small quantities $r \equiv \Delta m_{21}^2/|\Delta m_{31}^2| \approx 0.03$ and $s_{13}^2 < 0.05$ (at 3σ):

$$\text{BR}_{ee}^{\text{NH}, m_0=0} \approx s_{12}^4 r + 2s_{12}^2 s_{13}^2 \sqrt{r} \cos(\alpha_{32} - 2\delta), \quad (6.16)$$

$$\text{BR}_{e\mu}^{\text{NH}, m_0=0} \approx 2 [s_{12}^2 c_{12}^2 c_{23}^2 r + s_{23}^2 s_{13}^2 + 2s_{12} c_{12} s_{23} c_{23} s_{13} \sqrt{r} \cos(\alpha_{32} - \delta)], \quad (6.17)$$

$$\begin{aligned} \text{BR}_{\mu\mu}^{\text{NH}, m_0=0} \approx & s_{23}^4 + 2s_{23}^2 c_{23}^2 c_{12}^2 \sqrt{r} \cos \alpha_{32} + c_{23}^4 c_{12}^4 r \\ & - 4s_{23}^3 c_{23} s_{12} c_{12} s_{13} \sqrt{r} \cos(\alpha_{32} - \delta), \end{aligned} \quad (6.18)$$

$$\text{BR}_{e\tau}^{\text{NH}, m_0=0} \approx 2 [s_{12}^2 c_{12}^2 s_{23}^2 r + c_{23}^2 s_{13}^2 - 2s_{12} c_{12} s_{23} c_{23} s_{13} \sqrt{r} \cos(\alpha_{32} - \delta)], \quad (6.19)$$

$$\text{BR}_{\mu\tau}^{\text{NH}, m_0=0} \approx 2s_{23}^2 c_{23}^2 (1 - 2c_{12}^2 \sqrt{r} \cos \alpha_{32} + c_{12}^4 r). \quad (6.20)$$

For IH and $m_0 = 0, s_{13} = 0$ we have

$$\text{BR}_{ee}^{\text{IH}, m_0=0} = \frac{1}{2} \left(1 - \sin^2 2\theta_{12} \sin^2 \frac{\alpha_{12}}{2} \right), \quad (6.21)$$

$$\text{BR}_{e\mu}^{\text{IH}, m_0=0} = c_{23}^2 \sin^2 2\theta_{12} \sin^2 \frac{\alpha_{12}}{2}, \quad (6.22)$$

$$\text{BR}_{\mu\mu}^{\text{IH}, m_0=0} = \frac{c_{23}^4}{2} \left(1 - \sin^2 2\theta_{12} \sin^2 \frac{\alpha_{12}}{2} \right), \quad (6.23)$$

$$\text{BR}_{e\tau}^{\text{IH}, m_0=0} = s_{23}^2 \sin^2 2\theta_{12} \sin^2 \frac{\alpha_{12}}{2}, \quad (6.24)$$

$$\text{BR}_{\mu\tau}^{\text{IH}, m_0=0} = \frac{1}{4} \sin^2 2\theta_{23} \left(1 - \sin^2 2\theta_{12} \sin^2 \frac{\alpha_{12}}{2} \right), \quad (6.25)$$

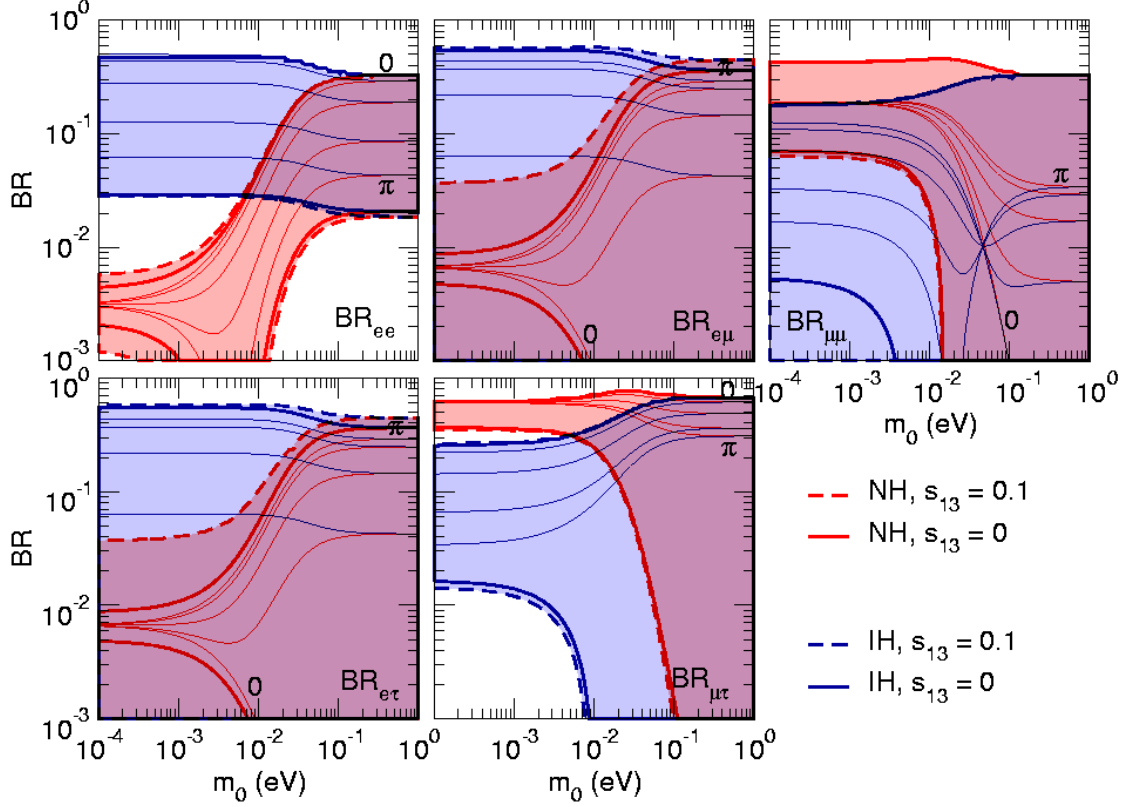


Figure 6.1: Branching ratios $\text{BR}(\Delta \rightarrow \ell_\alpha \ell_\beta)$ as function of the lightest neutrino mass m_0 for NH (light-red) and IH (dark-blue). The thick solid lines are for $s_{13} = 0$, and the thick dashed lines for $s_{13} = 0.1$, where the dependence on phases as well as the uncertainty of solar and atmospheric oscillation parameters at 2σ are included. The thin solid lines show the branchings for oscillation parameters fixed at the best fit points Eq. (1.4), $s_{13} = 0$, $\alpha_{32} = \pi$, and $\alpha_{12} = 0, \pi/4, \pi/2, 3\pi/4, \pi$.

and in the limit $m_0 \rightarrow \infty$ with $s_{13} = 0$ the branchings become

$$\text{BR}_{ee}^{\text{QD}} = \frac{1}{3} \left(1 - \sin^2 2\theta_{12} \sin^2 \frac{\alpha_{12}}{2} \right) = \frac{2}{3} \text{BR}_{ee}^{\text{IH}, m_0=0}, \quad (6.26)$$

$$\text{BR}_{e\mu}^{\text{QD}} = \frac{2}{3} c_{23}^2 \sin^2 2\theta_{12} \sin^2 \frac{\alpha_{12}}{2} = \frac{2}{3} \text{BR}_{e\mu}^{\text{IH}, m_0=0}, \quad (6.27)$$

$$\text{BR}_{\mu\mu}^{\text{QD}} = \frac{1}{3} \left[1 - \frac{1}{2} \sin^2 2\theta_{23} (1 - s_{12}^2 \cos \alpha_{31} - c_{12}^2 \cos \alpha_{32}) - c_{23}^4 \sin^2 2\theta_{12} \sin^2 \frac{\alpha_{12}}{2} \right], \quad (6.28)$$

$$\text{BR}_{e\tau}^{\text{QD}} = \frac{2}{3} s_{23}^2 \sin^2 2\theta_{12} \sin^2 \frac{\alpha_{12}}{2} = \frac{2}{3} \text{BR}_{e\tau}^{\text{IH}, m_0=0}, \quad (6.29)$$

$$\text{BR}_{\mu\tau}^{\text{QD}} = \frac{1}{3} \sin^2 2\theta_{23} \left(1 - s_{12}^2 \cos \alpha_{31} - c_{12}^2 \cos \alpha_{32} - \frac{1}{2} \sin^2 2\theta_{12} \sin^2 \frac{\alpha_{12}}{2} \right) \quad (6.30)$$

Note that for a vanishing lightest neutrino mass, $m_0 = 0$, there is only one physical Majorana phase, α_{32} for NH, and α_{12} for IH.

In the following we will explore the parameter dependencies of these branchings to obtain information on the neutrino mass spectrum and on Majorana phases. The rather wide ranges for the branchings in the cases of IH and QD spectrum suggest a strong dependence on the phases, and as we will see in Sec. 6.3.4 these are the cases where Majorana phases can be measured very efficiently. The determination of the mass spectrum is somewhat more subtle.

A clear signature for the NH with small m_0 is provided by BR_{ee} ⁶. Eq. (6.16) shows that for NH and $m_0 = 0$, BR_{ee} is suppressed by r and/or s_{13}^2 , and there is the upper bound $\text{BR}_{ee} < 5.3 \times 10^{-3}$ for the largest value of s_{12}^2 allowed at 2σ and $s_{13}^2 = 0.01$, in agreement with Fig.(6.1). In contrast, for IH with $m_0 < 0.01$ eV and for QD spectrum, Eqs. (6.21,6.26) give the lower bounds $\text{BR}_{ee} > (1 - \sin^2 2\theta_{12})/2 \approx 0.03$ and $\text{BR}_{ee} > (1 - \sin^2 2\theta_{12})/3 \approx 0.02$, respectively. Therefore, the characteristic signature of normal hierarchical spectrum is the suppression of Higgs decays into two electrons.

From a first glance at Fig.(6.1) one could expect that it might be difficult to distinguish IH and QD spectra, since there is always overlap between the allowed regions in the branchings. Indeed, if only branchings involving electrons and muons (BR_{ee} , $\text{BR}_{e\mu}$, $\text{BR}_{\mu\mu}$) are considered there is some degeneracy between IH and QD, especially if s_{13} is allowed to be close to the present bound. However, as we will show, due to the complementary dependence on the phases of all the $\text{BR}_{\alpha\beta}$ including also taus, the degeneracy is broken and these two cases can be disentangled. Consider, for example, $\text{BR}_{\mu\mu}$ and $\text{BR}_{\mu\tau}$: in the case of IH with $m_0 = 0$ they behave very similar as a function of α_{12} , see Eq. (6.23) and Eq. (6.25), whereas for QD they show opposite dependence, compare Eq. (6.28) and Eq. (6.30), and phases which give $\text{BR}_{\mu\mu}^{\text{QD}} = 0$ maximize $\text{BR}_{\mu\tau}^{\text{QD}}$.

Note that for $s_{13} = 0$ and $s_{23}^2 = 0.5$, $\text{BR}_{e\mu}$ and $\text{BR}_{e\tau}$ are identical. Nevertheless there is important complementarity between them. First, the uncertainty on s_{23}^2 , see Eq. (1.4), affects each of them significantly, and it reduces the final sensitivity if only $\text{BR}_{e\mu}$ is used in the analysis. But since $\text{BR}_{e\mu}$ and $\text{BR}_{e\tau}$ are related by the transformation $s_{23} \rightarrow c_{23}$, $c_{23} \rightarrow -s_{23}$ this uncertainty is cancelled if both of them are included in the fit. Second, it can be shown that the leading order term in s_{13} is the same for $\text{BR}_{e\mu}$ and $\text{BR}_{e\tau}$, apart from an opposite sign. Therefore, also the impact of s_{13} is strongly reduced if information from both of them is taken into account. One can observe from Fig.(6.1) that for small m_0 and NH, $\text{BR}_{e\mu}$ and $\text{BR}_{e\tau}$ show a significant dependence on s_{13} , while in the other cases the dependence is mild. The reason is a leading term linear in $\sqrt{r}s_{13}$ in Eqs. (6.17,6.19), whereas in all other cases s_{13} appears either in sub-leading terms or at least at second order.

⁶Note that the behaviour of BR_{ee} is the same as the effective neutrino mass probed in neutrinoless double beta-decay, which is also proportional to $|M_{ee}|$, see for example Ref. [158].

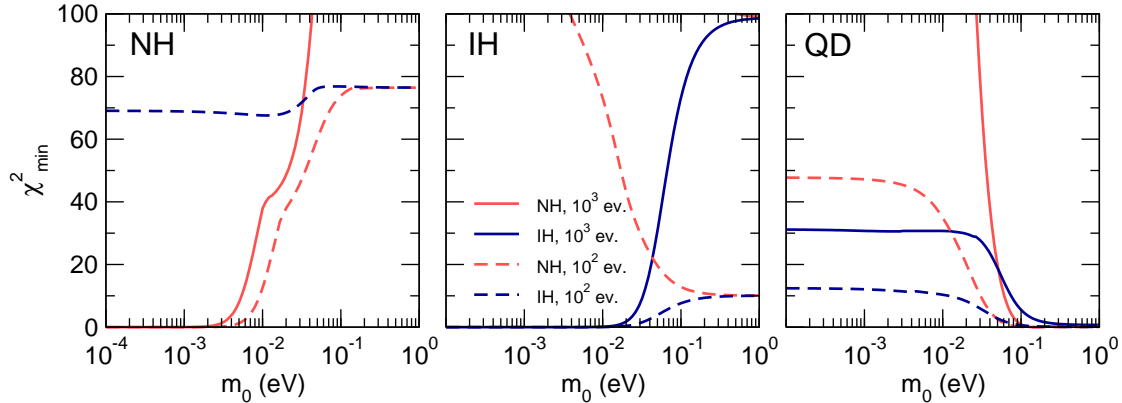


Figure 6.2: χ^2_{\min} vs m_0 assuming a true hierarchical spectrum with NH (left) and IH (middle), and a true QD spectrum (right). The χ^2 is shown for $\epsilon N_{2\Delta} = 100$ (dashed) and 1000 (solid) events, and $\sigma_{\text{norm}} = 20\%$. In the fit we assume either NH (light-red) or IH (dark-blue), and we minimize with respect to s_{13} and the phases. We adopt the following true parameter values. Left: $m_0 = 0$, NH, $\alpha_{32} = \pi$; middle: $m_0 = 0$, IH, $\alpha_{12} = 0$; right: $m_0 = 0.15$ eV, $\alpha_{12} = 0.1\pi$, $\alpha_{32} = 1.6\pi$; and always $s_{13} = 0$.

6.3.3 Determination of the neutrino mass spectrum

Let us now quantify the ability to determine the neutrino mass spectrum by performing a χ^2 analysis as described in section 6.3.1. In Fig.(6.2) we show the χ^2 by assuming that “data” are generated by a hierarchical spectrum with normal ordering (left), a hierarchical spectrum with inverted ordering (middle), or a QD spectrum (right). These data are fitted with both possibilities for the ordering (NH, light-red curves, and IH, dark-blue curves) and a value for m_0 shown on the horizontal axis. We minimize the χ^2 with respect to the other parameters, taking into account the current bound on s_{13} . The results are shown for a total number of doubly charged scalars decaying into like-sign leptons of $\epsilon N_{2\Delta} = 10^3$ (solid) and 10^2 (dashed).

First we discuss the sensitivity to hierarchical spectra with a very small lightest neutrino mass m_0 . The left panel of Fig.(6.2) shows that a NH with small m_0 can be identified with very high significance. An inverted hierarchical spectrum as well as a QD spectrum have $\Delta\chi^2 \gtrsim 60$ already for 100 events. An upper bound on the lightest neutrino mass of $m_0 \lesssim 0.01$ eV at 3σ can be established by LHC data. As discussed in the previous section this information comes mainly from the suppression of the decay into two electrons, which occurs only for normal hierarchical spectrum. An inverted hierarchical spectrum (middle panel) can be distinguished from a QD one at around 3σ with 100 events, where the χ^2 increases roughly linearly with the number of events. The ability to exclude a QD spectrum in case of a true IH depends on the true value of the Majorana phase α_{12} . The example chosen in Fig.(6.2), $\alpha_{12}^{\text{true}} = 0$, corresponds to the worst case; for all other values of α_{12} the χ^2 for QD is bigger.

Fig.(6.3) shows the ability to identify a hierarchical spectrum as a function of the true value for the Majorana phase, where for $m_0 = 0$ there is only one physical

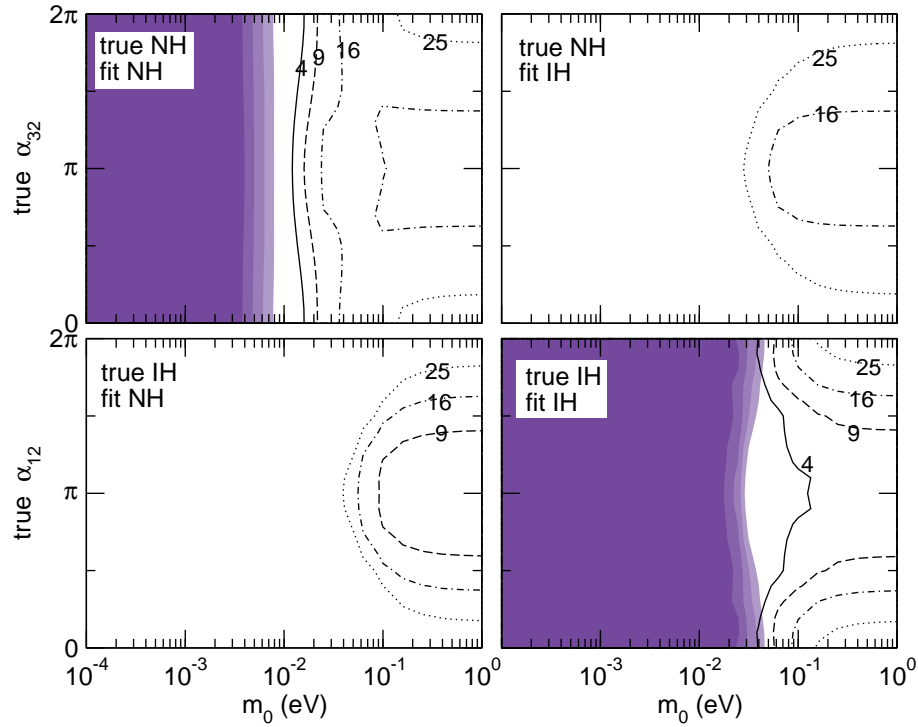


Figure 6.3: Determination of hierarchical neutrino mass spectra, $m_0^{\text{true}} = 0$, assuming 1000 Higgs pair decays. The upper (lower) panels are for a true NH (IH), and for the left (right) panels the fit is performed assuming a NH (IH). As a function of the true value of the Majorana phases we show contours $\chi^2 = 4, 9, 16, 25$ (from dark to light), minimizing with respect to all parameters except from m_0 . Coloured regions correspond to our standard analysis, whereas for the black contours we do not use decays into tau leptons.

phase. The shaded regions show that for 1000 events the true spectrum can be identified at 5σ significance, and an upper bound on the lightest neutrino mass $m_0 < 8 \times 10^{-3}$ eV for NH and $m_0 < 4 \times 10^{-2}$ eV for IH is obtained, independent of the true phase. For the black contours in Fig.(6.3) we do not use the information from decays into taus, i.e., we use only the lepton pairs (ee) , $(e\mu)$, $(\mu\mu)$. This analysis illustrates the importance of the tau events. For example, if tau events are not used an IH with $m_0 = 0$ cannot be distinguished from a QD spectrum for $\alpha_{12}^{\text{true}} \sim \pi$. Also the sensitivity to a NH is significantly reduced, which becomes even more severe if less events were available.

Now we move to the discussion of a true QD spectrum. As shown in the right panel of Fig.(6.2) also a QD spectrum can be identified quite well, and a lower bound on the lightest neutrino mass of $m_0 > 2(6) \times 10^{-2}$ eV at 3σ can be obtained for 100 (1000) events. Note that for the example shown in Fig.(6.2), 100 events give a $\Delta\chi^2 \approx 12.4$ for the IH with $m_0 = 0$, which corresponds roughly to an exclusion at 3.5σ . The potential to exclude a hierarchical inverted spectrum depends on the true values of the Majorana phases, and the true values of α_{12} and α_{32} adopted

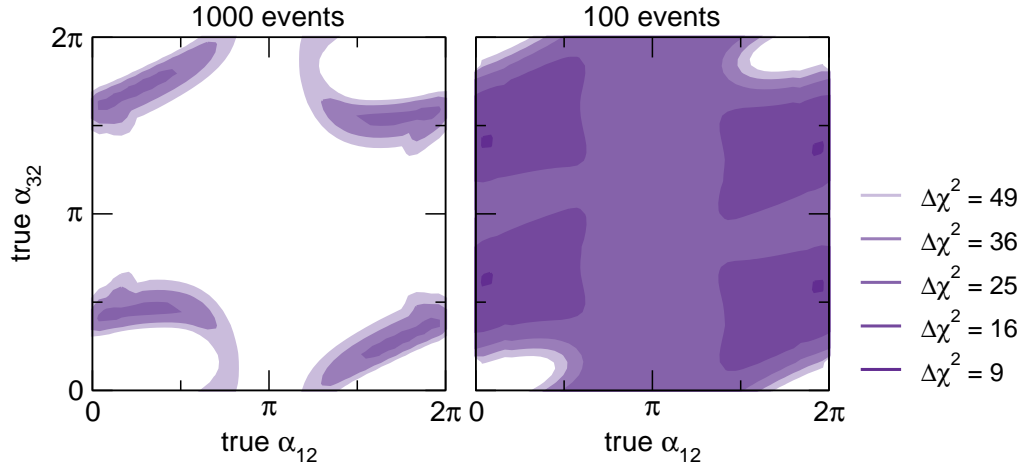


Figure 6.4: Exclusion of an IH with $m_0 = 0$ in the case of a true QD spectrum. We show χ^2 contours for 1000 events (left) and 100 events (right) in the plane of the true Majorana phases assuming a true QD spectrum ($m_0^{\text{true}} = 0.15$ eV, $s_{13}^{\text{true}} = 0$) fitted with IH and $m_0 = 0$, minimizing with respect to all other parameters.

in Fig.(6.2) correspond to the worst sensitivity. In Fig.(6.4) we show contours of $\Delta\chi^2$ for IH with $m_0 = 0$ assuming a true QD spectrum, in the plane of the true Majorana phases. For 1000 events we find some islands in the plane of α_{12} and α_{32} where the χ^2 reaches values as low as 30 (compare Fig.(6.2)), however in most parts of the parameter space the exclusion is at more than 7σ . For 100 events typically a significance better than 4σ is reached, but there are some notable regions ($-\pi/2 \lesssim \alpha_{12} \lesssim \pi/2$ and $\alpha_{32} \sim \pi/2, 3\pi/2$) with χ^2 values between 16 and 9.

Let us add that for the exclusion of an inverted hierarchical spectrum in the case of a true QD spectrum the branchings into tau leptons are crucial. If only electron and muon events are used in most regions of the parameter space an IH with $m_0 = 0$ can fit data from a QD spectrum. For (ee) , $(e\mu)$, $(\mu\mu)$ branchings a degeneracy between IH and QD appears due to the freedom in adjusting s_{13} , δ , θ_{23} and the Majorana phases. This effect is also apparent from the black contour lines in Fig.(6.3) (lower-right panel). The significance of this degeneracy depends on details such as the errors imposed on s_{13}^2 and s_{23}^2 , as well as on the systematical error σ_{norm} . As discussed in section 6.3.2, taking into account also decays into $e\tau$ and $\mu\tau$ is crucial to break this degeneracy, and in the full analysis used to calculate Figs.(6.2,6.4) the dependence on subtleties such as s_{13} and σ_{norm} is small.

6.3.4 Determination of Majorana phases

Let us now investigate the tantalizing possibility to determine the Majorana phases $\alpha_{ij} \equiv \alpha_i - \alpha_j$ from the doubly charged Higgs decays. Since the decay is governed by a single diagram without any interference term the decays are CP conserving, and therefore no explicit CP violating effects can be observed. Nevertheless, the branchings depend (in a CP conserving way) on the phases, which eventually may

allow to establish CP violating values for them. In general the measurement of Majorana phases is a very difficult task. Probably the only hope to access these phases will be neutrino-less double beta-decay in combination with an independent neutrino mass determination, where under very favorable circumstances [158] the phase α_{12} might be measurable.

We start by discussing some general properties of the branchings related to the Majorana phases. Using the PMNS parametrization of the neutrino mass matrix, Eq. (1.2,1.3) one can write:

$$\text{BR}_{\delta\rho} \propto |m_{\nu_{\delta\rho}}|^2 = \left| \sum_{i=1}^3 V_{\delta i} V_{\rho i} e^{i\alpha_i} m_i \right|^2, \quad (6.31)$$

where here α_i is the phase associated to each mass eigenstate. From this expression it is evident that for a vanishing lightest neutrino mass, $m_0 = 0$, there is only one physical Majorana phase, $\alpha_{32} = \alpha_3 - \alpha_2$ for NH and $\alpha_{12} = \alpha_1 - \alpha_2$ for IH. Next we note that since $V_{e3} \propto s_{13}$, it is clear that for $s_{13} = 0$ all branchings involving electrons can only depend on α_{12} .⁷ Since the small effects of s_{13} cannot be explored efficiently, the determination of both phases simultaneously necessarily involves $\text{BR}_{\mu\mu}$ and/or $\text{BR}_{\mu\tau}$, see also Eqs. (6.16) to (6.30). Furthermore, from Eq. (6.31) it can be seen that the branchings are invariant under

$$\alpha_{ij} \rightarrow 2\pi - \alpha_{ij}, \quad \delta \rightarrow 2\pi - \delta. \quad (6.32)$$

This symmetry is a consequence of the fact that there is no CP violation in the decays, and therefore the branchings have to be invariant under changing the signs of all phases simultaneously.

In Fig.(6.5) we show that for a QD spectrum the observation of the decay of 1000 doubly-charged Higgs pairs allows to determine both Majorana phases. We assume some true values for the two phases and then perform a fit leaving all parameters free, where for s_{13} we impose the constraint from present data. The actual accuracy to determine the phases depends on their true values, where we show three different examples in the three panels. For $\alpha_{12} = \alpha_{32} = \pi$ (left panel) the allowed region is the largest, however the phases can be constrained to a unique region. In the other two cases the accuracy is better, but some ambiguities are left. The symmetry from Eq. (6.32) is apparent in all panels, whereas in the case $\alpha_{12} = \alpha_{32} = \pi$ it does not introduce an ambiguity.

The features of Fig.(6.5) can be understood from Eqs. (6.26) to (6.30). In addition to the symmetry Eq. (6.32) one finds that in the limit $s_{13} = 0$ the phases α_{31} and α_{32} appear only in the particular combination

$$(s_{12}^2 \cos \alpha_{31} + c_{12}^2 \cos \alpha_{32}) \propto \cos(\alpha_{32} - \varphi) \quad \text{with} \quad \tan \varphi = \frac{s_{12}^2 \sin \alpha_{12}}{c_{12}^2 + s_{12}^2 \cos \alpha_{12}}, \quad (6.33)$$

⁷For the same reason only α_{12} can be tested in neutrino-less double beta-decay, where $|M_{ee}|$ is probed.

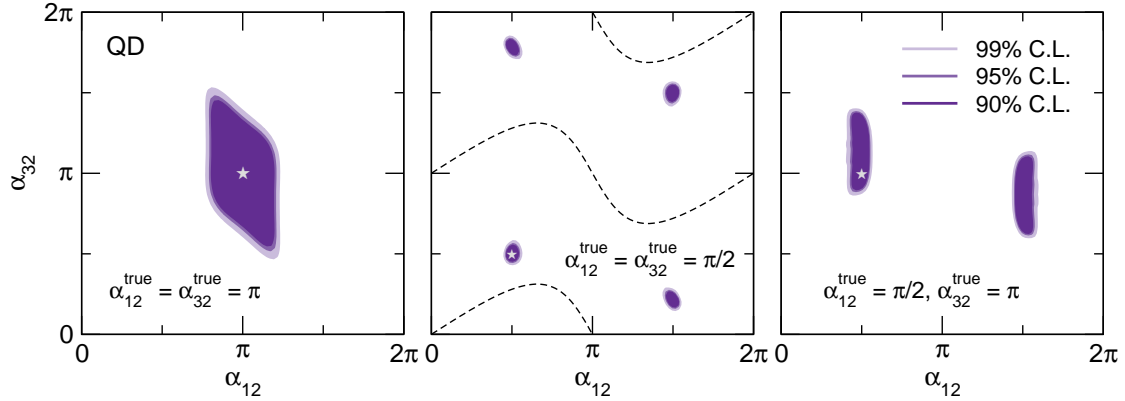


Figure 6.5: Determination of the Majorana phases for QD spectrum ($m_0 = 0.15$ eV) from 1000 doubly-charged Higgs pair events. We assume $s_{13}^{\text{true}} = 0$ and three example points for the true values of the Majorana phases given in each panel. The dashed lines in the middle panel correspond to the true values of the phases for which the degenerate solution according to Eq. (6.34) appears at a CP conserving value of α_{32} .

where we have used α_{12} and α_{32} as independent parameters. For constant α_{12} there are two values of α_{32} which leave this combination invariant: for each α_{32} we expect a degenerate solution at

$$\alpha'_{32} = 2\varphi - \alpha_{32}. \quad (6.34)$$

For $\alpha_{12} = \pi/2$ one finds $2\varphi \approx 0.28\pi$. In the case of $\alpha_{32} = \pi$ shown in the right panel of Fig.(6.5) this degenerate solution appears at $\alpha'_{32} \simeq 1.28\pi$, which cannot be resolved from the original one, and we are left with a two-fold ambiguity, due to Eq. (6.32). In the middle panel, for $\alpha_{12} = \alpha_{32} = \pi/2$, the ambiguity (6.34) leads to a separated solution around $\alpha'_{32} \simeq 1.78\pi$ and, together with the symmetry from Eq. (6.32) we end up with four degenerate solutions. However, in this case the individual regions are rather small, and the CP violating values of both phases can be established despite the presence of the four-fold ambiguity.

Note that the symmetry Eq. (6.32) does not mix CP conserving and violating values of the phases, whereas this can happen for the degeneracy Eq. (6.34). The dashed curves in the middle panel of Fig.(6.5) correspond to the true values of the phases, for which $\alpha'_{32} = 0$ or π . Hence, along these curves CP violating values for α_{32} cannot be established since the degeneracy is located at a CP conserving value.

Let us now discuss the potential to determine Majorana phases in case of hierarchical spectra. As mentioned above, in this case there is only one physical phase, α_{32} for NH and α_{12} for IH. In Fig.(6.6) we show the allowed interval for this phase which is obtained from the data as a function of its true value. In the fit the χ^2 is minimized with respect to all other parameters. The left panel shows that for NH even with 1000 events at most a 2σ indication can be obtained, on whether α_{32} is closer to zero or π . This can be understood from Eqs. (6.16) to (6.20), which show that α_{32} appears at least suppressed by \sqrt{r} . In contrast, as visible in the right panel,

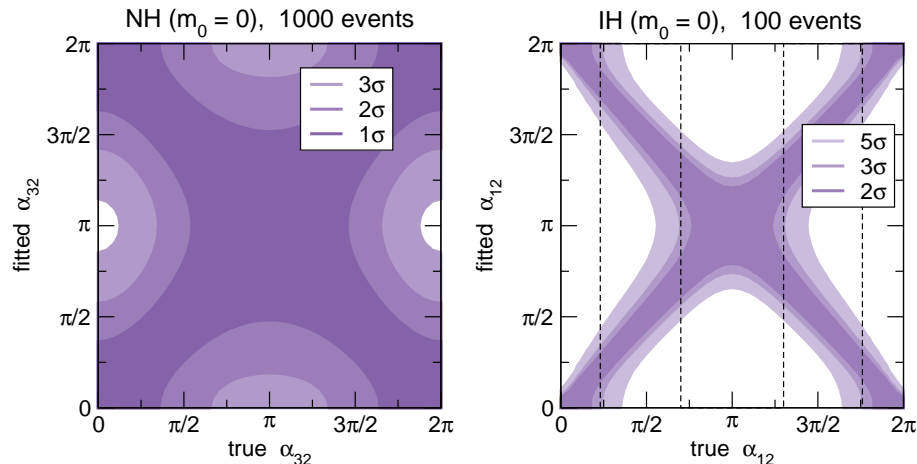


Figure 6.6: Determination of the Majorana phase for vanishing lightest neutrino mass. We assume $s_{13}^{\text{true}} = 0$. Left: 1, 2, 3 σ ranges for α_{32} as a function of its true value for NH assuming 1000 doubly-charged Higgs pair events. Right: 2, 3, 5 σ ranges for α_{12} as a function of its true value for IH assuming 100 doubly-charged Higgs pair events. The dashed vertical lines indicate the region where CP violating values of α_{12} can be established at 3 σ .

for IH a rather precise determination of α_{12} is possible already for 100 events, apart from the ambiguity $\alpha_{12} \rightarrow 2\pi - \alpha_{12}$. For α_{12} around $\pi/2$ or $3\pi/2$ its CP violating value can be established, as marked by the vertical lines in Fig.(6.6). The good sensitivity is obvious from Eqs. (6.21) to (6.25), which show a strong dependence of the leading terms in the branchings on α_{12} .

6.4 Summary and concluding remarks

In this work [4] we adopted the assumptions that (i) neutrino masses are generated by the VEV of a Higgs triplet, (ii) the doubly charged component of the triplet is light enough to be discovered at LHC, i.e., lighter than about 1 TeV, and (iii) it decays with a significant fraction into like-sign lepton pairs. We showed that under these assumptions LHC will provide very interesting information for neutrino physics. The reason is that the branching ratio of the doubly charged Higgs into like-sign leptons of flavor α and β , $\text{BR}(\Delta^{++} \rightarrow \ell_{\alpha}^{+} \ell_{\beta}^{+})$, is proportional to the modulus of the corresponding element of the neutrino mass matrix, $|m_{\nu_{\alpha\beta}}|^2$. Hence the flavor composition of like-sign lepton events at LHC provides a direct test of the neutrino mass matrix.

We showed that the type of the neutrino mass spectrum (normal hierarchical, inverted hierarchical, or quasi-degenerate) can be identified at the 3 σ level already with 100 doubly charged Higgs pairs $\Delta^{--}\Delta^{++}$ decaying into four leptons. Typically such a number of events will be achieved for doubly charged scalar masses below 600 GeV and 100 fb⁻¹ integrated luminosity, whereas for masses of 350 GeV of

order 1000 events will be obtained. We found that it is possible to decide whether the lightest neutrino mass is smaller or larger than roughly 0.01 eV, which marks the transition between hierarchical and quasi-degenerate spectra. If it is smaller the mass ordering (normal vs inverted) can be identified. A hierarchical spectrum with normal ordering has a distinct signature, namely a very small branching of the doubly charged Higgs decays into two electrons. Therefore, this mass pattern can easily be confirmed or ruled out at very high significance level. The other two possibilities for the neutrino mass spectrum, inverted hierarchical or quasi-degenerate, are somewhat more difficult to distinguish, but also in this case very good sensitivity is obtained, depending on the observed number of events.

In this respect the inclusion of final states involving tau leptons is important, since if only electrons and muons are considered a degeneracy between IH and QD spectra appears. In our analysis we conservatively assumed that events where one of the four charged leptons is a tau can be reconstructed efficiently, thanks to the kinematic constraints and the information on the invariant mass of the event available from events without a tau. Certainly a more realistic study including detailed simulations and event reconstruction should confirm the assumptions which we have adopted.

The decay of the doubly charged Higgs in this framework does not show explicit CP violation, since the decay is dominated by a tree-level diagram without any interference term which could induce CP violation. Nevertheless, the CP conserving branching ratios strongly depend on the Majorana CP phases of the lepton mixing matrix. Therefore, the framework considered here opens the fascinating possibility to measure the Majorana phases in the neutrino mass matrix via CP even observables. Our results show that for an inverted hierarchical spectrum as well as for quasi-degenerate neutrinos this is indeed possible. In the first case, there is only one physical phase, α_{12} , which can be determined up to an ambiguity $\alpha_{12} \leftrightarrow 2\pi - \alpha_{12}$ already with 100 events. In the case of a quasi-degenerate spectrum both Majorana phases can be measured, where, depending on the actual values some ambiguities might occur. In many cases CP violating values of the phases can be established.

Certainly the observation of a doubly charged scalar at LHC would be a great discovery of physics beyond the Standard Model. Of course this alone does by no means confirm the Higgs triplet mechanism for neutrino masses, since doubly charged particles decaying into leptons are predicted in many models. Therefore, in case such a particle is indeed found at LHC various consistency checks will have to be performed. It might turn out that the relation $\text{BR}(\Delta^{++} \rightarrow \ell_{\alpha}^{+} \ell_{\beta}^{+}) \propto |m_{\nu_{\alpha\beta}}|^2$ cannot be fulfilled for any neutrino mass matrix consistent with oscillation data. This would signal that a Higgs triplet cannot be the only source for neutrino masses. In this respect the information from decays into leptons of all flavors (including taus) will be important. For example, also in the Zee-Babu model [46] for neutrino masses doubly charged scalars might be found at LHC. However, in this case branchings into tau leptons are suppressed by powers of $(m_{\mu}/m_{\tau})^2$ with respect to muons [148, 47], whereas in the Higgs triplet model they are of similar size because of close to maximal θ_{23} mixing.

If LHC data on $\text{BR}(\Delta^{++} \rightarrow \ell_\alpha^+ \ell_\beta^+)$ will be consistent with a neutrino mass matrix from oscillation data, an analysis as pointed out here can be performed. Also in this case it will be of crucial importance to cross check the results with independent measurements, for example the determination of the neutrino mass ordering by oscillation experiments, or the measurement of the absolute neutrino mass in tritium beta-decay, neutrino-less double beta-decay or through cosmological observations. In particular, neutrino-less double beta-decay will provide a crucial test, since it gives an independent determination of the $|M_{ee}|$ element of the neutrino mass matrix, which—combined with information from oscillation experiments—will further constrain the allowed flavor structure of the di-lepton events at LHC. The next generation of neutrino-less double beta-decay experiments is expected to probe the regime of the QD neutrino spectrum within a timescale comparable to the LHC measurement. Information from searches for lepton flavor violating processes may be used as additional important consistency checks for the model.

In conclusion, a TeV scale Higgs triplet offers an appealing mechanism to provide mass to neutrinos, which can be directly tested at the LHC. Such a scenario opens the possibility to measure the Majorana phases of the lepton mixing matrix, which in general is a very difficult—if not a hopeless task.

Chapter 7

Conclusions

In this theses we have explored some phenomenological aspects of neutrino physics. In the first part, chapters 3 and 4, we considered the type I seesaw mechanism and we studied the connection between the CP violation responsible of Leptogenesis and that measurable at low energy experiments. In the second part of the theses we studied alternative models for neutrino masses. In chapter 5 we considered the Soft Leptogenesis mechanism in the context of the inverse seesaw model. And in chapter 6 we analyzed the synergies between collider physics and neutrino physics within the Higgs triplet model for neutrino masses.

The fact that neutrinos are massive is one of the more important signals of physics beyond the Standard Model. As we have stated several times along this theses, the type I seesaw mechanism provides one of the simplest ways to generate neutrino masses. Within the seesaw mechanism, three right-handed neutrinos with heavy Majorana masses are added to the Standard Model. These right-handed neutrinos couple to the lepton sector via yukawa interactions, and they induce tiny masses for left-handed neutrinos. This model suffers from a hierarchy problem, which can be solved if supersymmetry is considered.

On the other hand, within the type I seesaw mechanism it is possible to explain the Baryon Asymmetry of the Universe (BAU) through the Leptogenesis scenario. The out-of-equilibrium decay of heavy Majorana neutrinos violates lepton number and CP, generating an asymmetry in lepton number. The non-perturbative sphaleron processes present in the Standard Model can reconvert this lepton asymmetry into a baryon asymmetry. The CP violation required for leptogenesis are the phases present in the neutrino yukawa matrix. Some of this phases can be measured at low energy experiments (phases in the PMNS matrix): neutrino oscillation experiments can measure the Dirac CP violating phase, and the discovery of neutrino-less double beta decay would prove the Majorana nature of neutrinos and could put some constraints on the Majorana CP phases. Thus, an obvious question arises. Is the BAU sensitive to the phases measurable at low energy neutrino experiments?

We addressed this question in chapter 3. We assumed that the BAU was generated via flavored leptogenesis within the type I seesaw model and we studied if successful leptogenesis points towards a preferred range of values of the low energy

phases. This same question was addressed by other authors in previous works, in the case of Leptogenesis without flavor effects, and the answer they found was negative. We have shown that the answer does not change with the inclusion of flavor effects: for any value of the PMNS phases, it is possible to find a point in the space of unmeasurable seesaw parameters, such that leptogenesis works. We also provide an analytical proof of this fact.

In chapter 3 we give a parametrization of the BAU which is independent of the low energy phases. We express the BAU in terms of observables using the Casas-Ibarra matrix, then we find a parametrization of the unknown matrix R , for which the BAU is independent of the low energy phases. And finally we demonstrate that an enough BAU can be obtained for some values of the unknown parameters in the matrix R .

The answer we found can be expected. Given the large number of parameters, fixing a small number of observables, namely the neutrino oscillation parameters and the BAU, does not constraint the allowed parameter space. In chapter 4, we addressed the same question in the framework of Minimal Supergravity, because in this case more low energy observables could be available.

It is well known that neutrino yukawa couplings can lead to Lepton Flavor Violating (LFV) processes and Electric Dipole Moments (EDM) through Renormalization Group Equation running from high to low energies. In chapter 4 we presented the results of a scan of the seesaw parameter space in which we looked for points that reproduced neutrino oscillation parameters, gave a large enough BAU, and LFV rates big enough to be measured in upcoming experiments. We did not impose the EDMs as experimental inputs because we expected them to be suppressed. Then we studied if the experimental inputs implied a preferred range of values of the low energy phases.

We found, again, that there is no direct link between successful Leptogenesis and the low energy phases. By this we mean that for any value of the low energy phases, we can rearrange the unmeasurable parameters to obtain the right amount of BAU and LFV measurable in the next round of experiments. This study was performed both numerically and analytically. The numerical scan of the parameter space was done by a Markov Chain Monte Carlo simulation since, given the large number of parameters, a usual grid scan would have been prohibitive.

In the second part of this theses we have explored some phenomenological aspects of neutrino physics within two alternative models for neutrino masses. In the seesaw mechanism, in order to have small light neutrino masses, in general the right-handed neutrinos need to be very heavy. This is a drawback of the model because makes the mechanism untestable. Thus it is interesting to analyze other models in which neutrino masses arise due to physics at lower energy scales.

In chapter 5 we considered the inverse seesaw model as the source of neutrino masses. This model contains two right-handed neutrinos per generation and it is characterized by a small Majorana mass term μ , which suppresses the effective light neutrino mass matrix $m_\nu \sim \mu$. Thus, the right-handed neutrinos are expected to be lighter than in the usual seesaw scenario and, as a result, lepton flavor and CP

violating processes are highly enhanced.

We have studied the mechanism of Soft Leptogenesis within the supersymmetric version of this model, where lepton asymmetry is generated by sneutrino decays. In this framework the source of CP and lepton number violation is provided by the soft supersymmetry breaking parameters, together with the neutrino yukawa couplings and the lepton number violating coupling μ . The soft terms and μ remove the mass degeneracy between the sneutrino states, and due to their mixing they produce a CP asymmetry in their decay. This CP asymmetry can be large enough to produce the BAU.

We found that the CP asymmetry responsible of Soft Leptogenesis in the inverse seesaw model is not suppressed by any lepton number violating parameter. In the limit of lepton number conservation, although there is a CP asymmetry in sneutrino decays, it is not a lepton number asymmetry. We also stress that within this mechanism, the generation of the lepton asymmetry is consequence of thermal effects which are different for scalars and fermions. Our results show that successful Leptogenesis requires small values of the scalar bilinear and lepton number conserving parameter B , and a light neutrino mass spectrum strongly hierarchical.

Finally, in chapter 6 we studied the Higgs triplet model as the source of neutrino masses, under the assumption that the doubly charged component of the triplet is light enough to be produced at LHC and it decays into same sign leptons. We showed that under these circumstances LHC could provide very useful information about neutrinos, because the decay width of the scalar into two leptons of a given flavor is proportional to the modulus of the corresponding element of the neutrino mass matrix. In particular we studied the possibility of identifying the type of neutrino mass hierarchy and measuring the Majorana CP phases. Let us stress that doubly charged scalars appear in many extensions of the SM, therefore the discovery of such a doubly charged scalar at LHC is not a proof of the Higgs triplet model, and some consistency checks should be performed.

Our analysis shows that, within the above assumptions, LHC could decide whether the lightest neutrino mass is smaller or larger than 0.01 eV, which marks the transition between the hierarchical and degenerate spectra. If it is smaller, the type of hierarchy (normal or inverted) could be identified. We also show that, in the case of inverted hierarchy and for quasi-degenerate neutrinos, the CP Majorana phases could be measured, up to some degeneracies, via the CP even observables under consideration, namely the decay of the doubly charged scalars into same sign leptons. However, in the case of normal hierarchy this is not possible, due to the mild dependence of the branching ratios on the Majorana phases.

In summary, in this theses we have explored some phenomenological aspects of neutrino physics, and in particular we have studied possible consequences from a cosmological point of view, namely the generation of the Baryon Asymmetry of the Universe.

Conclusiones

En esta tesis hemos estudiado algunos aspectos fenomenológicos de física de neutrinos. En la primera parte de la tesis, los capítulos 3 y 4, consideramos el modelo seesaw tipo I y estudiamos la conexión entre la violación de CP responsable de la Leptogénesis y las fases de CP de bajas energías, que pueden ser medidas en los experimentos. En la segunda parte de la tesis, estudiamos algunos modelos de masas de neutrinos alternativos al seesaw estándar. En el capítulo 5 consideramos el mecanismo de Soft Leptogenesis en el contexto del modelo seesaw inverso. Y en el capítulo 6 asumimos que el modelo del triplete escalar da masa a los neutrinos, y analizamos lo que en LHC se podría aprender de ellos si este triplete fuese lo bastante ligero como para ser producido en el colisionador.

El hecho de que los neutrinos tienen masa constituye una de las evidencias más importantes de física más allá del Modelo Estándar. Como ya hemos comentado varias veces a lo largo de la tesis, el mecanismo seesaw es una de las maneras más simples de generar las masas de los neutrinos. En este mecanismo se asume la existencia de tres singletes neutros, neutrinos pesados, con masas de Majorana. Estos neutrinos pesados interactúan únicamente con el sector leptónico a través de acoplamientos de tipo Yukawa, y generan pequeñas masas para los neutrinos ligeros. Este modelo sufre el llamado problema de jerarquías, que puede solucionarse si se considera Supersimetría.

Por otro lado, el mecanismo seesaw de tipo I, aparte de generar satisfactoriamente las masas de los neutrinos, permite explicar la asimetría bariónica presente en el Universo a través de la Leptogénesis. Las desintegraciones de los neutrinos pesados violan número leptónico y la simetría CP; si estas desintegraciones ocurren fuera del equilibrio térmico, se genera una asimetría en número leptónico. Los procesos no perturbativos conocidos como esfalerones, y que ocurren en el marco del Modelo Estándar, pueden convertir esta asimetría leptónica en asimetría bariónica. La violación de CP, un requisito indispensable para generar la asimetría bariónica, está presente en la Leptogénesis debido a las seis fases complejas de la matriz de yukawas de los neutrinos. Algunas de estas fases se pueden medir en los experimentos (las tres fases de la matriz de mezcla PMNS): los experimentos de oscilaciones de neutrinos podrían medir la fase de Dirac, mientras que el descubrimiento de la desintegración doble beta sin neutrinos, además de probar que los neutrinos son de tipo Majorana, pondría algunas restricciones en las dos fases de Majorana. Así que se plantea una pregunta obvia: ¿es la asimetría bariónica sensible a los valores de las fases accesibles a los experimentos?

En el capítulo 3 nos planteamos esta pregunta. En este capítulo asumimos que la asimetría bariónica se produjo a través de la leptogénesis con efectos de sabor en el marco del modelo seesaw tipo I, y estudiamos si este requisito restringe el rango de posibles valores de las fases de bajas energías, las fases de la matriz PMNS. Esta misma cuestión fue considerada por otros autores en un trabajo previo al nuestro, donde se consideraba la Leptogénesis sin efectos de sabor, y la respuesta que encontraron fue negativa. Nosotras hemos demostrado que la respuesta no cambia si los efectos de sabor son tomados en consideración: para cualquier valor de las fases de la matriz PMNS, es posible encontrar un punto en el espacio de parámetros de alta energía –no accesible a los experimentos– para el que se puede generar con éxito la asimetría bariónica. Este hecho lo hemos demostrado también analíticamente.

En el capítulo 3 encontramos una parametrización de la asimetría bariónica que es independiente de las fases de baja energía. Escribimos la asimetría bariónica en términos de observables utilizando la matriz de Casas-Ibarra, y luego encontramos una expresión para la matriz R tal que la asimetría bariónica es independiente de las fases de baja energía. Finalmente demostramos que bajo esta parametrización es posible encontrar puntos en el espacio de parámetros en los que se genera con éxito la asimetría bariónica.

Hay que decir que la respuesta que encontramos no es sorprendente. Dado el gran número de parámetros libres del modelo, el hecho de fijar unos pocos observables (los parámetros de oscilación de neutrinos y la asimetría bariónica), no reduce la región permitida del espacio de parámetros. Por ello, en el capítulo 4 nos planteamos la misma cuestión pero en el marco de Minimal Supergravity, pues en este caso podría haber nuevos observables a bajas energías.

Es bien conocido que los acoplamientos de Yukawa de los neutrinos pueden dar lugar a procesos que violan sabor leptónico (LFV) y momentos dipolares eléctricos (EDM), a través de las ecuaciones del grupo de renormalización. En el capítulo 4 presentamos los resultados de un “scan” del espacio de parámetros del seesaw en el que buscábamos puntos que fueran capaces de reproducir los observables medidos de oscilación de neutrinos y la asimetría bariónica, y a la vez generaran procesos LFV que pudieran medirse en la próxima generación de experimentos. A continuación estudiamos si todos estos requisitos experimentales constriñen el rango de valores permitido para las fases.

Nuestra respuesta es, de nuevo, que no existe una relación directa entre la Leptogénesis y los valores de las fases medibles en los experimentos. Con esto queremos decir que para cualesquiera valores de las fases de la matriz PMNS, es posible encontrar un punto del espacio de parámetros en el que se genera con éxito la asimetría bariónica y se obtienen procesos LFV que se medirían en los experimentos futuros. Este estudio lo hemos hecho de manera analítica y de manera numérica. En el estudio numérico utilizamos las simulaciones Markov Chain Monte Carlo, que son capaces de escanear con éxito un espacio de parámetros con muchos grados de libertad.

En la segunda parte de esta tesis hemos explorado algunos modelos de masas

de neutrinos alternativos al seesaw estándar. En el marco del mecanismo seesaw tipo I, para poder generar las pequeñas masas de los neutrinos ligeros, en general es necesario que las masas de Majorana de los neutrinos pesados sean enormes. Esto supone un inconveniente, pues hace que el modelo no pueda ser comprobado. Así que es interesante analizar modelos en los que la generación de masa de los neutrinos implica nueva fenomenología a escalas energéticas más bajas, y que por tanto podrían ser probados.

En el capítulo 5 consideramos el modelo seesaw inverso. En este modelo se incorporan dos singletes neutros por cada familia de leptones y está caracterizado por una pequeña masa de Majorana μ , que suprime las masas de los neutrinos ligeros $m_\nu \sim \mu$. Así que los singletes neutros pueden ser más ligeros que en el caso seesaw estándar y, como resultado, los procesos que violan sabor leptónico y los procesos que violan CP pueden ser observados.

En el capítulo 5 consideramos la versión supersimétrica de este modelo y estudiamos la Soft Leptogénesis, en la que la asimetría leptónica es generada en la desintegración de los sneutrinos. En este contexto, la fuente de violación de CP y de número leptónico son los términos “soft” que rompen Supersimetría, junto con los acoplamientos de Yukawa de los neutrinos y el término μ que viola número leptónico por ser una masa de Majorana. Estos términos “soft” junto con el término μ , rompen la degeneración de masa de los sneutrinos y hacen que, debido a las mezclas entre ellos, generen una asimetría de CP en su desintegración. Esta asimetría es suficientemente grande como para explicar la asimetría bariónica del Universo.

Nuestro estudio demuestra que la asimetría de CP relevante en la Soft Leptogénesis no se encuentra suprimida por ningún término que viole número leptónico. En el límite en que se conserva número leptónico, aunque existe una asimetría de CP en la desintegración de los sneutrinos, ésta no es una asimetría en número leptónico, que se conserva estrictamente. También hacemos hincapié en que en este mecanismo, la asimetría leptónica generada es consecuencia de los efectos térmicos que rompen supersimetría, ya que son esencialmente diferentes para escalares y fermiones. Nuestros resultados muestran que para generar con éxito la asimetría bariónica es necesario que el acoplamiento escalar bilineal B , que conserva número leptónico, sea muy pequeño, y que el espectro de masa de los neutrinos ligeros sea fuertemente jerárquico.

Finalmente, en el capítulo 6 estudiamos el modelo del triplete de Higgs como origen de las masas de los neutrinos, bajo la suposición de que la componente doblemente cargada de este triplete es lo suficientemente ligera como para ser producida en el LHC y que se desintegra a dos leptones de igual carga eléctrica. Demostramos que en estas circunstancias, LHC podría ser de gran utilidad para la física de neutrinos. La razón es que la anchura de desintegración de este escalar en dos leptones de cierto sabor es proporcional al módulo al cuadrado del correspondiente elemento de la matriz de masa de los neutrinos. En particular estudiamos la posibilidad de identificar el tipo de jerarquía de masa y de medir las fases de Majorana de la matriz de mezcla PMNS. Hemos de decir que un escalar doblemente cargado, como el que aquí tratamos, no es algo exclusivo del modelo del triplete de Higgs. Así que, en el

caso de que LHC descubriera tales escalares, habría que contrastar esos resultados con otras medidas experimentales.

Nuestro análisis muestra que, bajo las suposiciones expuestas arriba, LHC podría decidir si la masa del neutrino más ligero es mayor o menor que 0.01 eV , que es el límite que marca la transición entre un espectro de masas jerárquico y uno degenerado. Además, si es menor, se podría identificar el tipo de jerarquía (normal o invertida). También demostramos que, en el caso de jerarquía inversa y para un espectro casi degenerado de masas, las fases de Majorana se podrían medir, excepto por ciertas degeneraciones. Mientras que en el caso de jerarquía normal, debido a la escasa dependencia de las anchuras de desintegración en las fases de Majorana, éstas no podrían ser medidas.

En definitiva, en esta tesis hemos explorado diversos aspectos fenomenológicos de física de neutrinos, y en particular hemos estudiado una de sus posibles consecuencias desde el punto de vista cosmológico, la generación de la asimetría bariónica presente en el Universo.

Bibliography

- [1] S. Davidson, J. Garayoa, F. Palorini and N. Rius, Phys. Rev. Lett. **99** (2007) 161801.
- [2] S. Davidson, J. Garayoa, F. Palorini and N. Rius, JHEP **0809** (2008) 053.
- [3] J. Garayoa, M. C. Gonzalez-Garcia and N. Rius, JHEP **0702** (2007) 021.
- [4] J. Garayoa and T. Schwetz, JHEP **0803** (2008) 009.
- [5] B. T. Cleveland *et al.*, Astrophys. J. **496** (1998) 505.
- [6] J. N. Abdurashitov *et al.* [SAGE Collaboration], J. Exp. Theor. Phys. **95** (2002) 181 [Zh. Eksp. Teor. Fiz. **122** (2002) 211].
- [7] M. Altmann *et al.* [GNO COLLABORATION Collaboration], Phys. Lett. B **616** (2005) 174.
- [8] J. Hosaka *et al.* [Super-Kamiokande Collaboration], Phys. Rev. D **73** (2006) 112001.
- [9] B. Aharmim *et al.* [SNO Collaboration], Phys. Rev. Lett. **101** (2008) 111301.
- [10] C. Arpesella *et al.* [The Borexino Collaboration], Phys. Rev. Lett. **101** (2008) 091302.
- [11] Y. Ashie *et al.* [Super-Kamiokande Collaboration], Phys. Rev. D **71** (2005) 112005.
- [12] S. Abe *et al.* [KamLAND Collaboration], Phys. Rev. Lett. **100** (2008) 221803.
- [13] E. Aliu *et al.* [K2K Collaboration], Phys. Rev. Lett. **94** (2005) 081802.
- [14] P. Adamson *et al.* [MINOS Collaboration], Phys. Rev. Lett. **101** (2008) 131802.
- [15] T. Schwetz, M. Tortola and J. W. F. Valle, New J. Phys. **10** (2008) 113011.
- [16] S. Hannestad, arXiv:0710.1952 [hep-ph].

- [17] P. Minkowski, Phys. Lett. B **67** (1977) 421; M. Gell-Mann, P. Ramond and R. Slansky, *Proceedings of the Supergravity Stony Brook Workshop*, New York 1979, eds. P. Van Nieuwenhuizen and D. Freedman; T. Yanagida, *Proceedings of the Workshop on Unified Theories and Baryon Number in the Universe*, Tsukuba, Japan 1979, eds. A. Sawada and A. Sugamoto; R. N. Mohapatra, G. Senjanovic, *Phys.Rev.Lett.* **44** (1980) 912.
- [18] A. Santamaria, Phys. Lett. B **305**, 90 (1993).
- [19] A. Broncano, M. B. Gavela and E. E. Jenkins, Phys. Lett. B **552** (2003) 177 [Erratum-ibid. B **636** (2006) 330].
- [20] S. Davidson and A. Ibarra, JHEP **0109** (2001) 013.
- [21] S. Davidson, arXiv:hep-ph/0409339.
- [22] J. A. Casas and A. Ibarra, Nucl. Phys. B **618** (2001) 171.
- [23] F. Borzumati and A. Masiero, Phys. Rev. Lett. **57** (1986) 961.
- [24] J. Hisano *et al.*, Phys. Rev. D **53** (1996) 2442; J. Hisano and D. Nomura, Phys. Rev. D **59** (1999) 116005.
- [25] S Lavignac, I Masina and C Savoy, *Phys. Lett.* **B520** (2001), 269-278; Petcov, S. T. and Rodejohann, W. and Shindou, T. and Takanishi, Y.", *Nucl. Phys.* **B739** (2006) 208-233; T. Blazek and S. F. King, Nucl. Phys. B **662** (2003) 359.
- [26] Y. Farzan and M. E. Peskin, Phys. Rev. D **70**, 095001 (2004).
- [27] A. Pilaftsis and T. E. J. Underwood, Phys. Rev. D **72** (2005) 113001.
- [28] R.N. Mohapatra and J.W.F. Valle, Phys. Rev. **D34** (1986) 1642 .
- [29] E. Akhmedov, M. Lindner, E. Schnapka and J. W. F. Valle, Phys. Rev. D **53** (1996) 2752; Phys. Lett. B **368** (1996) 270.
- [30] S. M. Barr, Phys. Rev. Lett. **92** (2004) 101601; S. M. Barr and I. Dorsner, Phys. Lett. B **632** (2006) 527.
- [31] M. C. Gonzalez-Garcia and J. W. F. Valle, Phys. Lett. B **216** (1989) 360.
- [32] G. B. Gelmini and M. Roncadelli, Phys. Lett. B **99** (1981) 411.
- [33] J. C. Pati and A. Salam, Phys. Rev. D **10** (1974) 275 [Erratum-ibid. D **11** (1975) 703]; R. N. Mohapatra and J. C. Pati, Phys. Rev. D **11** (1975) 566; G. Senjanovic and R. N. Mohapatra, Phys. Rev. D **12** (1975) 1502.

- [34] N. Arkani-Hamed, A. G. Cohen, E. Katz and A. E. Nelson, JHEP **0207** (2002) 034; C. Csaki, J. Hubisz, G. D. Kribs, P. Meade and J. Terning, Phys. Rev. D **67** (2003) 115002; T. Han, H. E. Logan, B. McElrath and L. T. Wang, Phys. Rev. D **67** (2003) 095004; S. Chang and J. G. Wacker, Phys. Rev. D **69** (2004) 035002.
- [35] T. Han, H. E. Logan, B. Mukhopadhyaya and R. Srikanth, Phys. Rev. D **72** (2005) 053007.
- [36] W. Grimus, R. Pfeiffer and T. Schwetz, Eur. Phys. J. C **13**, 125 (2000).
- [37] M. Magg and C. Wetterich, Phys. Lett. B **94** (1980) 61; G. Lazarides, Q. Shafi and C. Wetterich, Nucl. Phys. B **181** (1981) 287; R. N. Mohapatra and G. Senjanovic, Phys. Rev. D **23** (1981) 165.
- [38] J. Schechter and J. W. F. Valle, Phys. Rev. D **22** (1980) 2227.
- [39] E. Ma and U. Sarkar, Phys. Rev. Lett. **80** (1998) 5716.
- [40] A. Hektor, M. Kadastik, M. Muntel, M. Raidal and L. Rebane, Nucl. Phys. B **787**, 198 (2007).
- [41] T. Han, B. Mukhopadhyaya, Z. Si and K. Wang, Phys. Rev. D **76**, 075013 (2007).
- [42] M. Kakizaki, Y. Ogura and F. Shima, Phys. Lett. B **566**, 210 (2003).
- [43] E. Ma, M. Raidal and U. Sarkar, Phys. Rev. Lett. **85** (2000) 3769; E. Ma, M. Raidal and U. Sarkar, Nucl. Phys. B **615** (2001) 313.
- [44] A. Abada, C. Biggio, F. Bonnet, M. B. Gavela and T. Hambye, JHEP **0712** (2007) 061; Phys. Rev. D **78**, 033007 (2008).
- [45] B. Bajc, M. Nemevsek and G. Senjanovic, Phys. Rev. D **76** (2007) 055011.
- [46] A. Zee, Nucl. Phys. B **264** (1986) 99; K. S. Babu, Phys. Lett. B **203** (1988) 132.
- [47] M. Nebot, J. F. Oliver, D. Palao and A. Santamaria, Phys. Rev. D **77** (2008) 093013.
- [48] A. Zee, Phys. Lett. B **93** (1980) 389 [Erratum-ibid. B **95** (1980) 461].
- [49] M. Hirsch and J. W. F. Valle, New J. Phys. **6** (2004) 76 [arXiv:hep-ph/0405015].
- [50] C. Amsler et al. (Particle Data Group), Phys. Lett. B **667**, 1 (2008).
- [51] F. Iocco, G. Mangano, G. Miele, O. Pisanti and P. D. Serpico, arXiv:0809.0631 [astro-ph].

- [52] E. Komatsu *et al.* [WMAP Collaboration], arXiv:0803.0547 [astro-ph].
- [53] A. D. Sakharov, Pisma Zh. Eksp. Teor. Fiz. **5** (1967) 32 [JETP Lett. **5** (1967 SOPUA,34,392-393.1991 UFNAA,161,61-64.1991) 24].
- [54] G. 't Hooft, Phys. Rev. Lett. **37** (1976) 8.
- [55] F. R. Klinkhamer and N. S. Manton, Phys. Rev. D **30** (1984) 2212.
- [56] M. Fukugita and T. Yanagida, Phys. Lett. B **174** (1986) 45.
- [57] S. Davidson, E. Nardi and Y. Nir, Phys. Rept. **466** (2008) 105.
- [58] L. Covi, E. Roulet and F. Vissani, Phys. Lett. B **384** (1996) 169.
- [59] O. Vives, Phys. Rev. D **73** (2006) 073006.
- [60] G. Engelhard, Y. Grossman, E. Nardi and Y. Nir, Phys. Rev. Lett. **99** (2007) 081802.
- [61] P. Di Bari and A. Riotto, arXiv:0809.2285 [hep-ph].
- [62] A. Abada *et al.*, JCAP **0604** (2006) 004.
- [63] E. Nardi *et al.*, JHEP **0601** (2006) 164.
- [64] A. Abada *et al.*, JHEP **0609** (2006) 010.
- [65] E. W. Kolb and S. Wolfram, Nucl. Phys. B **172**, 224 (1980) [Erratum-ibid. B **195**, 542 (1982)].
- [66] W. Buchmuller, P. Di Bari and M. Plumacher, Annals Phys. **315** (2005) 305.
- [67] J. A. Harvey and M. S. Turner, Phys. Rev. D **42** (1990) 3344.
- [68] A. Basboll and S. Hannestad, JCAP **0701**, 003 (2007).
- [69] S. Davidson and A. Ibarra, Phys. Lett. B **535** (2002) 25.
- [70] M. Y. Khlopov and A. D. Linde, Phys. Lett. B **138** (1984) 265; J. R. Ellis, J. E. Kim and D. V. Nanopoulos, Phys. Lett. B **145** (1984) 181; J. R. Ellis, D. V. Nanopoulos and S. Sarkar, Nucl. Phys. B **259** (1985) 175; T. Moroi, H. Murayama and M. Yamaguchi, Phys. Lett. B **303** (1993) 289; M. Kawasaki, K. Kohri and T. Moroi, Phys. Lett. B **625** (2005) 7; For a recent discussion, see: K. Kohri, T. Moroi and A. Yotsuyanagi, Phys. Rev. D **73** (2006) 123511. C. Bird, K. Koopmans and M. Pospelov, Phys. Rev. D **78** (2008) 083010; F. D. Steffen, Phys. Lett. B **669** (2008) 74.
- [71] M. Kawasaki, K. Kohri, T. Moroi and A. Yotsuyanagi, arXiv:0804.3745 [hep-ph].

- [72] T. Kanzaki, M. Kawasaki, K. Kohri and T. Moroi, Phys. Rev. D **75** (2007) 025011; J. L. Diaz-Cruz, J. R. Ellis, K. A. Olive and Y. Santoso, JHEP **0705** (2007) 003.
- [73] W. Buchmuller, L. Covi, K. Hamaguchi, A. Ibarra and T. Yanagida, JHEP **0703** (2007) 037; A. Ibarra and D. Tran, JCAP **0807** (2008) 002; K. Ishiwata, S. Matsumoto and T. Moroi, arXiv:0805.1133 [hep-ph].
- [74] Y. Grossman, T. Kashti, Y. Nir and E. Roulet, Phys. Rev. Lett. **91**, 251801 (2003).
- [75] G. D'Ambrosio, G. F. Giudice and M. Raidal, Phys. Lett. B **575**, 75 (2003).
- [76] Y. Grossman, T. Kashti, Y. Nir and E. Roulet, JHEP **0411** (2004) 080.
- [77] G. F. Giudice *et al.*, Nucl. Phys. B **685** (2004) 89.
- [78] G. C. Branco *et al.*, Nucl. Phys. B **617** (2001) 475.
- [79] T. Fujihara *et al.*, Phys. Rev. D **72** (2005) 016006.
- [80] S. Pascoli, S. T. Petcov and A. Riotto, Phys. Rev. D **75** (2007) 083511.
- [81] S. Pascoli, S. T. Petcov and A. Riotto, Nucl. Phys. B **774** (2007) 1.
- [82] G. C. Branco, R. Gonzalez Felipe and F. R. Joaquim, Phys. Lett. B **645** (2007) 432.
- [83] S. Antusch, S. F. King and A. Riotto, JCAP **0611** (2006) 011.
- [84] A. Anisimov, S. Blanchet and P. Di Bari, JCAP **0804** (2008) 033.
- [85] E. Molinaro and S. T. Petcov, arXiv:0803.4120 [hep-ph].
- [86] S. Blanchet, P. Di Bari and G. G. Raffelt, JCAP **0703** (2007) 012.
- [87] R. Barbieri *et al.*, Nucl. Phys. B **575** (2000) 61.
- [88] F. X. Josse-Michaux and A. Abada, JCAP **0710**, 009 (2007).
- [89] K. Hamaguchi, H. Murayama and T. Yanagida, Phys. Rev. D **65** (2002) 043512.
- [90] M. Raidal *et al.*, Eur. Phys. J. C **57**, 13 (2008).
- [91] S. Antusch and A. M. Teixeira, JCAP **0702** (2007) 024.
- [92] E. K. Akhmedov, M. Frigerio and A. Y. Smirnov, JHEP **0309** (2003) 021.
- [93] S. T. Petcov and T. Shindou, Phys. Rev. D **74** (2006) 073006.
- [94] J. R. Ellis and M. Raidal, Nucl. Phys. B **643** (2002) 229.

- [95] F. R. Joaquim, I. Masina and A. Riotto, *Int. J. Mod. Phys. A* **22**, 6253 (2007).
- [96] D. J. C. MacKay, “Information Theory, Inference, and Learning Algorithms”, Cambridge University Press.
- [97] W. R. Gilks, S. Richardson and D. J. Spiegelhalter, “Markov Chain Monte Carlo in Practice”, Chapman and Hall.
- [98] L. Calibbi, J. J. Perez and O. Vives, arXiv:0804.4620 [hep-ph].
- [99] S. Ritta and the MEG Collaboration, *Nucl. Phys. Proc. Suppl.* 162 (2006) 279.
- [100] A. G. Akeroyd *et al.* [SuperKEKB Physics Working Group], arXiv:hep-ex/0406071.
- [101] D. DeMille *et al.*, *Phys. Rev. A* 61, (2000) 05250; L.R. Hunter *et al.*, *Phys. Rev. A* 65, (2002) 030501(R); D. Kawall, F. Bay, S. Bickman, Y. Jiang, and D. DeMille, *Phys. Rev. Lett.* 92 (2004) 133007.
- [102] J. P. Miller *et al.* [EDM Collaboration], AIP Conf. Proc. **698** (2004) 196.
- [103] J. Hisano and K. Tobe, *Phys. Lett. B* **510** (2001) 197.
- [104] K. Hagiwara, A. D. Martin, D. Nomura and T. Teubner, *Phys. Lett. B* **649** (2007) 173.
- [105] D. W. Hertzog, J. P. Miller, E. de Rafael, B. Lee Roberts and D. Stockinger, arXiv:0705.4617 [hep-ph].
- [106] T. Moroi, *Phys. Rev. D* **53** (1996) 6565 [Erratum-*ibid.* D **56** (1997) 4424].
- [107] M. Davier, *Nucl. Phys. Proc. Suppl.* **169** (2007) 288.
- [108] J. R. Ellis, J. Hisano, M. Raidal and Y. Shimizu, *Phys. Lett. B* **528** (2002) 86.
- [109] I. Masina, *Nucl. Phys. B* **671** (2003) 432.
- [110] A. Bandyopadhyay *et al.* [ISS Physics Working Group], arXiv:0710.4947 [hep-ph].
- [111] M. Cirelli and A. Strumia, *JCAP* **0612** (2006) 013; S. Hannestad and G. G. Raffelt, *JCAP* **0611** (2006) 016; U. Seljak, A. Slosar and P. McDonald, *JCAP* **0610** (2006) 014.
- [112] C. Kraus *et al.*, *Eur. Phys. J. C* **40** (2005) 447.
- [113] H. V. Klapdor-Kleingrothaus *et al.*, *Eur. Phys. J. A* **12** (2001) 147.
- [114] D. A. Demir and Y. Farzan, *JHEP* **0510** (2005) 068.

- [115] S. Davidson, JHEP **0303** (2003) 037.
- [116] F. X. Josse-Michaux and A. Abada, JCAP **0710** (2007) 009.
- [117] P. H. Frampton, S. L. Glashow and T. Yanagida, Phys. Lett. B **548**, 119 (2002); W. l. Guo, Z. z. Xing and S. Zhou, Int. J. Mod. Phys. E **16**, 1 (2007).
- [118] A. Ibarra and G. G. Ross, Phys. Lett. B **591** (2004) 285; A. Ibarra, JHEP **0601** (2006) 064.
- [119] E. A. Baltz and P. Gondolo, JHEP **0410** (2004) 052; M. Kunz, R. Trotta and D. Parkinson, Phys. Rev. D **74** (2006) 023503.
- [120] B. C. Allanach, C. G. Lester and A. M. Weber, JHEP **0612** (2006) 065.
- [121] L. Verde *et al.* [WMAP Collaboration], Astrophys. J. Suppl. **148** (2003) 195.
- [122] W. Buchmuller, P. Di Bari and M. Plumacher, Nucl. Phys. B **643** (2002) 367.
- [123] E. Ma, N. Sahu and U. Sarkar, J. Phys. G **32**, L65 (2006).
- [124] P. Di Bari, Nucl. Phys. B **727** (2005) 318.
- [125] G. 't Hooft, Lecture given at Cargese Summer Inst., Cargese, France, Aug. 26 - Sep. 8, 1979.
- [126] J. Bernabeu, A. Santamaria, J. Vidal, A. Mendez and J. W. F. Valle, Phys. Lett. B **187** (1987) 303; G. C. Branco, M. N. Rebelo and J. W. F. Valle, Phys. Lett. B **225** (1989) 385; N. Rius and J. W. F. Valle, Phys. Lett. B **246** (1990) 249; M. C. Gonzalez-Garcia and J. W. F. Valle, Mod. Phys. Lett. A **7** (1992) 477; D. Tommasini, G. Barenboim, J. Bernabeu and C. Jarlskog, Nucl. Phys. B **444** (1995) 451; F. Deppisch, T. S. Kosmas and J. W. F. Valle, Nucl. Phys. B **752** (2006) 80.
- [127] M. Dittmar, A. Santamaria, M. C. Gonzalez-Garcia and J. W. F. Valle, Nucl. Phys. B **332** (1990) 1; M. C. Gonzalez-Garcia, A. Santamaria and J. W. F. Valle, Nucl. Phys. B **342** (1990) 108.
- [128] P. Hernandez and N. Rius, Nucl. Phys. B **495**, 57 (1997).
- [129] E. Nardi, E. Roulet and D. Tommasini, Phys. Lett. B **327** (1994) 319; E. Nardi, E. Roulet and D. Tommasini, Phys. Lett. B **344** (1995) 225.
- [130] Y. Farzan, Phys. Rev. D **69**, 073009 (2004).
- [131] A. Pilaftsis, Phys. Rev. **D56** (1997) 5431.
- [132] G. D'Ambrosio, T. Hambye, A. Hektor, M. Raidal and A. Rossi, Phys. Lett. B **604** (2004) 199.

- [133] S. F. King, Nucl. Phys. B **576** (2000) 85.
- [134] Y. Grossman, R. Kitano and H. Murayama, JHEP **0506**, 058 (2005).
- [135] A. D. Medina and C. E. M. Wagner, JHEP **0612**, 037 (2006).
- [136] F. Pisano and V. Pleitez, Phys. Rev. D **46** (1992) 410; P. H. Frampton, Phys. Rev. Lett. **69** (1992) 2889; M. B. Tully and G. C. Joshi, Phys. Rev. D **64**, 011301 (2001); J. C. Montero, C. A. de S. Pires and V. Pleitez, Phys. Lett. B **502** (2001) 167.
- [137] N. Sahu and U. Sarkar, Phys. Rev. D **76**, 045014 (2007); J. McDonald, N. Sahu and U. Sarkar, JCAP **0804**, 037 (2008).
- [138] I. Dorsner and I. Mocioiu, Nucl. Phys. B **796**, 123 (2008).
- [139] J. F. Gunion, J. Grifols, A. Mendez, B. Kayser and F. I. Olness, Phys. Rev. D **40** (1989) 1546; J. F. Gunion, R. Vega and J. Wudka, Phys. Rev. D **42** (1990) 1673.
- [140] K. Huitu, J. Maalampi, A. Pietila and M. Raidal, Nucl. Phys. B **487**, 27 (1997).
- [141] J. F. Gunion, C. Loomis and K. T. Pitts, Proceedings of Snowmass 96, Colorado, 25 Jun – 12 Jul 1996, pp LTH096, hep-ph/9610237.
- [142] B. Dion, T. Gregoire, D. London, L. Marleau and H. Nadeau, Phys. Rev. D **59** (1999) 075006.
- [143] M. Muhlleitner and M. Spira, Phys. Rev. D **68** (2003) 117701.
- [144] G. Azuelos, K. Benslama and J. Ferland, J. Phys. G **32**, 73 (2006).
- [145] A. G. Akeroyd and M. Aoki, Phys. Rev. D **72**, 035011 (2005).
- [146] G. Abbiendi *et al.* [OPAL Coll.], Phys. Lett. B **526** (2002) 221; J. Abdallah *et al.* [DELPHI Coll.], Phys. Lett. B **552** (2003) 127; P. Achard *et al.* [L3 Coll.], Phys. Lett. B **576** (2003) 18.
- [147] V. M. Abazov *et al.* [D0 Coll.], Phys. Rev. Lett. **93** (2004) 141801; D. E. Acosta *et al.* [CDF Coll.], Phys. Rev. Lett. **93** (2004) 221802; Phys. Rev. Lett. **95** (2005) 071801.
- [148] K. S. Babu and C. Macesanu, Phys. Rev. D **67** (2003) 073010; D. Aristizabal Sierra and M. Hirsch, JHEP **0612**, 052 (2006).
- [149] D. Aristizabal Sierra, M. Hirsch, J. W. F. Valle and A. Villanova del Moral, Phys. Rev. D **68**, 033006 (2003).
- [150] C. S. Chen, C. Q. Geng, J. N. Ng and J. M. S. Wu, JHEP **0708** (2007) 022.

-
- [151] W. Porod, M. Hirsch, J. Romao and J. W. F. Valle, Phys. Rev. D **63** (2001) 115004.
- [152] D. Aristizabal Sierra and D. Restrepo, JHEP **0608** (2006) 036.
- [153] S. M. Bilenky, J. Hosek and S. T. Petcov, Phys. Lett. B **94** (1980) 495.
- [154] E. J. Chun, K. Y. Lee and S. C. Park, Phys. Lett. B **566**, 142 (2003).
- [155] F. Cuypers and S. Davidson, Eur. Phys. J. C **2** (1998) 503; A. de Gouvea and S. Gopalakrishna, Phys. Rev. D **72** (2005) 093008.
- [156] A. E. Nelson and S. M. Barr, Phys. Lett. B **246**, 141 (1990);
J. A. Harvey and M. S. Turner, Phys. Rev. D **42**, 3344 (1990);
K. Hasegawa, Phys. Rev. D **70** (2004) 054002.
- [157] P. Huber, M. Lindner, M. Rolinec, T. Schwetz and W. Winter, Phys. Rev. D **70** (2004) 073014.
- [158] S. Pascoli, S. T. Petcov and T. Schwetz, Nucl. Phys. B **734** (2006) 24.

Agradecimientos

Después de estos cuatro o cinco años en el IFIC, me voy haciendo un balance muy positivo y quiero aprovechar estos agradecimientos para mostrar mi satisfacción. Creo que todo lo que he aprendido y las oportunidades que se me han presentado son una experiencia única que no olvidaré.

A la primera persona que quiero agradecer todo esto es a “mi jefa”, Nuria, porque sin ella no habría llegado hasta aquí. Todo el trabajo de esta tesis se lo debo a ella que me ha ido guiando y enseñando durante todo este tiempo. Y no sólo le estoy agradecida en lo profesional, también en lo personal, porque siempre ha respetado mis decisiones, nunca me ha puesto problemas para ir a mi aire, y ¡hasta me dejaba ir de estancia con Andreu! Muchas gracias por todo.

También quiero dar las gracias a todas las personas con las que he tenido la oportunidad de trabajar, por el ambiente tan agradable de trabajo y porque ellas también han contribuido a sacar adelante esta tesis. Gracias Concha González-García, Federica Palorini, Óscar Vives, Sacha Davidson, Sergio Pastor, Tegua Pinto y Thomas Schwetz.

Afortunadamente no todo es trabajo, y he disfrutado a lo largo de estos años de muchos buenos ratos en compañía de mis amigos del IFIC: Martín, Paola, Paula, Natxo, Fabio, Diego Milanés, Alberto, Zahara, Diego Aristizábal, Urbano, Tegua... y algún que otro desterrado a la Universidad: ¡¡Iván!!, Catalina, Jacobo, Enrique, Ana... Segur que les bombes no haurien sigut el mateix sense Ricard, i tampoc els dos mesos en Hamburg en la seua companyia i la de Mariam.

Mi familia se merece una mención muy especial, porque siempre me han apoyado en mis decisiones y escuchado mis rollos. Gracias a mis padres, Juan y Julia, a mi hermana Ana y mi cuñaaaaao Luis. Y por supuesto miles de gracias a Andreu, porque con él todo es mucho más fácil y mejor.

Y en último lugar, pero no por ello menos importantes, quiero recordar a mis amigos de la Pandilla del Infiern versión extendida: Fet y Alba, Aida y Pepe Toni, Ari e Iván, Feli y Álex, Germán, Carlos, y Goyo y María, porque son estupendos y me recuerdan cada viernes que hay vida más allá del IFIC. Chicos, a partir de ahora me denegarán el acceso al búnker y seré una pobre mortal más. ¡¡Gracias a todos!!

Que me quiten lo bailao.